A DISSERTATION FOR THE DEGREE OF DOCTOR OF PHILOSOPHY

Mutation frequency, stability, mechanism, and induction efficiency of mutants induced by diverse gamma-ray treatments in *Cymbidium*

감마선 처리에 의해 유도된 심비디움 돌연변이체의
돌연변이 발생빈도 및 안정성, 기작, 유도효율
증진 연구

February, 2020

Sang Hoon Kim

MAJOR IN HORTICULTURAL SCIENCE AND BIOTECHNOLOGY

DEPARTMENT OF PLANT SCIENCE

THE GRADUATE SCHOOL OF SEOUL NATIONAL UNIVERSITY

A DISSERTATION FOR THE DEGREE OF DOCTOR OF PHILOSOPHY

Mutation frequency, stability, mechanism, and induction efficiency of mutants induced by diverse gamma-ray treatments in *Cymbidium*

감마선 처리에 의해 유도된 심비디움 돌연변이체의
돌연변이 발생빈도 및 안정성, 기작, 유도효율
증진 연구

February, 2020

Sang Hoon Kim

MAJOR IN HORTICULTURAL SCIENCE AND BIOTECHNOLOGY
DEPARTMENT OF PLANT SCIENCE
THE GRADUATE SCHOOL OF SEOUL NATIONAL UNIVERSITY

Mutation frequency, stability, mechanism, and induction efficiency of mutants induced by diverse gamma-ray treatments in *Cymbidium*

Sang Hoon Kim

Department of Plant Science, Seoul National University

ABSTRACT

Mutation breeding techniques using physical mutagens (e.g., γ-rays, X-rays, and ion beams) have been widely used to develop mutant cultivars in diverse plant species. In 226 plant species, 3,308 mutants developed with physical mutagens have been registered in the Mutant Variety Database of the joint Food and Agriculture Organization of the United Nations/International Atomic Energy Agency. Especially, this technique is a useful method to improve one or two characteristics of elite cultivars. In seed propagated crops, the broad studies on mutation induction, optimal radiation dose, mutation efficiency, and so on have been conducted. However, in the vegetatively propagated plant species except chrysanthemum the studies have been performed restrictively and especially on

Cymbidium. In this study, I focused on the analysis of optimal γ-irradiation condition, mutation frequency, stability of chimeras, mutation mechanism, and induction efficiency of mutation in *Cymbidium*.

To analyze the effects of the total dose and irradiation duration on the growth of *Cymbidium* hybrid, samples were irradiated with seven total doses of γ-rays (0, 20, 40, 60, 80, 100, and 120 Gy) and five irradiation durations (1, 4, 8, 16, and 24 h). Survival and multiplication rates were measured at 3 and 6 months after irradiation (MAI), whereas the regeneration rate was analyzed at 9 MAI. The optimal doses (LD_{50}) for each irradiation duration were estimated: 1 h, 16.1 Gy; 4 h, 23.6 Gy; 8 h, 37.9 Gy; 16 h, 37.9 Gy; and 24 h, 40.0 Gy. The estimated optimal doses were duration-dependent at irradiation durations shorter than 8 h, but not at irradiation durations exceeding 8 h. Using the results of the first experiment as a reference, mutant populations were constructed using diverse γ-irradiation conditions as follows: RB003, irradiation conditions of 50 Gy/ 24 h, 50 Gy/ 16 h, 50 Gy/ 8 h, 35 Gy/ 4 h, and 25 Gy/ 1 h; RB012, irradiation conditions of 40 Gy/ 24 h, 40 Gy/ 16 h, 40 Gy/ 8 h, 30 Gy/ 4 h, 20 Gy/ 1 h, 30 Gy/ 24 h, and 30-30 Gy/ 24 h [re-irradiation of the population treated with 30 Gy/ 24 h]. In the RB003 and RB012 populations, the highest mutation frequency was identified as 4.06% (irradiation condition of 35 Gy/ 4 h) and 1.51% (20 Gy/ 1 h), respectively. Compared with the RB012 population γ-irradiated with 30 Gy/ 24 h, there was no difference on the mutation frequency of the re-irradiated (30-30 Gy/ 24 h) population: 30 Gy/ 24 h, mutation frequency of 0.68%; 30-30 Gy/ 24 h, 0.67%. These results indicate the mutations induced by a short-term treatment may be

similar to those induced by a treatment over a longer period. Additionally, leaf-color mutants was identified as relatively stable chimera types, but leaf-shape mutants was unstable and the stability of chimeras was different depending on the type and the location of a mutation on the cell layers.

A mutant displaying light-green leaves, obtained by γ-ray-based mutagenesis of a *Cymbidium*, was subjected to RNA sequencing (RNA-seq) to identify genes associated with leaf color. A total of 144,918 unigenes obtained from more than 25 million generated reads were assigned to 22 metabolic pathways in the Kyoto Encyclopedia of Genes and Genomes database. In addition, Gene Ontology was used to classify the predicted functions of unigenes into 73 functional groups. The RNA-seq analysis identified 2,267 genes differentially expressed between wild-type and mutant *Cymbidium*. Genes involved in chlorophyll biosynthesis and degradation as well as metal ion transport were identified and further evaluated by quantitative real-time PCR. No change was detected in genes involved in chlorophyll biosynthesis. In contrast, seven genes involved in ion transport were down-regulated, and chlorophyllase 2, associated with chlorophyll degradation, was up-regulated. Taken together, our results suggest that alteration in chlorophyll metabolism and/or ion transport regulate leaf color in *Cymbidium*.

This study was approached from the theoretical background that de-condensed chromatins are readily affected by radiation. I selected leaf color of *Cymbidium* as target traits for trait-targeted mutagenesis, and focused on genes encoding proteins in chlorophyll biosynthetic pathways. Light modulation was

used to control the expression of genes related to chlorophyll biosynthesis in *Cymbidium*. γ-irradiation was conducted when genes encoding proteins of chlorophyll pathways were highly expressed. Light modulation followed by γ-ray treatment resulted in a 1.4–2.0-fold increase in the mutation frequency of leaf-color compared with γ-ray treatment alone without light modulation in *Cymbidium*. These results indicate that the highly expressed condition of genes associated with specific trait is readily affected by radiation, resulting in an increased frequency of mutation related to the target trait.

The information presented herein regarding optimal γ-irradiation condition, mutation frequency, stability of chimeras, mutation mechanism, and induction efficiency of mutation will be useful for the mutation breeding of *Cymbidium*.

Key words: gamma-ray, mutation, frequency, stability, mechanism, induction efficiency

Student number: 2013-30323

CONTENTS

ABSTRACT i

LIST OF TABLES xi

LIST OF FIGURES xiii

LIST OF ABBREVIATION xvii

GENERAL INTRODUCTION 1

REFERENCES 6

CHAPTER I. Effects of the total dose and duration of γ-irradiation on the growth responses and induced SNPs of a *Cymbidium* hybrid

ABSTRACT 11

INTRODUCTION 12

MATERIALS AND METHODS 16

Plant materials 16

γ-Irradiation 16

Evaluation of PLB growth responses 17

DNA extraction 17

GBS analysis 18

RESULTS 20

Effects of the total dose and irradiation duration on PLB growth responses 20

Estimated 50% lethal dose (LD_{50}) and 50% reduction dose (RD_{50}).. 26

Evaluation of heterozygosity, natural variation, and induced SNPs. 29

DISCUSSION 32

Effects of the total dose and irradiation duration on PLB growth responses 32

Optimal γ-irradiation for inducing mutations 35

Genome complexity and induced SNPs 36

REFERENCES 39

CHAPTER II. Frequency, spectrum, and stability of leaf mutants induced by diverse γ-ray treatments in two *Cymbidium* hybrids

ABSTRACT 44

INTRODUCTION 45

MATERIALS AND METHODS 49

Plant materials 49

Optimal γ-ray dose determination 49

Mutant population construction 50

Phenotype and stability analysis of leaf mutants 50

RESULTS 52

Effects of γ-irradiation on rhizome growth parameters 52

Comparison of mutation frequency and spectrum among γ-irradiated populations 55

Evaluation of stability among leaf mutants 60

DISCUSSION 64

Optimal γ-irradiation condition for mutation induction 64

Frequency and spectrum of induced leaf mutants 65

Effects of short-term irradiation and re-irradiation on mutation induction. 66

Stability of induced chimera mutants 68

REFERENCES 70

CHAPTER III. Transcriptome analysis to identify candidate genes associated with the yellow-leaf phenotype of a *Cymbidium* mutant generated by γ-irradiation

ABSTRACT 74

INTRODUCTION 75

MATERIALS AND METHODS 78

Plant materials 78

RNA extraction 78

Quantitative real-time PCR (qRT-PCR) analysis 78

Chl and carotenoid content assay 79

RNA sequencing and *de novo* assembly 80

Functional annotation 80

Identification of differentially expressed genes between wild type and S12 mutant 81

RESULTS 83

Reduced accumulation of Chls and carotenoids in the S12 mutant 83

The implicated role of ion transport and Chl catabolism in the S12 phenotype according to DEG analysis.. 92

DISCUSSION 109

REFERENCES 113

CHAPTER IV. γ-irradiation combined with light modulation increases the frequency of leaf-color mutation in *Cymbidium*

ABSTRACT 121

INTRODUCTION 122

MATERIALS AND METHODS 126

Plant materials 126

Light modulation 126

Chl analysis 127

RNA extraction and RT-qPCR analysis 127

γ-ray treatments and evaluation of induced leaf mutants 128

Statistical analyses 129

RESULTS 130

Effect of light modulation on Chl degradation and biosynthesis 130

Effect of light modulation on Chl pathway gene expression 135

Induction frequency of Chl-related leaf-color mutants 137

DISCUSSION 141

Light modulation up-regulates gene expression in Chl pathway 141

Light modulation followed by γ-ray treatment increases leaf-color mutation 143

REFERENCES 145

GENERAL CONCLUSION 152

ABSTRACT IN KOREAN 156

LIST OF TABLES

Chapter I

Table I-1. Information regarding the barcode adapters used for the genotyping-by-sequencing analysis..... 19

Table I-2. Summary of the sequencing results, construction of the reference sequence, and the genome complexity of *Cymbidium* hybrid RB001..... 22

Chapter II

Table II-1. Regeneration, mutation frequency, and spectrum of leaf mutants derived from diverse γ-ray treatments in the *Cymbidium* hybrids 'RB003' and 'RB012' 57

Table II-2. Stability of leaf mutants induced by γ-irradiation in the *Cymbidium* hybrid 'RB003' and 'RB012' populations..... 62

Chapter III

Table III-1. Summary of RNA sequencing and *de novo* transcriptome assembly results 85

Table III-2. Functional categorization of assembled unigenes in KEGG pathways 86

Table III-3. Functional annotation of differentially expressed genes based on DAVID 94

Table III-4. Differentially expressed genes with increased expression levels that likely lead to higher enzymatic activities 95

Table III-5. Differentially expressed genes with decreased expression levels that likely lead to lower enzymatic activities 96

Table III-6. Primers used for qRT-PCR analysis 102

Table III-7. Functional classification of differentially expressed genes identified by KEGG clusters of orthologous genes (KOG) analysis..... 103

LIST OF FIGURES

Chapter I

Figure I-1. Survival and multiplication rates of *Cymbidium* hybrid RB001 PLBs at 3 months after γ-irradiation 23

Figure I-2. Survival and multiplication rates of *Cymbidium* hybrid RB001 PLBs at 6 months after γ-irradiation 24

Figure I-3. Regeneration rate of *Cymbidium* hybrid RB001 PLBs at 9 months after γ-irradiation. 25

Figure I-4. Comparison of the LD_{50} and RD_{50} of *Cymbidium* hybrid RB001 PLBs at 3, 6, and 9 months after γ-irradiation. 28

Figure I-5. Comparison of the induced SNPs among five γ-irradiated *Cymbidium* hybrid RB001 populations based on a *de novo* genotyping-by-sequencing analysis. 31

Chapter II

Figure II-1. Relative weight, survival, multiplication, and relative regeneration rate of *Cymbidium* hybrid 'RB003' and 'RB012' rhizomes at 3, 6, and 9 months after γ-irradiation. 54

Figure II-2. Diverse leaf-color or -shape mutants derived from *Cymbidium* hybrids 'RB003' and 'RB012' 59

Figure II-3. Segregation in the selected mutant RB012-S17 63

Chapter III

Figure III-1. Morphological phenotypes of typical wild-type and S12 mutant plants of *Cymbidium* hybrid RB003. 88

Figure III-2. Relative levels of chlorophylls *a* and *b* and carotenoids in the wild-type and S12 mutant. 89

Figure III-3. Distribution of annotated sequences based on Gene Ontology (GO) analysis 90

Figure III-4. Distribution of annotated sequences based on Kyoto Encyclopedia of Genes and Genomes (KEGG) pathway analysis. ... 91

Figure III-5. Venn diagram showing numbers of genes with altered expressions in the S12 mutant compared with wild-type. 97

Figure III-6. Gene Ontology (GO) functional classification of differentially expressed genes (DEGs) 98

Figure III-7. Eukaryotic clusters of orthologous genes (KOG) annotations of differentially expressed genes (DEGs) 99

Figure III-8. KEGG pathway representation of differentially expressed genes (DEGs) in the S12 mutant 100

Figure III-9. Schematic diagram of reads mapped to genes encoding proteins involved in chlorophyll biosynthesis and degradation. 107

Figure III-10. Quantitative real-time PCR analysis of 16 genes showing altered expression in the RNA-seq analysis 108

Chapter IV

Figure IV-1. Chlorophyll degradation after dark treatment in rhizomes of *Cymbidium* hybrids RB003 and RB012. 132

Figure IV-2. Chlorophyll accumulation after light treatment in rhizomes of *Cymbidium* hybrids RB003 and RB012 133

Figure IV-3. Chlorophyll contents of light-treated rhizomes in *Cymbidium* hybrids RB003 and RB012..... 134

Figure IV-4. Relative expression of six genes involved in chlorophyll biosynthesis and degradation during light treatment of *Cymbidium* hybrids RB003 and RB012..... 136

Figure IV-5. Representative leaf-color and -shape mutants induced by light modulation followed by γ-irradiation in *Cymbidium* hybrids RB003 and RB012. 139

Figure IV-6. Regeneration, total mutation, and chlorophyll-related mutation rates of mutant populations induced by light modulation followed by γ-irradiation in *Cymbidium* hybrids RB003 and RB012 140

LIST OF ABBREVIATION

PLBs	Protocorm-like bodies
GBS	Genotyping-by-sequencing
SNPs	Single nucleotide polymorphisms
SAM	Shoot apical meristem
LD_{50}	50% lethal dose
RD_{50}	50% reduction dose
GO	Gene ontology
DAVID	Database for annotation, visualization, and integrated discovery
KEGG	Kyoto encyclopedia of genes and genomes
KOG	Eukaryotic clusters of orthologous genes
DEGs	Differentially expressed genes
Chl	Chlorophyll
HEMD	Uroporphyrinogen-III synthase
HEME2	Uroporphyrinogen decarboxylase 2
PORA	Protochlorophyllide oxidoreductase A
CHLG	Chlorophyll synthase
CLH2	Chlorophyllase 2
RCCR	Red Chl catabolite reductase

GENERAL INTRODUCTION

The Orchidaceae is among the largest families of angiosperms, and is composed of approximately 736 genera and about 28,000 species (Chase et al. 2015). Among the diverse genera in the family, *Dendrobium*, *Phalaenopsis*, *Oncidium*, and *Cymbidium* are important floricultural crops in Asian countries (Sarmah et al. 2017). In particular, *Cymbidium* is economically important in northeastern Asia, including Korea, China, and Japan (Choi et al. 2006). *Cymbidium* species are conveniently divided into two groups on the basis of the native habitat and climate region, i.e., temperate and subtropical or tropical regions (Kang et al. 2009, Ryu et al. 2013). There are continuous demands for development of new *Cymbidium* cultivars on account of the attractiveness of the foliage as well as the flower colors and fragrance. To date, many *Cymbidium* cultivars have been developed via natural selection or artificial cross-breeding, although transformation has also been developed in *Cymbidium* breeding (Chin et al. 2007). However, development of a new *Cymbidium* cultivar by means of cross-breeding is time-consuming because of the long vegetative growth stage.

Mutation breeding techniques involving physical mutagens (e.g., γ-rays and X-rays) or chemical mutagens (e.g., ethyl methanesulfonate and *N*-nitroso-

N-methylurea) have been broadly used to induce mutations in diverse plant species. For example, 3,303 mutants of 226 plant species (including two *Cymbidium* and two *Oncidium* mutants) mainly developed with physical mutagens have been registered in the Mutant Variety Database of the joint Food and Agriculture Organization of the United Nations/International Atomic Energy Agency (IAEA 2019). Mutation breeding with a physical mutagen combined with *in vitro* tissue culture has been used to shorten the breeding period (Lee et al. 2016), implying that a method involving γ-radiation and *in vitro* tissue culture may be useful for *Cymbidium* breeding.

Regarding mutation breeding with physical mutagens, the optimal irradiation condition refers to the condition that induces desirable genomic mutations, with minimal radiation damages. Researchers have used the 30%–50% lethal dose ($LD_{30–50}$) for constructing a mutant population (Kodym et al. 2012). However, Yamaguchi et al. (2009) revealed that the mutation frequency is highest at a shoulder dose, which is approximately the LD_{10} in rice (i.e., seed-propagated plant species). To the best of my knowledge, there is relatively little published research regarding the optimal irradiation condition for vegetatively propagated plant species. Lee et al. (2016) and Kodym et al. (2012) respectively suggested that the 50% reduction dose (RD_{50}) and the $RD_{30–50}$ were the optimal conditions for inducing mutations. Researchers have considered the total

irradiation dose for inducing mutations in diverse plant species, but there has been relatively little consideration given to the dose rate and irradiation duration, which are also crucial factors. Previous studies on oat and maize indicated that mutations are more effectively induced with increasing dose rates, even if the total dose remains the same (Mabuchi and Matsumura 1964; Nishiyama et al. 1966). However, Yamaguchi et al. (2008) reported that the mutation frequency for chrysanthemum is dependent on the total dose, not the dose rate. In contrast, Kim et al. (2016) suggested that a specific irradiation duration or dose rate may effectively induce mutations in chrysanthemum.

In addition, the ratio of DNA double-strand breaks (DSBs) induced by γ-ray treatment was higher in decondensed chromatin than in condensed chromatin in human cells (Takata et al. 2013). Heterochromatin, a strongly packed type of DNA, RNA, and protein, was less sensitive to DNA DSBs by γ-ray treatment than euchromatin, a slightly packed type in human cells (Venkatesh et al. 2016). Hase et al. (2010) suggested that the mutation of specific genes by radiation may be affected by controlling the expression of target genes. Recently, the proposed hypothesis was experimentally elucidated in chrysanthemum (Kim et al. 2019).

The treatment of seeds, buds (tip/node cuttings), callus, and rhizomes with a mutagen induces chimeras in M_1 plants, because mutations are induced in individual cells and regenerated shoots are recovered from pre-existing

multicellular meristems (Geier 2012). Geier (2012) suggested that plant regeneration via adventitious buds or somatic embryos, which permits the genetic background to be retained, might be useful to dissociate the chimera in vegetatively propagated plants. In the majority of angiosperms, the shoot apical meristem (SAM) is composed of three layers: the outer meristem layer (L1), the second meristem layer (L2), and the inner corpus (L3) (Filippis et al. 2013, Frank and Chitwood 2016). Mutagen-treated plants are composed of heterogeneous cells in the three layers, which can be categorized into three chimera types: sectorial chimeras, which have an unstable heterogenomic population of cells traversing more than one layer of the SAM; mericlinal chimeras, which have an unstable heterogenomic population of cells within a single layer of the SAM; and periclinal chimeras, which have a stable, uniform, and genetically distinguished layer of cells of the SAM (Geier 2012, Frank and Chitwood 2016). The phenotypes of mutants are diverse according to the type and extent of these chimeras. Thus, an understanding of chimerism is necessary to develop a new *Cymbidium* mutant cultivar by mutagenesis.

The leaf color phenotype has been extensively studies in rice and has provided insights into the steps involved in chlorophyll biosynthesis and degradation, chloroplast developments, tetrapyrrole synthesis, and photosynthesis (Deng et al. 2014). These studies have led to the isolation of

diverse leaf colors and patterns including albino, light and purple green leaves, as well as striped and zebra-patterned leaves (Deng et al. 2012). Thus far, over 50 genes contributing to leaf color have been characterized in rice and 13 of these function in chlorophyll biosynthesis (Jung et al. 2003, Lee et al. 2005, Zhang et al. 2006, Liu et al. 2007, Wu et al. 2007, Wang et al. 2010, Huang et al. 2013, Sakuraba et al. 2013, Tian et al. 2013, Zhou et al. 2013, Ma et al. 2017, Qin et al. 2017). These studies suggest that genes regulating leaf color can, directly or indirectly, contribute to chlorophyll biosynthesis and/or structure of the chloroplast and that chlorophyll and anthocyanin content are major contributors to the leaf color. Zhu et al. (2015) suggested that the yellow-striped leaves of a *Cymbidium sinense* variant were due to an increase in chlorophyll degradation.

In this study, I focused on the analysis of optimal γ-irradiation condition, mutation frequency, stability of chimeras, mutation mechanism, and induction efficiency of mutation in *Cymbidium*.

REFERENCES

Chase MW, Cameron KM, Freudenstein JV, Pridgeon AM, Salazar G, van den Berg C, Schuiteman A. 2015. An updated classification of Orchidaceae. Bot J Linn Soc. 177: 151–174.

Chin DP, Mishiba K, Mii M. 2007. *Agrobacterium*-mediated transformation of protocorm-like bodies in *Cymbidium*. Plant Cell Rep. 26: 735–743.

Choi SH, Kim MJ, Lee JS, Ryu KH. 2006. Genetic diversity and phylogenetic relationships among and within species of oriental cymbidiums based on RAPD analysis. Sci Hortic. 108: 79–85.

Deng X, Zhang H, Wang Y, Shu Z, Wang G, Wang G. 2012. Research advances on rice leaf-color mutant genes. Hybrid Rice. 27(5): 9–14.

Deng XJ, Zhang HQ, Wang Y, He F, Liu JL, Xiao X, et al. 2014. Mapped clone and functional analysis of leaf-color gene Ygl7 in a rice hybrid (*Oryza sativa* L. ssp. *indica*). PLoS ONE. 9(6): e99564.

Filippis I, Lopez-Cobollo R, Abbott J, Butcher S, Bishop GJ. 2013. Using a periclinal chimera to unravel layer-specific gene expression in plants. Plant J. 75: 1039–1049.

Frank MH, Chitwood DH. 2016. Plant chimeras: The good, the bad, and the 'Bizzaria'. Dev Biol. 419: 41–53.

Geier T. 2012. Chimeras: Properties and dissociation in vegetatively propagated plants. *In*: Shu QY, Forster BP, Nakagawa H (eds.) Plant Mutation Breeding and Biotechnology, CAB International, Wallingford; FAO, Rome, pp. 191–202.

Hase Y, Okamura M, Takeshita D, Narumi I, Tanaka A. 2010. Efficient induction of flower-color mutants by ion beam irradiation in petunia seedlings treated with high sucrose concentration. Plant Biotechnol. 27: 99–103.

Huang J, Qin F, Zang G, Kang Z, Zou H, Hu F, et al. 2013. Mutation of OsDET1 increases chlorophyll content in rice. Plant Sci. 210: 241–249.

[IAEA] International Atomic Energy Agency. 2019. IAEA Mutant Variety

Database [Dataset]. The joint FAO/IAEA Mutant Variety Database; [accessed 2019]. https://mvd.iaea.org/#!Home.

Jung KH, Hur J, Ryu CH, Choi Y, Chung YY, Miyao A, et al. 2003. Characterization of a rice chlorophyll-deficient mutant using the T-DNA gene-trap system. Plant Cell Physiol. 44(5): 463–472.

Kang KW, Park KS, Mo SY, Kim DH, Kang SY. 2009. A new *Cymbidium* orchid variety "Daegook" bred by *in vitro* mutagenesis. Kor J Breed Sci. 41: 510–514.

Kim SH, Kim YS, Jo YD, Kang SY, Ahn JW, Kang BC, Kim JB. 2019. Sucrose and methyl jasmonate modulate the expression of anthocyanin biosynthesis genes and increase the frequency of flower-color mutants in chrysanthemum. Sci Hortic. 256: 108602.

Kim YS, Sung SY, Jo YD, Lee HJ, Kim SH. 2016. Effects of gamma ray dose rate and sucrose treatment on mutation induction in chrysanthemum. Eur J Hortic Sci. 81: 212–218.

Kodym A, Afza R, Forster BP, Ukai Y, Nakagawa H, Mba C. 2012. Methodology for physical and chemical mutagenic treatments. *In*: Shu QY, Forster BP, Nakagawa H (eds.) Plant Mutation Breeding and Biotechnology, CAB International, Wallingford; FAO, Rome, pp. 169–180.

Lee S, Kim JH, Yoo ES, Lee CH, Hirochika H, An G. 2005. Differential regulation of chlorophyll a oxygenase genes in rice. Plant Mol Biol. 57(6): 805–818.

Lee YM, Lee HJ, Kim YS, Kang SY, Kim DS, Kim JB, Ahn JW, Ha BK, Kim SH. 2016. Evaluation of the sensitivity to ionizing γ-radiation of a *Cymbidium* hybrid. J Hortic Sci Biotechnol. 91: 109–116.

Liu W, Fu Y, Hu G, Si H, Zhu L, Wu C, et al. 2007. Identification and fine mapping of a thermo-sensitive chlorophyll deficient mutant in rice (*Oryza sativa* L.). Planta. 226(3): 785–795.

Mabuchi T, Matsumura S. 1964. Dose rate dependence of mutation rates from γ-irradiated pollen grains of maize. Jpn J Genet. 39: 131–135.

Ma X, Sun X, Li C, Huan R, Sun C, Wang Y, et al. 2017. Map-based cloning and characterization of the novel yellow-green leaf gene ys83 in rice (*Oryza sativa*). Plant Physiol Biochem. 111: 1–9.

Nishiyama I, Ikushima T, Ichikawa S. 1966. Radiological studies in plants–XI: Further studies on somatic mutations induced by X-rays at the *al* locus of diploid oats. Radiat Bot. 6: 211–218.

Qin R, Zeng D, Liang R, Yang C, Akhter D, Alamin M, et al. 2017. Rice gene SDL/RNRS1, encoding the small subunit of ribonucleotide reductase, is required for chlorophyll synthesis and plant growth development. Gene. 627: 351–362.

Ryu J, So HS, Bae SH, Kang HS, Lee BC, Kang SY, Lee HY, Bae CH. 2013. Genetic diversity of *in vitro* cultured *Cymbidium* spp. irradiated with electron beam. Kor J Breed Sci. 45: 8–18.

Sakuraba Y, Rahman ML, Cho SH, Kim YS, Koh HJ, Yoo SC, et al. 2013. The rice faded green leaf locus encodes protochlorophyllide oxidoreductase B and is essential for chlorophyll synthesis under high light conditions. Plant J. 74(1): 122–133.

Sarmah D, Kolukunde S, Sutradhar M, Singh BK, Mandal T, Mandal N. 2017. A review on: *In vitro* cloning of orchids. Int J Curr Microbiol Appl Sci. 6: 1909–1927.

Takata H, Hanafusa T, Mori T, Shimura M, Iida Y, Ishikawa K, Yoshikawa K, Yoshikawa Y, Maeshima K. 2013. Chromatin compaction protects genomic DNA from radiation damage. PLoS ONE 8(10): e75622.

Tian X, Ling Y, Fang L, Du P, Sang X, Zhao F, et al. 2013. Gene cloning and functional analysis of yellow green leaf3 (*ygl3*) gene during the whole-plant growth stage in rice. Gene Genomics. 35(1): 87–93.

Venkatesh P, Panyutin IV, Remeeva E, Neumann RD, Panyutin IG. 2016. Effect of chromatin structure on the extent and distribution of DNA double strand breaks produced by ionizing radiation; comparative study of hESC and differentiated cells lines. Int J Mol Sci. 17: 58.

Wang P, Gao J, Wan C, Zhang F, Xu Z, Huang X, et al. 2010. Divinyl chlorophyll(ide) *a* can be converted to monovinyl chlorophyll(ide) *a* by a divinyl reductase in rice. Plant Physiol. 153(3): 994–1003.

Wu Z, Zhang X, He B, Diao L, Sheng S, Wang J, et al. 2007. A chlorophyll-deficient rice mutant with impaired chlorophyllide esterification in chlorophyll biosynthesis. Plant Physiol. 145(1): 29–40.

Yamaguchi H, Hase Y, Tanaka A, Shikazono N, Degi K, Shimizu A, Morishita

T. 2009. Mutagenic effects of ion beam irradiation on rice. Breed Sci. 59: 169–177.

Yamaguchi H, Shimizu A, Degi K, Morishita T. 2008. Effects of dose and dose rate of gamma ray irradiation on mutation induction and nuclear DNA content in chrysanthemum. Breed Sci. 58: 331–335.

Zhang H, Li J, Yoo JH, Yoo SC, Cho SH, Koh HJ, et al. 2006. Rice *Chlorina-1* and *Chlorina-9* encode ChlD and ChlI subunits of Mg-chelatase, a key enzyme for chlorophyll synthesis and chloroplast development. Plant Mol Biol. 62(3): 325–337.

Zhou K, Ren Y, Lv J, Wang Y, Liu F, Zhou F, et al. 2013. *Young Leaf Chlorosis 1*, a chloroplast-localized gene required for chlorophyll and lutein accumulation during early leaf development in rice. Planta. 237(1): 279–292.

Zhu G, Yang F, Shi S, Li D, Wang Z, Liu H, et al. 2015. Transcriptome characterization of *Cymbidium sinense* 'Dharma' using 454 pyrosequencing and its application in the identification of genes associated with leaf color variation. PLoS ONE. 10(6): e0128592.

CHAPTER I

Effects of the total dose and duration of γ-irradiation on the growth responses and induced SNPs of a *Cymbidium* hybrid

This research has been published in *International Journal of Radiation Biology* [2020; doi: 10.1080/09553002.2020.1704303].

ABSTRACT

Ionizing radiation has been used for developing new cultivars of diverse plant species, including *Cymbidium* orchid species. The effects of the total dose on mutation induction has been investigated; however, there is relatively little research on the influence of the dose rate or irradiation duration. Thus, I analyzed the effects of the total dose and irradiation duration on the growth of *Cymbidium* hybrid RB001 protocorm-like bodies (PLBs). I completed a genotyping-by-sequencing analysis to compare the induced SNPs among five γ-irradiated populations with similar growth responses (LD_{50}) to γ-rays. The optimal time to assess the effects of the γ-irradiation was at 6 months after the treatment. On the basis of the survival rate of γ-irradiated PLBs, the optimal doses (LD_{50}) for each irradiation duration were estimated: 1 h, 16.1 Gy; 4 h, 23.6 Gy; 8 h, 37.9 Gy; 16 h, 37.9 Gy; and 24 h, 40.0 Gy. The estimated optimal doses were duration-dependent at irradiation durations shorter than 8 h, but not at irradiation durations exceeding 8 h. A SNP comparison revealed a lack of significant differences among the mutations induced by γ-irradiations. These results indicate the irradiation duration affects PLB growth in response to γ-rays. Moreover, the mutations induced by a short-term treatment may be similar to those induced by a treatment over a longer period.

INTRODUCTION

Orchidaceae, which is one of the largest families of angiosperms, includes approximately 736 genera and about 28,000 species (Chase et al. 2015). In the countries belonging to the Association of Southeast Asian Nations, *Dendrobium*, *Phalaenopsis*, *Oncidium*, and *Cymbidium* orchid species are considered typical cash crops (Sarmah et al. 2017). However, *Cymbidium* species are especially economically important in northeastern Asia, including Korea, China, and Japan (Choi et al. 2006). The demand for new *Cymbidium* cultivars has continued to increase in these countries because of the popularity of the flower colors and fragrances as well as the desirable leaf appearance. Many *Cymbidium* cultivars were mainly developed via natural selection or cross-breeding, although transformation-based techniques have also been used for *Cymbidium* breeding (Chin et al. 2007). However, the development of a new *Cymbidium* cultivar with traditional cross-breeding techniques is time-consuming because of the long vegetative growth stage. Moreover, there are restrictions regarding the release of transgenic plants to market in many countries.

Mutation breeding techniques involving physical mutagens (e.g., γ-rays and X-rays) or chemical mutagens (e.g., ethyl methanesulfonate and *N*-nitroso-

N-methylurea) have been broadly used to induce mutations in diverse plant species. For example, 3,303 mutants of 226 plant species (including two *Cymbidium* and two *Oncidium* mutants) mainly developed with physical mutagens have been registered in the Mutant Variety Database of the joint Food and Agriculture Organization of the United Nations/International Atomic Energy Agency (IAEA 2019). Mutation breeding with a physical mutagen combined with *in vitro* tissue culture has been used to shorten the breeding period (Lee et al. 2016b), implying that a method involving γ-radiation and *in vitro* tissue culture may be useful for *Cymbidium* breeding.

Regarding mutation breeding with physical mutagens, the optimal irradiation condition refers to the condition that induces desirable genomic mutations, with minimal radiation damages. Researchers have used the 30%–50% lethal dose ($LD_{30–50}$) for constructing a mutant population (Kodym et al. 2012). However, Yamaguchi et al. (2009) revealed that the mutation frequency is highest at a shoulder dose, which is approximately the LD_{10} in rice (i.e., seed-propagated plant species). To the best of our knowledge, there is relatively little published research regarding the optimal irradiation condition for vegetatively propagated plant species. Lee et al. (2016b) and Kodym et al. (2012) respectively suggested that the 50% reduction dose (RD_{50}) and the $RD_{30–50}$ were the optimal conditions for inducing mutations. Researchers have considered the total

irradiation dose for inducing mutations in diverse plant species, but there has been relatively little consideration given to the dose rate and irradiation duration, which are also crucial factors. Previous studies on oat and maize indicated that mutations are more effectively induced with increasing dose rates, even if the total dose remains the same (Mabuchi and Matsumura 1964; Nishiyama et al. 1966). However, Yamaguchi et al. (2008) reported that the mutation frequency for chrysanthemum is dependent on the total dose, not the dose rate. In contrast, Kim et al. (2016) suggested that a specific irradiation duration or dose rate may effectively induce mutations in chrysanthemum.

The recent development of next-generation sequencing technology has provided researchers with a cost-effective and rapid means to analyze DNA variants at the whole-genome level (Lee et al. 2016a; Tsai et al. 2017). For example, mutations, such as single base substitutions, deletions, and insertions, have been revealed by the whole-genome re-sequencing of *Arabidopsis thaliana* and rice (Hase et al. 2018; Cui et al. 2019). Genotyping-by-sequencing (GBS) technologies based on a next-generation sequencing platform are also applicable to studies of population genomics, association mapping, and large-scale detection of single nucleotide polymorphisms (SNPs) (Narum et al. 2013; Uitdewilligen et al. 2013; Ryu et al. 2019).

Lee et al. (2016b) determined the optimal dose by comparing the

physiological and physical responses of protocorm-like bodies (PLBs). In this study, I investigated the effects of the total dose and irradiation duration on PLBs and compared the induced SNPs among five γ-irradiated populations.

MATERIALS AND METHODS

Plant materials

The PLBs of *Cymbidium* hybrid RB001 [(*C. sinense* × *C. goeringii*) × *Cymbidium* spp.] were analyzed according to a slightly modified version of a method described by Lee et al. (2016b). Specifically, the PLBs were cultured at 24 ± 1 °C with a 16-h photoperiod provided by white fluorescent lights (PPFD = 50 μmol m^{-2} s^{-1}) on medium (pH 5.35) comprising 0.2% Hyponex (N:P:K = 6.5:6:19; Hyponex Japan Co., Ltd., Osaka, Japan), 0.1% Hyponex (N:P:K = 20:20:20), 3% sucrose (Duchefa B.V., Haarlem, The Netherlands), 0.3% peptone (Duchefa B.V.), 0.075% activated charcoal (Sigma-Aldrich, St Louis, MO, USA), and 0.38% plant agar (Duchefa B.V.).

γ-Irradiation

Samples were irradiated with seven total doses of γ-rays (0, 20, 40, 60, 80, 100, and 120 Gy) emitted from a ^{60}Co source (150 TBq capacity; AECL, Canada) and five irradiation durations (1, 4, 8, 16, and 24 h) at the Korea Atomic Energy Research Institute, Jeongeup, Korea. Irradiation was conducted at 25 ± 3 °C with a 24-h photoperiod provided by white fluorescent lights (PPFD = 20

μmol m^{-2} s^{-1}). The γ-irradiated-PLBs were immediately transferred to fresh culture medium.

Evaluation of PLB growth responses

The growth of γ-irradiated PLBs was evaluated based on three growth parameters. Survival and multiplication rates of PLBs were measured at 3 and 6 months after irradiation, whereas the regeneration rate was analyzed at 9 months. The γ-irradiated PLBs were sub-cultured every 3 months. The experiments were performed with 10 biological replicates, with nine PLBs per replicate. Linear regression analysis was separately conducted for two irradiation duration ranges (1 to 8 h and 8 to 24 h) to compare estimated LD_{50} and RD_{50} among five γ-treated populations.

DNA extraction

Genomic DNA was extracted from the leaves of plants regenerated from each γ-irradiated and untreated control PLB with the DNeasy Plant Mini Kit (Qiagen, Hilden, Germany) and quantified with the NanoDrop 2000 spectrophotometer (Thermo Fisher Scientific, MA, USA). Six samples from each

treatment (36 samples in total) were used for a comparison of the induced SNP mutations among the γ-irradiated populations.

GBS analysis

A GBS library was constructed with the restriction enzyme *Ape*KI (GCWGC) (New England Biolabs Inc., MA, USA) and 36 barcode adapters (Table I-1) as described by Elshire et al. (2011), with minor modifications. The library was sequenced with the NextSeq 500 system (Illumina, CA, USA) (150-bp single-end reads). The raw reads were assigned to individual samples with barcode adapters using the Stacks tool (Catchen et al. 2013). The reads were then trimmed to 120 bp with quality control constraints (Q-score > 20) using the Trimmomatic tool (Bolger et al. 2014). The reference sequence was *de novo* assembled and SNPs were analyzed with the *de novo* SNP detection pipeline of the Stacks tool. The GBS analysis was performed by C & K Genomics Inc. (Seoul, Korea).

Table I-1. Information regarding the barcode adapters used for the genotyping-by-sequencing analysis

Sample	Barcode	Sample	Barcode
Control_1	AACT	40 Gy_8 h_1	AAGCA
Control_2	CCTA	40 Gy_8 h_2	GGTGTACA
Control_3	TTAC	40 Gy_8 h_3	AACCGTAT
Control_4	AGGC	40 Gy_8 h_4	CCAATGTAA
Control_5	GCAT	40 Gy_8 h_5	TTGTACGGT
Control_6	TAGA	40 Gy_8 h_6	GGTGCAATA
20 Gy_1 h_1	CTGT	40 Gy_16 h_1	GACGGT
20 Gy_1 h_2	AGAGA	40 Gy_16 h_2	CTAAGA
20 Gy_1 h_3	CGCGT	40 Gy_16 h_3	ACGTAT
20 Gy_1 h_4	TCTGA	40 Gy_16 h_4	CGTGTA
20 Gy_1 h_5	AACAT	40 Gy_16 h_5	GCTCGA
20 Gy_1 h_6	CCACA	40 Gy_16 h_6	ATCGAT
30 Gy_4 h_1	CGTAA	40 Gy_24 h_1	TGCCAT
30 Gy_4 h_2	ACATT	40 Gy_24 h_2	ACAGTA
30 Gy_4 h_3	TTCCA	40 Gy_24 h_3	CGTAGT
30 Gy_4 h_4	GTGGA	40 Gy_24 h_4	TTCTGGA
30 Gy_4 h_5	AATCGTTA	40 Gy_24 h_5	GAGACGT
30 Gy_4 h_6	CACTA	40 Gy_24 h_6	ACACAGT

RESULTS

Effects of the total dose and irradiation duration on PLB growth responses

The survival rate of γ-irradiated PLBs clearly decreased at irradiations less than 40 Gy, but dose-dependent responses were not detected at irradiations exceeding 40 Gy (Figure I-1A). However, the multiplication rate of the γ-irradiated PLBs rapidly decreased with increasing doses. Additionally, the PLBs exhibited highly limited growth responses when irradiated at more than 60 Gy (Figure I-1B). On the basis of these two growth parameters, the PLB growth responses varied depending on the irradiation durations (Figure I-1). Moreover, at doses exceeding 60 Gy, the PLBs exhibited extremely limited growth, but several PLBs survived in all treatments (Figure I-1A). Furthermore, there was no detectable regeneration of PLBs for all treatments (including the control treatment) during the first 3 months of the study period.

The effects of γ-rays on PLBs were also examined based on two growth parameters at 6 months after the γ-ray treatments. In response to the 8-, 16-, and 24-h γ-irradiations, similar decreasing patterns were observed for the two analyzed growth parameters. Specifically, the survival and multiplication rates

decreased to nearly 0 in response to 80 Gy (Figure I-2). In contrast, the decreasing patterns due to the irradiation durations of 1 and 4 h differed from those induced by the irradiation durations greater than 8 h, with two growth parameters decreasing to nearly 0 in response to 60 Gy (Figure I-2). At 3 months after the γ-ray treatments, several PLBs γ-irradiated at doses greater than 60 Gy remained viable (Figure I-1A), but almost all PLBs γ-irradiated at doses exceeding 80 Gy were dead at 6 months after irradiation (Figure I-2A). The multiplication rates of the 60 Gy-treated PLBs were close to 0 at 3 months after irradiation (Figure I-1B), but some PLBs γ-irradiated for 8, 16, and 24 h recovered somewhat at 6 months (Figure I-2B).

Regenerated PLBs were detected in the control and γ-irradiated populations from about 7 and 8 months after treatments, respectively. The PLB regeneration rates were finally scored at 9 months after irradiation. The regeneration pattern for the γ-irradiated PLBs was similar to the multiplication rate changes of γ-irradiated PLBs at 3 months after treatments (Figure I-1B, 3). In response to all treatments, the regeneration rates decreased with increasing doses. Additionally, the regeneration rates decreased to 0 in response to 40 Gy for the 1- and 4-h treatments and 60 Gy for the 8-, 16-, and 24-h treatments (Figure I-3).

Table I-2. Summary of the sequencing results, construction of the reference sequence, and the genome complexity of *Cymbidium* hybrid RB001

Category	Estimated value
Sequencing results	
Raw clusters	187,443,640
Trimmed clusters	154,665,489
Sequencing yield (Mbp)	23,354
Reference sequence construction	
Number of catalogs	590,047
Catalog length (bp)	120
Reference sequence (bp)	70,805,640
Genome complexity[†]	
Heterozygosity (kbp^{-1})	2.395
Natural variation (kbp^{-1})	0.222 (Transition, 0.091; Transversion, 0.131)

[†]Calculations are based on the sequence information for the six controls.

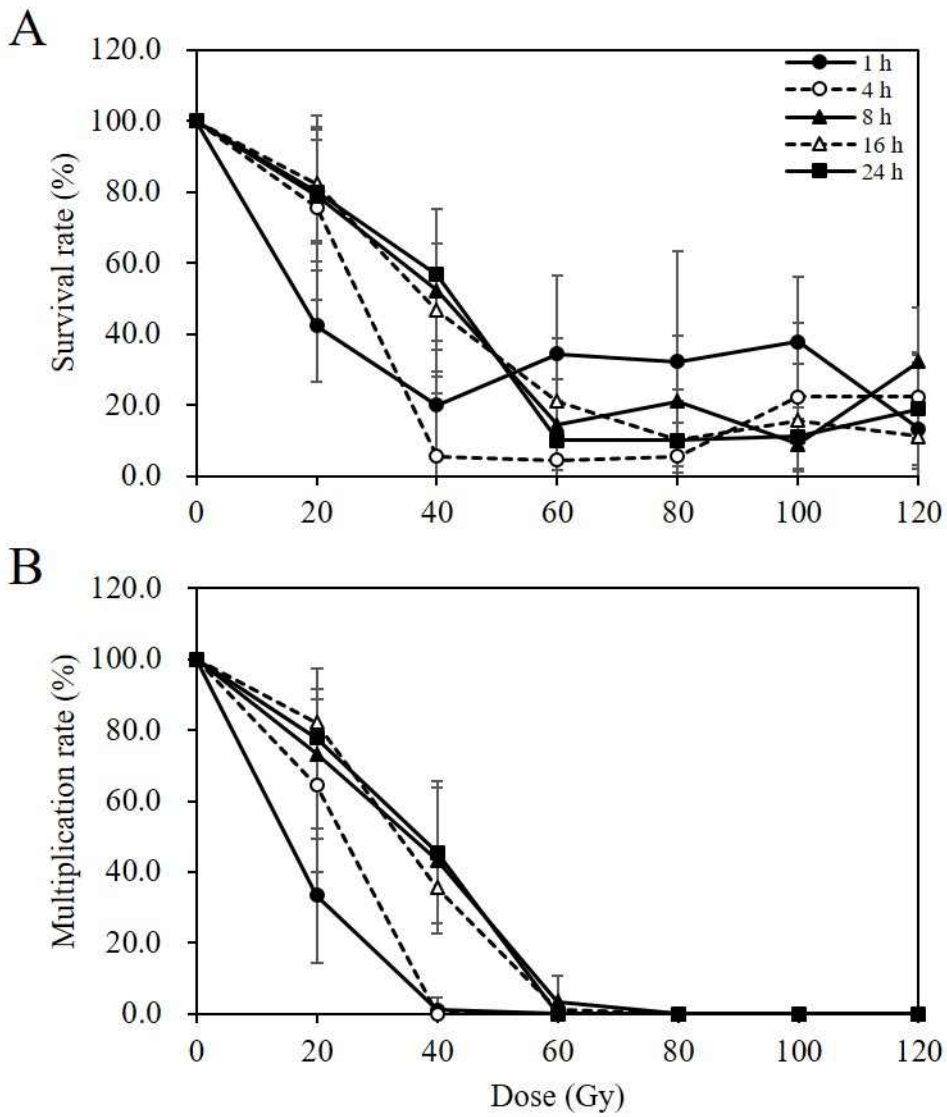

Figure I-1. Survival and multiplication rates of *Cymbidium* hybrid RB001 PLBs at 3 months after γ-irradiation. A, survival rate of PLBs; B, multiplication rate of PLBs. Error bars indicate the standard error of the mean (n = 10, biological replicates).

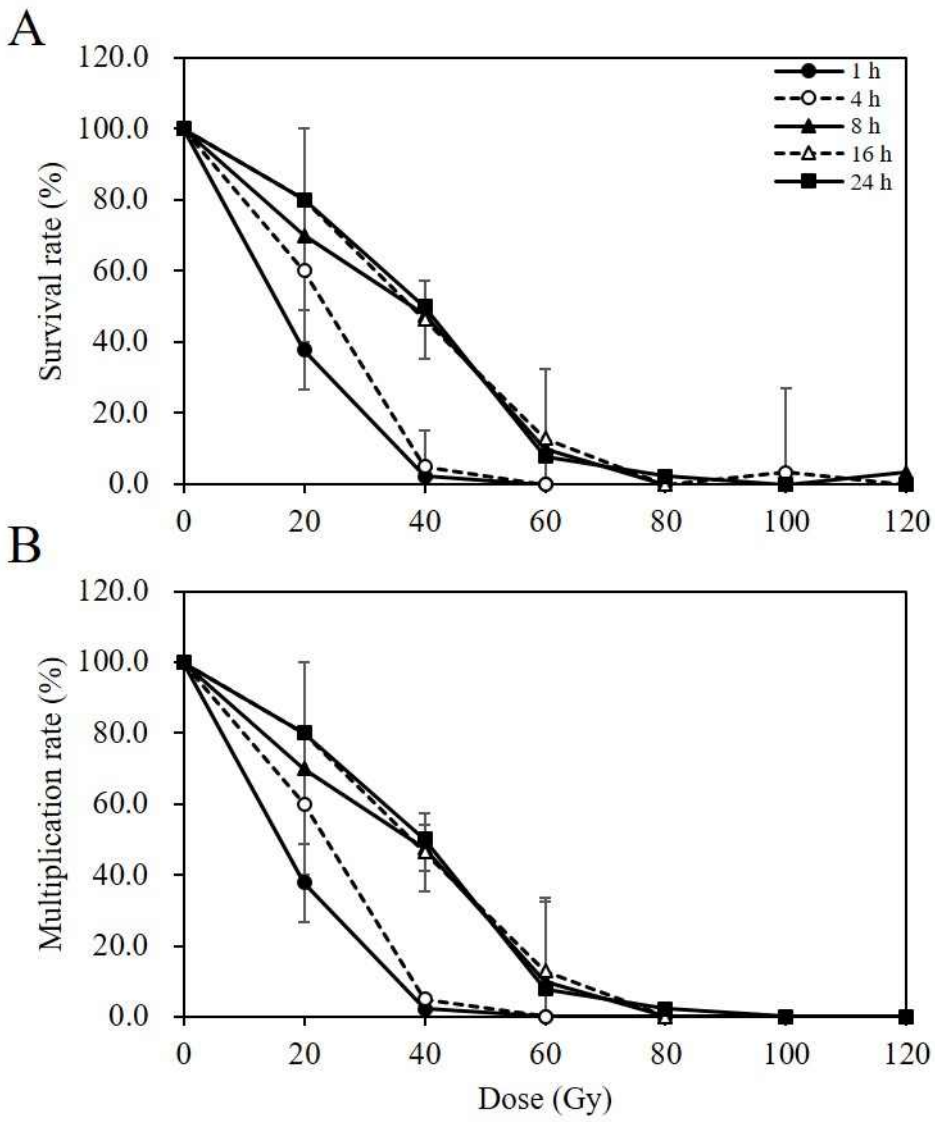

Figure I-2. Survival and multiplication rates of *Cymbidium* hybrid RB001 PLBs at 6 months after γ-irradiation. A, survival rate of PLBs; B, multiplication rate of PLBs. Error bars indicate the standard error of the mean (n = 10, biological replicates).

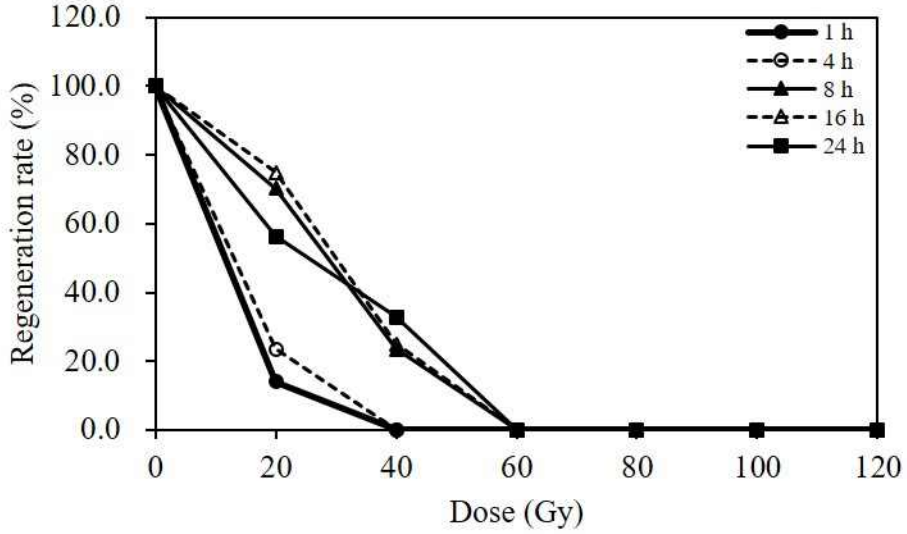

Figure I-3. Regeneration rate of *Cymbidium* hybrid RB001 PLBs at 9 months after γ-irradiation.

Estimated 50% lethal dose (LD_{50}) and 50% reduction dose (RD_{50})

At 3 months after the γ-irradiation of PLBs, the LD_{50} values estimated for the analyzed irradiation durations were 17.3 Gy (irradiation for 1 h), 27.3 Gy (4 h), 41.2 Gy (8 h), 38.1 Gy (16 h), and 42.9 Gy (24 h). The estimated RD_{50} values based on the multiplication rate were 15.0 Gy (irradiation for 1h), 24.5 Gy (4 h), 35.6 Gy (8 h), 33.8 Gy (16 h), and 37.2 Gy (24 h) (Figure I-4A). An analysis of the irradiation durations from 1 to 8 h revealed the estimated LD_{50} and RD_{50} values were significantly correlated with the irradiation duration based on the survival ($p < 0.01$) and multiplication ($p < 0.05$) rates (Figure 4A). However, the estimated LD_{50} and RD_{50} values based on the survival and multiplication rates differed a little because not all surviving PLBs multiplied. At 6 months after the γ-ray treatments of PLBs, the estimated LD_{50} values were 16.1 Gy (irradiation for 1 h), 23.6 Gy (4 h), 37.9 Gy (8 h), 37.9 Gy (16 h), and 40.0 Gy (24 h). The estimated RD_{50} values for each irradiation duration were as follows: 1 h, 16.1 Gy (based on the multiplication rate at 6 months) and 11.6 Gy (based on the regeneration rate at 9 months); 4 h, 23.6 Gy (multiplication rate) and 13.1 Gy (regeneration rate); 8 h, 37.9 Gy (multiplication rate) and 27.6 Gy (regeneration rate); 16 h, 37.9 Gy (multiplication rate) and 28.9 Gy (regeneration rate); and 24 h, 40.0 Gy (multiplication rate) and 27.8 Gy (regeneration rate) (Figure I-4B). An examination of the irradiation duration from 1 to 8 h indicated the estimated

LD_{50} and RD_{50} values were correlated with the irradiation duration based on the survival, multiplication, and regeneration rates; however, this correlation was not significant (Figure I-4B). Additionally, the estimated LD_{50} and RD_{50} values based on the survival and multiplication rates overlapped because all of the γ-irradiated PLBs were stable.

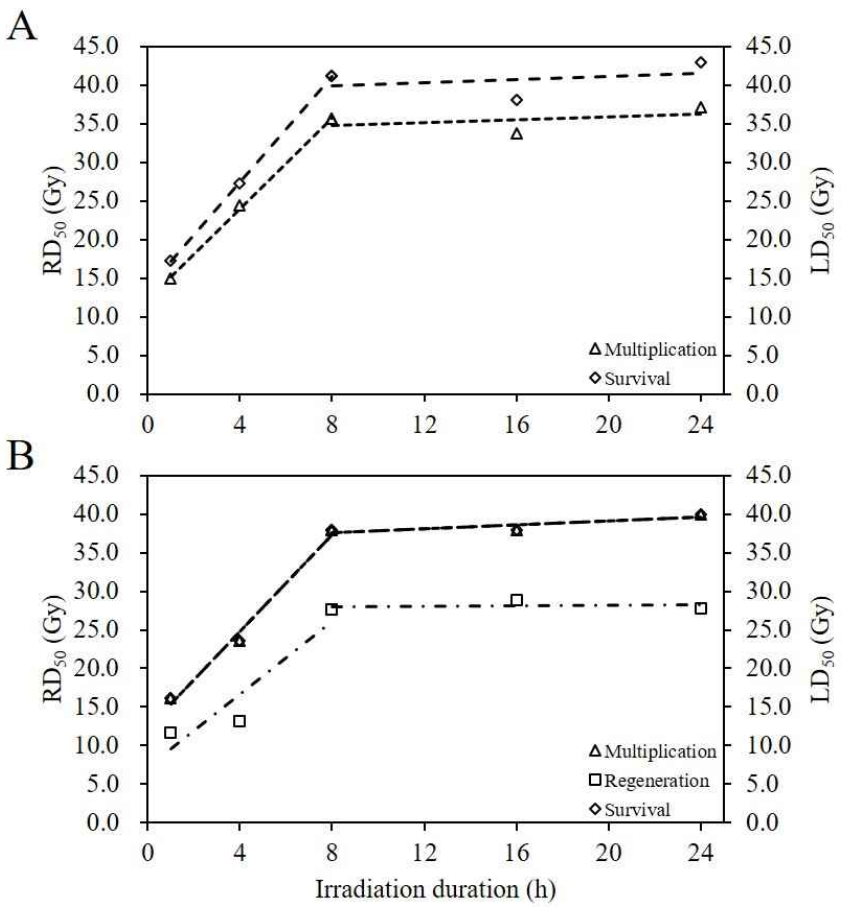

Figure I-4. Comparison of the LD_{50} and RD_{50} of *Cymbidium* hybrid RB001 PLBs at 3, 6, and 9 months after γ-irradiation. A, LD_{50} and RD_{50} at 3 months after γ-irradiation; B, LD_{50} and RD_{50} at 6 and 9 months after γ-irradiation. Linear regressions were separately analyzed for two irradiation duration ranges (1 to 8 h and 8 to 24 h). A: survival rate, y = 3.418x + 13.791, r = 0.999** (1 to 8 h) and y = 0.106x + 39.033, r = 0.349 (8 to 24 h); and multiplication rate, y = 2.934x + 12.320, r = 0.999* (1 to 8 h) and y = 0.1x + 33.933, r = 0.470 (8 to 24 h). B: survival rate, y = 3.139x + 12.264, r = 0.995 (1 to 8 h) and y = 0.131x + 36.5, r = 0.886 (8 to 24 h); multiplication rate, y = 3.139x + 12.264, r = 0.995 (1 to 8 h) and y = 0.131x + 36.5, r = 0.866 (8 to 24 h); and regeneration rate, y = 2.358x + 7.215, r = 0.937 (1 to 8 h) and y = 0.013x + 27.9, r = 0.143 (8 to 24 h). * and ** represent significant differences at the 95% and 99% levels, respectively.

Evaluation of heterozygosity, natural variation, and induced SNPs

A GBS library was constructed for 36 samples [i.e., six control samples and six samples for each of the five γ-irradiation treatments, which exhibited similar growth responses (LD_{50}) to γ-irradiation]. The sequencing results, construction of the reference sequence, and the genome complexity are summarized in Table 2. A total of 187,443,640 clusters comprising 23,354 Mbp nucleotides were produced and then trimmed to 154,665,489 clusters. The *Cymbidium* hybrid RB001 reference sequence (70 Mbp) was *de novo* assembled with 590,047 catalogs trimmed to 120 bp and then analyzed regarding heterozygosity, natural variation, and induced SNPs. The heterozygosity rate was estimated as 2.395 kbp^{-1}, whereas the natural variation rate was 0.222 kbp^{-1} (transition and transversion were 0.091 and 0.131, respectively). Genome complexity was calculated based on the sequence information for the six control samples. The induced mutations among five γ-irradiated populations were compared according to the SNPs detected by the GBS analysis. On the basis of all γ-irradiated populations, 20.02 SNPs Mbp^{-1} were detected (transition, 7.06 Mbp^{-1}; transversion, 12.98 Mbp^{-1}) (Figure I-5). A similar SNP rate was calculated for all five γ-irradiated populations: 20 Gy/1 h, 20.5 SNPs Mbp^{-1} (transition, 7.5; transversion, 13.0); 30 Gy/4 h, 20.9 SNPs Mbp^{-1} (transition, 7.1;

transversion, 13.8); 40 Gy/8 h, 20.3 SNPs Mbp^{-1} (transition, 6.5; transversion, 13.8); 40 Gy/16 h, 19.8 SNPs Mbp^{-1} (transition, 7.4; transversion, 12.4); and 40 Gy/24 h, 18.6 SNPs Mbp^{-1} (transition, 6.8; transversion, 11.9). Moreover, the transversion rate was higher than the transition rate for all γ-irradiated populations (Figure I-5).

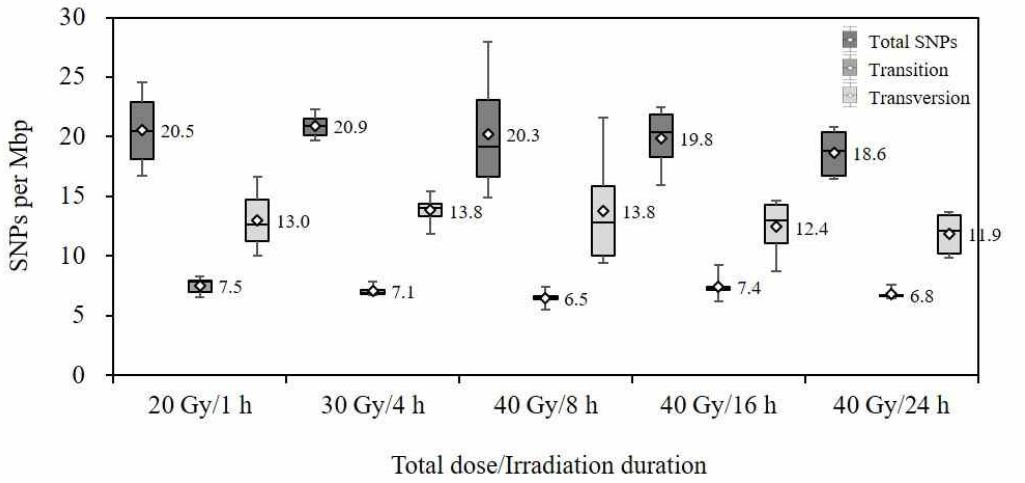

Figure I-5. Comparison of the induced SNPs among five γ-irradiated *Cymbidium* hybrid RB001 populations based on a *de novo* genotyping-by-sequencing analysis.

DISCUSSION

Effects of the total dose and irradiation duration on PLB growth responses

Determining the optimal irradiation conditions for inducing desirable mutations, while minimizing other DNA damages, is a crucial part of plant mutation breeding. The total dose is an important factor for inducing mutations in diverse plant species and has been used for determining optimal irradiation conditions, although there is some variability in the suggested doses reported by different researchers [e.g., Yamaguchi et al. 2009 (LD_{10}); Kodym et al. 2012 ($LD_{30–50}$ and $RD_{30–50}$); and Lee et al. 2016b (RD_{50})]. However, the dose rate and irradiation duration are also crucial factors for inducing mutations. Unfortunately, researchers and breeders have generally not focused on these factors. Studies on the dose rate were mainly conducted in the mid-1960s and mid-1970s (Mabuchi and Matsumura 1964; Nishiyama et al. 1966; Dewey 1969; Killion et al. 1971; Bottino et al. 1975). Nishiyama et al. (1966) and Mabuchi and Matsumura (1964) suggested that higher dose rates induce mutations more effectively than lower dose rates in oat and maize, even if the total dose is the same. Conversely, Natarajan and Maric (1961) indicated that mutations are induced more effectively at a low dose rate than at a high dose rate in barley and maize. In contrast, in a

study of chrysanthemum, Yamaguchi et al. (2008) revealed that the mutation frequency is dependent on the total dose, not the dose rate, although the DNA contents are affected by both the total γ-ray dose and dose rate. These contradictory results regarding the effects of the dose rate may be confusing for researchers interested in mutation induction.

To the best of our knowledge, there are no published reports describing the relationship between the total dose and irradiation duration (or dose rate) in orchids, especially *Cymbidium* species. Regarding germinating barley seeds, Bottino et al. (1975) reported that at a dose rate lower than 15 Gy h^{-1}, increases in the dose rate (and decreases in the irradiation duration) caused the total dose required to induce a specific growth inhibition level to decrease (i.e., increased effectiveness). Additionally, a linear relationship on a double logarithmic plot was observed in the dose rate range of 0.3–15 Gy h^{-1} (irradiation duration of 0.03–0.3 h). Additional increases in the dose rate resulted in an increase in the total dose required for a specific growth inhibition level (i.e., decreased effectiveness). Moreover, this change in effectiveness occurred at 0.3–0.4 h, which was within the time required for one mitotic cycle (11.5 h). Thus, this change in effectiveness may depend on chromosome size, DNA contents, or mitotic cycle time, which vary among species. The correlation between the total dose and irradiation duration was previously proposed by Kim et al. (2016). They

reported that a specific irradiation duration may be effective for inducing mutations in chrysanthemum. In the current study, another change in effectiveness was detected at the 8 h time-point (Figure I-4). At irradiation durations shorter than 8 h, increases in the irradiation duration (and decreases in the dose rate) resulted in increases in the LD_{50} and RD_{50} values based on the survival, multiplication, and regeneration rates of PLBs (i.e., decreased effectiveness). Additionally, at irradiation durations longer than 8 h, increases in the irradiation duration (and decreases in the dose rate) were associated with slight increases or no changes to the above-mentioned LD_{50} and RD_{50} values (i.e., decreased or unaffected effectiveness) (Figure I-4).

The repair mechanism is responsible for minimizing the effects of a long-term radiation treatment. Moreover, radiation-induced damages are repaired primarily in the S phase of the DNA replication cycle during the interphase of the cell cycle (Kodym et al. 2012). A radiobiological hypothesis has been proposed that the dose per cell cycle determines the extent of radiation effects in dividing cells continuously exposed to radiation. This hypothesis implies that a shorter cell cycle or a longer irradiation duration decreases the effects of a treatment dose (Kodym et al. 2012). Our LD_{50} and RD_{50} response curves (Figure I-4) are consistent with the suggested hypothesis. Furthermore, 8 h may represent the reference time for the *Cymbidium* hybrid RB001 cell cycle.

Optimal γ-irradiation for inducing mutations

Kodym et al. (2012) suggested that the effects of radiation on seedling height should be assessed when the first true leaves of the control are fully grown, whereas the survival rate of the radiation-treated plants should be calculated at maturity. However, in the current study, I focused on the growth responses of PLBs (i.e., vegetative tissues). Therefore, it may be appropriate to determine the sensitivity of PLBs to radiation after the growth responses of γ-irradiated PLBs have stabilized. Thus, it may be better to assess the effects of a γ-irradiation at 6 months rather than at 3 months after the treatment because at 3 months, several PLBs irradiated at high doses (> 60 Gy) are alive, but are not multiplying. Of the three growth parameters used to evaluate the γ-irradiated PLBs, the survival rate were used to calculate the following optimal doses (LD_{50}): 1 h, 16.1 Gy; 4 h, 23.6 Gy; 8 h, 37.9 Gy; 16 h, 37.9 Gy; and 24 h, 40.0 Gy (Figure I-4B). As mentioned above, there are inconsistencies regarding the reported effects of the dose rate on mutation induction. Additionally, it may be easier to determine the optimal condition for inducing mutations by adjusting the irradiation duration rather than the dose rate. Therefore, the effects of irradiation duration should be clarified.

Genome complexity and induced SNPs

Comparing the mutation frequency with the phenotype is a convenient way to analyze the effects of irradiation duration. However, I analyzed the induced SNPs in plants regenerated from the γ-irradiated PLBs to more accurately compare the five γ-irradiated populations with similar growth responses (LD_{50}) to γ-rays (Figure I-5). Previous investigations indicated that *Cymbidium* species have a relatively large genome comprising 3.05 Gb [based on *Cymbidium sinense* (Jacks.); Jones et al. 1998] or 4.10 Gb [based on four *Cymbidium* species; Leitch et al. 2009]. In contrast, the genome of *Phalaenopsis equestris* was estimated to consist of 1.16 Gb, with a heterozygosity of about 0.4% (Cai et al. 2015). Yan et al. (2015) reported that the *Dendrobium officinale* genome comprises 1.35 Gb, with a heterozygosity of about 0.48%. The genomes of *A. thaliana* and rice (i.e., model plant species) comprise 157 and 466 Mb, respectively (Yu et al. 2002; Bennett et al. 2003). These results confirm that orchids have a large and complex genome, with the genome of *Cymbidium* species approximately 20-fold larger than that of *A. thaliana*. The heterozygosity of *Cymbidium* hybrid RB001 was calculated as 0.24%, but this may be an underestimation because of the size of the genome and the limited information derived from the *de novo* GBS analysis. Lee et al. (2016a) completed a whole-genome re-sequencing of a soybean mutant exposed to γ-rays, and estimated a

SNP rate of 342 SNPs Mbp^{-1} (1 per 2,925 bp), with 67.5% of all SNPs identified as transitions. In another study, a SNP rate of 365 SNPs Mbp^{-1} (1 per 2,736 bp) was calculated following a whole-genome re-sequencing of a γ-irradiated early-maturing rice mutant, and transitions were 2-times more abundant than transversions (Hwang et al. 2014). On the basis of a whole-genome re-sequencing experiment, Shirasawa et al. (2016) estimated SNP rates of 0.125 SNPs Mbp^{-1} (1 per 8 Mbp) and 1.25 SNPs Mbp^{-1} (1 per 0.8 Mbp) for tomato (cv. Micro-Tom) mutants treated with γ-rays and ethyl methanesulfonate, respectively, with transition-to-transversion ratios of 0.9 and 2.9, respectively. In the current study, the estimated SNP and transversion rates induced by γ-irradiation in *Cymbidium* hybrid RB001 were greater than those of rice and soybean, but not of tomato. These differences may be due to the diversity in the genome size, repair mechanisms, and other characteristics that vary among plant species. Moreover, the analysis may have been limited by the restricted genome coverage of the assembled reference sequence. Additionally, I did not detect a significant difference among the induced SNPs of five γ-irradiated populations, although two populations (20 Gy/1 h and 30 Gy/4 h) were exposed to radiation levels that exceeded the LD_{50}. These results indicate that irradiations over a short period may induce mutations that are similar to those induced by a longer irradiation period. Furthermore, the information presented herein regarding the correlation

between the total dose and the irradiation duration and the suggested optimal dose may be relevant for the mutation breeding of orchid species, including *Cymbidium* species.

REFERENCES

Bennett MD, Leitch IJ, Price HJ, Johnston S. 2003. Comparison with *Caenorhabditis* (~100 Mb) and Drosophila (~175 Mb) using flow cytometry show genome size in Arabidopsis to be ~157 Mb and thus ~25 % larger than the Arabidopsis genome initiative estimate of ~125 Mb. Ann Bot. 91:547–557.

Bolger AM, Lohse M, Usadel B. 2014. Trimmomatic: a flexible trimmer for Illumina sequence data. Bioinformatics 30:2114–2120.

Bottino PJ, Sparrow AH, Schwemmer SS, Thompson KH. 1975. Interrelation of exposure and exposure rate in germinaing seeds of barley and its concurrence with dose-rate theory. Radiat Bot. 15:17–27.

Cai J, Liu X, Vanneste K, Proost S, Tsai WC, Liu KW, Chen LJ, He Y, Xu Q, Bian C, et al. 2015. The genome sequence of the orchid *Phalaenopsis equestris*. Nat Genet. 47:65–72.

Catchen J, Hohenlohe PA, Bassham S, Amores A, Cresko WA. 2013. Stacks: an analysis tool set for population genomics. Mol Ecol. 22:3124–3140.

Chase MW, Cameron KM, Freudenstein JV, Pridgeon AM, Salazar G, van den Berg C, Schuiteman, A. 2015. An updated classification of Orchidaceae. Bot J Linn Soc. 177:151–174.

Chin DP, Mishiba K, Mii M. 2007. *Agrobacterium*-mediated transformation of protocorm-like bodies in *Cymbidium*. Plant Cell Rep. 26:735–743.

Choi SH, Kim MJ, Lee JS, Ryu KH. 2006. Genetic diversity and phylogenetic relationships among and within species of oriental cymbidiums based on RAPD analysis. Sci Hortic. 108:79–85.

Cui T, Luo S, Du Y, Yu L, Yang J, Li W, Chen X, Li X, Wang J, Zhou L. 2019. Research of photosynthesis and genomewide resequencing on a yellow-leaf *Lotus japonicus* mutant induced by carbon ion beam irradiation. Grassl Sci. 65:41–48.

Dewey DL. 1969. An oxygen-dependent X-ray dose-rate effect in *Serratia*

marcescens. Radiat Res. 38:467–474.

Elshire RJ, Glaubitz JC, Sun Q, Poland JA, Kawamoto K, Buckler ES, Mitchell SE. 2011. A robust, simple genotyping-by-sequencing (GBS) approach for high diversity species. PLoS ONE 6:e19379.

Hase Y, Satoh K, Kitamura S, Oono Y. 2018. Physiological status of plant tissue affects the frequency and types of mutations induced by carbon-ion irradiation in Arabidopsis. Sci Rep. 8:1394.

Hwang SG, Hwang JG, Kim DS, Jang CS. 2014. Genome-wide DNA polymorphism and transcriptome analysis of an early-maturing rice mutant. Genetica 142:73–85.

[IAEA] International Atomic Energy Agency. 2019. IAEA Mutant Variety Database [Dataset]. The joint FAO/IAEA Mutant Variety Database; [accessed 2019]. https://mvd.iaea.org/#!Home.

Jones WE, Kuehnle AR, Arumuganathan K. 1998. Nuclear DNA content of 26 orchid (*Orchidaceae*) genera with emphasis on *Dendrobium*. Ann Bot. 82:189–194.

Killion DD, Constantin MJ. 1971. Acute gamma irradiation of the wheat plant: effects of exposure, exposure rate, and developmental stage on survival, height, and grain yield. Radiat Bot. 11:367–373.

Killion DD, Constantin MJ, Siemer EG. 1971. Acute gamma irradiation of the soybean plant: effects of exposure, exposure rate, and developmental stage on growth and yield. Radiat Bot. 11:225–232.

Kim YS, Sung SY, Jo YD, Lee HJ, Kim SH. 2016. Effects of gamma ray dose rate and sucrose treatment on mutation induction in chrysanthemum. Eur J Hortic Sci. 81:212–218.

Kodym A, Afza R, Forster BP, Ukai Y, Nakagawa H, Mba C. 2012. Methodology for physical and chemical mutagenic treatments. In: Shu QY, Forster BP, Nakagawa H, editors. Plant Mutation Breeding and Biotechnology. Wallingford: CAB International; Rome: FAO; p. 123–134.

Lee KJ, Kim DS, Kim JB, Jo SH, Kang SY, Choi HI, Ha BK. 2016a. Identification of candidate genes for an early-maturing soybean mutant by genome resequencing analysis. Mol Gen Genom. 291:1561–1571.

Lee YM, Lee HJ, Kim YS, Kang SY, Kim DS, Kim JB, Ahn JW, Ha BK, Kim

SH. 2016b. Evaluation of the sensitivity to ionizing γ-radiation of a *Cymbidium* hybrid. J Hortic Sci Biotechnol. 91:109–116.

Leitch IJ, Kahandawala I, Suda J, Hanson L, Ingrouille MJ, Chase MW, Fay MF. 2009. Genome size diversity in orchids: consequences and evolution. Ann Bot. 104:469–481.

Mabuchi T, Matsumura S. 1964. Dose rate dependence of mutation rates from γ-irradiated pollen grains of maize. Jpn J Genet. 39:131–135.

Narum SR, Buerkle CA, Davey JW, Miller MR, Hohenlohe PA. 2013. Genotyping-by-sequencing in ecological and conservation genomics. Mol Ecol. 22:2841–2847.

Nishiyama I, Ikushima T, Ichikawa S. 1966. Radiological studies in plants–XI: Further studies on somatic mutations induced by X-rays at the *al* locus of diploid oats. Radiat Bot. 6:211–218.

Ryu J, Kim WJ, Im J, Kang KW, Kim SH, Jo YD, Kang SY, Lee JH, Ha BK. 2019. Single nucleotide polymorphism (SNP) discovery through genotyping-by-sequencing (GBS) and genetic characterization of *Dendrobium* mutants and cultivars. Sci Hortic. 244:225–233.

Sarmah D, Kolukunde S, Sutradhar M, Singh BK, Mandal T, Mandal N. 2017. A review on: *In vitro* cloning of orchids. Int J Curr Microbiol Appl Sci. 6:1909–1927.

Shirasawa K, Hirakawa H, Nunome T, Tabata S, Isobe S. 2016. Genome-wide survey of artificial mutations induced by ethyl methanesulfonate and gamma rays in tomato. Plant Biotechnol J. 14:51–60.

Tsai WC, Dievart A, Hsu CC, Hsiao TT, Chiou SY, Huang H, Chen HH. 2017. Post genomics era for orchid research. Bot Stud. 58:61.

Uitdewilligen JGAML, Wolters AMA, D'hoop BB, Borm TJA, Visser RGF, van Eck HJ. 2013. A next-generation sequencing method for genotyping-by-sequencing of highly heterozygous autotetraploid potato. PLoS ONE 8:e62355.

Yamaguchi H, Hase Y, Tanaka A, Shikazono N, Degi K, Shimizu A, Morishita T. 2009. Mutagenic effects of ion beam irradiation on rice. Breed Sci. 59:169–177.

Yamaguchi H, Shimizu A, Degi K, Morishita T. 2008. Effects of dose and dose

rate of gamma ray irradiation on mutation induction and nuclear DNA content in chrysanthemum. Breed Sci. 58:331–335.

Yan L, Wang X, Liu H, Tian Y, Lian J, Yang R, Hao S, Wang X, Yang S, Li Q, et al. 2015. The genome of *Dendrobium officinale* illuminates the biology of the important traditional Chinese orchid herb. Mol Plant 8:922–934.

Yu J, Hu S, Wang J, Wong GKS, Li S, Liu B, Deng Y, Dai L, Zhou Y, Zhang X, et al. 2002. A draft sequence of the rice genome (*Oryza sativa* L. ssp. *indica*). Science 296:79–92.

CHAPTER II

Frequency, spectrum, and stability of leaf mutants induced by diverse γ-ray treatments in two *Cymbidium* hybrids

This research has been submitted in *Breeding Science*.

ABSTRACT

Ionizing radiation combined with *in vitro* tissue culture has been used for development of new cultivars in diverse crops. The effects of ionizing radiation on mutation induction have been analyzed on several orchid species, including *Cymbidium*. Limited information is available on the comparison of mutation frequency and spectrum based on phenotypes in *Cymbidium* species. In addition, the stability of induced chimera mutants in *Cymbidium* is unknown. In this study, I analyzed the radiation-sensitivity, mutation frequency, and spectrum of mutants induced by diverse γ-ray treatments, and analyzed the stability of induced chimera mutants in the *Cymbidium* hybrid cultivars 'RB003' and 'RB012'. The optimal γ-irradiation conditions of each cultivar differed as follows: RB003, mutation frequency of 4.06% (under 35 Gy/4 h); RB012, 1.51% (20 Gy/1 h). Re-irradiation of γ-rays broadened the mutation spectrum observed in RB012. The stability of leaf-color chimera mutants was higher than that of leaf-shape chimeras, and stability was dependent on the chimera type and location of a mutation in the cell layers of the shoot apical meristem. These results indicated that short-term γ-irradiation was more effective to induce mutations in *Cymbidium*. Information on the stability of chimera mutants will be useful for mutation breeding of diverse ornamental plants.

INTRODUCTION

The Orchidaceae is among the largest families of angiosperms, and is composed of approximately 736 genera and about 28,000 species (Chase et al. 2015). Among the diverse genera in the family, *Dendrobium*, *Phalaenopsis*, *Oncidium*, and *Cymbidium* are important floricultural crops in Asian countries (Sarmah et al. 2017). In particular, *Cymbidium* is economically important in northeastern Asia, including Korea, China, and Japan (Choi et al. 2006). *Cymbidium* species are conveniently divided into two groups on the basis of the native habitat and climate region, i.e., temperate and subtropical or tropical regions (Kang et al. 2009, Ryu et al. 2013). There is continuous demand for development of new *Cymbidium* cultivars on account of the attractiveness of the foliage as well as the flower colors and fragrance. To date, many *Cymbidium* cultivars have been developed via natural selection or artificial cross-breeding, although transformation has also been applied in *Cymbidium* breeding (Chin et al. 2007). However, development of a new *Cymbidium* cultivar by means of cross-breeding is time-consuming because of the long vegetative growth stage.

Mutation breeding techniques using physical mutagens (e.g., γ-rays, X-rays, and ions) or chemical mutagens (e.g., ethyl methanesulfonate, *N*-nitroso-*N*-

methylurea, and colchicine) have been widely used to develop mutant cultivars in diverse plant species, including food and ornamental crops. In 226 plant species, 3,308 mutants, including two *Cymbidium* mutants, that were predominantly (approximately 77.5%) developed using physical mutagens have been registered in the Mutant Variety Database of the joint Food and Agriculture Organization of the United Nations/International Atomic Energy Agency (IAEA 2019). Among the diverse ornamental plants registered on the database, the most numerous mutants are those of chrysanthemum (*Chrysanthemum* spp., 274 mutants) followed by rose (*Rosa* spp., 67 mutants), dahlia (*Dahlia* spp., 36 mutants), alstroemeria (*Alstroemeria* spp., 35 mutants), streptocarpus (*Streptocarpus* spp., 30 mutants), and carnation (*Dianthus caryophyllus*, 28 mutants) (IAEA 2019). The combination of treatment with a physical mutagen and *in vitro* tissue culture has been used to shorten the breeding period of orchids (Luan et al. 2012, Lee et al. 2016). Thus, integration of γ-irradiation and *in vitro* tissue culture may be an efficient procedure for development of mutant cultivars in *Cymbidium*.

The treatment of seeds, buds (tip/node cuttings), callus, and rhizomes with a mutagen induces chimeras in M_1 plants, because mutations are induced in individual cells and regenerated shoots are recovered from pre-existing multicellular meristems (Geier 2012). In seed-propagated plants, the induced

chimera is commonly dissociated by selfing of M_1 plants, whereas, in vegetatively propagated plants chimera dissociation by selfing is of limited use because selfing results in loss of the desirable original characters. Geier (2012) suggests that plant regeneration via adventitious buds or somatic embryos, which permits the genetic background to be retained, may be useful to dissociate the chimera in vegetatively propagated plants. In the majority of angiosperms, the shoot apical meristem (SAM) is composed of three layers: the outer meristem layer (L1), the second meristem layer (L2), and the inner corpus (L3) (Filippis et al. 2013, Frank and Chitwood 2016). Mutagen-treated plants are composed of heterogeneous cells in the three layers, which can be categorized into three chimera types: sectorial chimeras, which have an unstable heterogenomic population of cells traversing more than one layer of the SAM; mericlinal chimeras, which have an unstable heterogenomic population of cells within a single layer of the SAM; and periclinal chimeras, which have a stable, uniform, and genetically distinguished layer of cells of the SAM (Geier 2012, Frank and Chitwood 2016). The phenotypes of mutants are diverse according to the type and extent of these chimeras. Thus, an understanding of chimerism is necessary to develop a new *Cymbidium* mutant cultivar by mutagenesis.

In the present study, I evaluated the optimal γ-ray dose to induce mutations in *Cymbidium*, and compared the mutation frequency and spectrum of

leaf mutants induced by diverse γ-ray treatments. In addition, I investigated the stability of chimera mutants using plants secondarily regenerated from selected rhizomes and the primary regenerated mutant plant.

MATERIALS AND METHODS

Plant materials

Two *Cymbidium* hybrid (*C. sinense* × *C. goeringii*) cultivars, 'RB003' and 'RB012', were used in this study. Rhizomes of the two cultivars were cultured at 24 ± 1 °C under a 16-h photoperiod provided by white fluorescent light (photosynthetic photon flux density = 50 μmol m^{-2} s^{-1}) on medium (pH 5.35) comprising 0.2% Hyponex (N:P:K = 6.5:6:19; Hyponex Japan Co., Ltd., Osaka, Japan), 0.1% Hyponex (N:P:K = 20:20:20), 3% sucrose (Duchefa B.V., Haarlem, The Netherlands), 0.3% peptone (Duchefa B.V.), 0.075% activated charcoal (Sigma-Aldrich, St Louis, MO, USA), and 0.38% plant agar (Duchefa B.V.).

Optimal γ-ray dose determination

Rhizomes of the two cultivars were irradiated with six doses of γ-rays (0, 20, 40, 60, 80, or 100 Gy) emitted from a ^{60}Co source (150 TBq capacity; AECL, Canada) for 24 h at the Korea Atomic Energy Research Institute, Jeongeup, Korea. The γ-irradiated rhizomes were immediately transferred to fresh culture medium. The growth of γ-irradiated rhizomes was evaluated based on four

growth parameters. Relative weight, survival, and multiplication rate of rhizomes were measured at 3 and 6 months after irradiation, whereas the relative regeneration rate was analyzed at 9 months. The γ-irradiated rhizomes were subcultured at 3-month intervals. The experiments were performed with five biological replicates, with seven rhizomes per replicate.

Mutant population construction

Mutant populations of the two cultivars were constructed using diverse γ-irradiation conditions as follows: RB003, irradiation conditions of 50 Gy/24 h, 50 Gy/16 h, 50 Gy/8 h, 35 Gy/4 h, and 25 Gy/1 h; RB012, irradiation conditions of 40 Gy/24 h, 40 Gy/16 h, 40 Gy/8 h, 30 Gy/4 h, 20 Gy/1 h, 30 Gy/24 h, and 30-30 Gy/24 h [re-irradiation after mutant selection on the population treated with 30 Gy/ 24 h]. The experiments for each γ-irradiation condition were performed with about 40 and 50 culture bottles (seven rhizomes per culture bottle) for RB003 and RB012, respectively except the irradiation condition of 30–30 Gy/24 h on RB012, which was conducted with about 200 culture bottles.

Phenotype and stability analysis of leaf mutants

Phenotype analysis of the mutant populations derived from RB003 and RB012 was conducted at three time points until 10 and 12 months after γ-ray treatment, respectively. The stability of mutants was analyzed on newly regenerated plants from two selected mutant tissues: the primary mutant plant regenerated from γ-irradiated rhizomes and its closely attached about 1 cm-sized rhizome.

RESULTS

Effects of γ-irradiation on rhizome growth parameters

At 3 months after γ-irradiation, the relative weight of the γ-irradiated rhizomes of the cultivars RB003 and RB012 gradually decreased with increase in γ-ray dose. At 6 months after γ-irradiation, the responses of rhizomes to γ-irradiation were more distinct; rhizome growth was strongly inhibited at γ-ray doses of more than 60 and 40 Gy in RB003 and RB012, respectively (Figure II-1A). All γ-irradiated rhizomes of the two cultivars survived, including after 100 Gy treatment, at 3 and 6 months after irradiation (Figure II-1B). However, at 3 months after γ-irradiation the multiplication rate of the γ-irradiated rhizomes rapidly decreased at doses of more than 60 and 40 Gy in RB003 and RB012, respectively. In addition, at 6 months after γ-irradiation multiplication was not observed at doses of more than 80 Gy in the two cultivars (Figure II-1C). The γ-irradiated rhizomes were regenerated from about 8 months after irradiation in the two cultivars, although regeneration of the control was detected from 7 months after initial culture. Therefore, the relative regeneration rate of γ-irradiated populations was evaluated at 9 months after irradiation. The regeneration of

RB003 rhizomes decreased in a dose-dependent manner and strongly inhibited regeneration was observed at doses of more than 60 Gy. However, RB012 rhizomes irradiated with 20 Gy showed a higher rate of regeneration compared with that of the control, and at doses of exceeding 40 Gy regeneration was strongly suppressed (Figure II-1D).

Given that all γ-irradiated populations survived during the first 6 months after treatment, it was impossible to estimate the 50% lethal dose (LD_{50}) for the two cultivars (Figure II-1B). At 3 months after γ-irradiation of rhizomes, the 50% reduction dose (RD_{50}) for the two cultivars was estimated as follows: RB003, 30.0 Gy (based on the relative weight) and 58.2 Gy (based on the multiplication rate); and RB012, 29.0 Gy (based on the relative weight) and 33.5 Gy (based on the multiplication rate). At 6 months, the estimated RD_{50} for each cultivar was as follows: RB003, 34.4 Gy (based on the relative weight) and 52.5 Gy (based on the multiplication rate); and RB012, 30.6 Gy (based on the relative weight) and 44.1 Gy (based on the multiplication rate) (Figure II-1A, C). At 9 months, the RD_{50} based on the relative regeneration rates for each cultivar was 47.4 Gy and 34.4 Gy for RB003 and RB012, respectively (Figure II-1D).

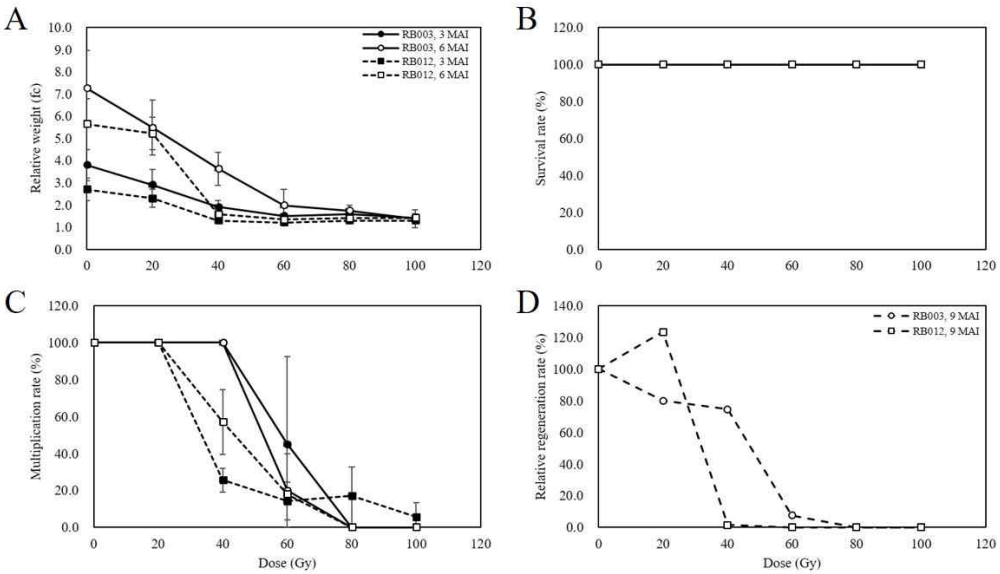

Figure II-1. Relative weight, survival, multiplication, and relative regeneration rate of *Cymbidium* hybrid 'RB003' and 'RB012' rhizomes at 3, 6, and 9 months after γ-irradiation. A, Relative weight of rhizomes; B, survival rate of rhizomes; C, multiplication rate of rhizomes; D, relative regeneration rate of rhizomes. fc, fold-change. MAI, months after irradiation. Error bars indicate the standard error of the mean (n = 5).

Comparison of mutation frequency and spectrum among γ-irradiated populations

A previous study revealed that the RD_{50} of protocorm-like bodies (PLBs) for γ-irradiation duration of 24 h was reduced with decrease in irradiation duration as follows: 40.0 Gy (for irradiation duration of 24 h), 37.9 Gy (16 and 8 h), 23.6 Gy (4 h), and 16.1 Gy (1 h) (Kim et al. 2019). Therefore, based on the RD_{50} values calculated from the multiplication and relative regeneration rates for an irradiation duration of 24 h, γ-irradiated populations of the two cultivars were constructed using suggested doses for each irradiation duration of 1, 4, 8, and 16 h. In addition, repeat irradiation (30–30 Gy/24 h) was conducted to identify the effect of re-irradiation of γ-rays on RB012 rhizomes (Table II-1).

Regeneration was reduced in γ-irradiated populations of the two cultivars; in particular, the treatments 40 Gy/16 h, 40 Gy/8 h, and 30 Gy/4 h applied to RB012 rhizomes induced severely decreased regeneration of γ-irradiated rhizomes. In addition, regeneration was reduced by 42.4% after re-irradiation (30–30 Gy/24 h) of the RB012 population initially γ-irradiated with 30 Gy/24 h (Table II-1). In the RB003 populations, the mutation frequency was elevated with increase in γ-ray dose rate as follows: 50 Gy/24 h, mutation rate of 0.35%; 50 Gy/16 h, 0.81%; and 50 Gy/8 h, 3.73%. In addition, the two populations γ-irradiated with 50 Gy/8 h and

35 Gy/4 h showed the same regeneration rate of 9.33% as well as similar mutation frequencies: 50 Gy/8 h, mutation rate of 3.73%; and 35 Gy/4 h, 4.06%. Under these irradiation conditions, the mutation frequency and spectrum were the highest observed among the γ-irradiated RB003 populations (Table II-1). In the RB012 populations, the regeneration rate decreased precipitously with increase in γ-ray dose rate as follows: 40 Gy/24 h, regeneration rate of 13.88%; 40 Gy/16 h, 5.45%; and 40 Gy/8 h, 0.33%. The two populations γ-irradiated with 40 Gy/24 h and 20 Gy/1 h showed similar regeneration rates (13.88% and 13.07%, respectively) as well as similar mutation frequencies: 40 Gy/24 h, mutation frequency of 1.42%; and 20 Gy/1 h, 1.51%. The highest mutation frequency observed was 3.24% in the irradiation condition 30 Gy/4 h; however, it is impossible to consider this is to be the optimal irradiation condition because of the severely reduced regeneration. The highest mutation spectrum was observed in the population γ-irradiated with 20 Gy/1 h, which also showed the second-highest mutation frequency of 1.51% (Table II-1). Compared with the RB012 population γ-irradiated with 30 Gy/24 h, the mutation spectrum of the re-irradiation (30–30 Gy/24 h) population was broader, although no difference in mutation frequency was observed (Table II-1). In the γ-irradiated populations of the two cultivars, diverse leaf-color or -shape mutants were observed and the proportion of leaf-color mutants was higher than that of leaf-shape mutants (Table II-1, Figure II-2).

Table II-1. Regeneration, mutation frequency, and spectrum of leaf mutants derived from diverse γ-ray treatments in the *Cymbidium* hybrids 'RB003' and 'RB012'

Total dose/ irradiation duration	No. of regenerants per cultured bottle	No. of mutants (%)	Description of mutants (No. of mutants)		Mutation spectrum
			Leaf color	Leaf shape	
RB003					
Control	16.25	–	–	–	–
50 Gy/24 h	7.49	1 (0.35)	Comb/yellow broad stripe (1)	–	1
50 Gy/16 h	9.11	3 (0.81)[a]	Comb (1), bright green/yellow large spot (1), yellow marginal stripe (1)	Wrinkle (1)	4
50 Gy/8 h	9.33	11 (3.73)	Bright green/yellow large spot (1), bright green (2), comb (3), comb/yellow broad stripe (1), bright green/comb (1),	Abnormal (2), dwarf (1), wrinkle (4)	8
35 Gy/4 h	9.33	14 (4.06)	Yellow marginal stripe (1), bright green (2), comb/yellow broad stripe (1), yellow marginal/narrow stripe (1), bright green/yellow large spot (3)	Wrinkle (5), dwarf (1)	7
25 Gy/1 h	10.25	7 (2.13)	Bright green/comb (2), bright green/yellow large spot (2), yellow marginal stripe (1)	Abnormal (2)	4

[a] A mutant showing more than two characteristics was counted as only one.

Table II-1. Continued.

Total dose/ irradiation duration	No. of regenerants per cultured bottle	No. of mutants (%)	Description of mutants (No. of mutants)		Mutation spectrum
			Leaf color	Leaf shape	
RB012					
Control	50.00	–	–	–	–
40 Gy/24 h	13.88	9 (1.42)	Yellow narrow stripe (1), yellow large spot (4), snakeskin (2), yellow marginal stripe (2),	–	4
40 Gy/16 h	5.45	1 (0.23)	Yellow marginal stripe (1)	–	1
40 Gy/8 h	0.33	–	–	–	–
30 Gy/4 h	1.96	3 (3.24)	Yellow marginal stripe (2), yellow large spot (1)	–	2
20 Gy/1 h	13.07	10 (1.51)	Yellow marginal stripe (2), yellow large spot (3), bright green (1), snakeskin (2), yellow narrow stripe (1), yellow broad stripe (1)	–	6
30 Gy/24 h	21.41	4 (0.68)	Yellow large spot (1), yellow marginal stripe (2)	Abnormal (1)	3
30–30 Gy/ 24 h	12.33	21 (0.67)	Yellow narrow stripe (1), yellow marginal stripe (6), yellow broad stripe (3), bright green (1), yellow large spot (5), snakeskin (1),	Wrinkle (1), dwarf (1), abnormal (2)	9

Figure II-2. Diverse leaf-color or -shape mutants derived from *Cymbidium* hybrids 'RB003' and 'RB012'. A, RB003 control; B, leaf mutants derived from RB003; C, RB012 control; D, leaf mutants derived from RB012. Scale bar: 1 cm.

Evaluation of stability among leaf mutants

A total of 101 leaf-color or -shape mutants (52 mutants derived from RB003 and 49 from RB012) were tested to analyze the stability of the induced chimera mutants (Table II-2). The chimera stability of the first selected mutant plant induced by regeneration of γ-irradiated rhizomes was higher than that of the rhizome closely attached to the mutant plant: RB003, plant (43.4%), rhizome (33.3%); and RB012, plant (33.3%), rhizome (18.6%). The leaf-color mutants were observed to be relatively stable chimera types, but the leaf-shape mutants were unstable in the two cultivars. The most stable chimera type was the yellow marginal stripe types, which showed stability of 50.0% (from the rhizome) and 83.3% (from the plant) (estimated to be a periclinal chimera, a mutation of the L2 layer of the SAM), followed by yellow broad stripe types with stability of 50.0% (rhizome) and 66.6% (plant) (estimated to be a periclinal chimera, a mutation of the L3 layer of the SAM), yellow narrow stripe types with 25.5% (rhizome) and 100% (plant) (estimated to be a mericlinal chimera, a mutation of the L3 layer), bright green types with 25.0% (rhizome) and 50.0% (plant) (estimated to be a sectorial chimera, a mutation of the L2 and L3 layers), yellow large spot types with 12.5% (rhizome) and 12.5% (plant), and comb types with 0% (rhizome) and 33.3% (plant) (estimated to be a mericlinal chimera, a mutation of the L3 layer) (Table II-2). In the case of the selected mutant RB012-S17, the

phenotype of the first selected mutant plant induced by regeneration of γ-irradiated rhizomes with 40 Gy/24 h was of the yellow narrow stripe type; however, newly regenerated *in vitro* plants from the rhizome closely attached to the mutant plant segregated in the M_1V_1 generation, and the yellow broad stripe type ultimately selected was stabilized in the M_1V_5 generation (Figure II-3).

Table II-2. Stability of leaf mutants induced by γ-irradiation in the *Cymbidium* hybrid 'RB003' and 'RB012' populations

Characteristic	No. of mutants	Stability (%)	
		Rhizome[a]	Plant[b]
RB003			
Yellow marginal stripe, color	3	–	3/3 (100.0)
Yellow broad stripe, color	3	–	1/2 (50.0)
Yellow narrow stripe, color	1	–	1/1 (100.0)
Bright green, color	15	2(2[c])/6 (33.3)	3/6 (50.0)
Yellow large spot, color	7	2/2 (100.0)	1/2 (50.0)
Comb, color	7	0/1 (0.0)	1/3 (33.3)
Dwarf, shape	2	–	–
Wrinkle, shape	10	0/3 (0.0)	0/5 (0.0)
Abnormal, shape	4	–	0/1 (0.0)
Total	52	4(2)/12 (33.3)	10/23 (43.4)
RB012			
Yellow marginal stripe, color	14	5(2)/10 (50.0)	2/3 (66.7)
Yellow broad stripe, color	4	2(1)/4 (50.0)	1/1 (100.0)
Yellow narrow stripe, color	4	1(2)/4 (25.0)	2/2 (100.0)
Bright green, color	2	0/2 (0.0)	–
Yellow large spot, color	15	0/14 (0.0)	0/6 (0.0)
Snakeskin, color	5	0/5 (0.0)	–
Dwarf, shape	1	0/1 (0.0)	–
Wrinkle, shape	1	0/1 (0.0)	0/1 (0.0)
Abnormal, shape	3	0/2 (0.0)	0/2 (0.0)
Total	49	8(5)/43 (18.6)	5/15 (33.3)

[a] Rhizome closely attached to the selected mutant plant.

[b] This is the first mutant plant induced by regeneration of γ-irradiated rhizomes.

[c] Segregation.

Figure II-3. Segregation in the selected mutant RB012-S17. A, The first mutant plant regenerated from γ-irradiated rhizomes; B, segregation of newly regenerated plants from the first selected rhizomes in the M_1V_1 generation. Scale bar: 1 cm.

DISCUSSION

Optimal γ-irradiation condition for mutation induction

In plant mutation breeding, the optimal irradiation condition is considered to be the most important factor to induce desirable mutants with the minimum collateral DNA damage. Irradiation dose has been mainly used for determination of the optimal irradiation condition in diverse plant species, including orchids (Abu Hassan et al. 2016, Ahmad et al. 2006, Dehgahi and Joniyasa 2017, Luan et al. 2012, Okamura et al. 2015, Ryu et al. 2013, Yamaguchi et al. 2009a, b). However, the optimal doses suggested by previous researchers differ: e.g., Yamaguchi et al. (2009b) (LD_{10} in rice seeds); Kodym et al. (2012) ($LD_{30–50}$ and $RD_{30–50}$ in crop seeds); Suprasanna et al. (2012) ($LD_{20–30}$ in *in vitro* tissues); and Lee et al. (2016) (RD_{50} in *Cymbidium* PLBs). Furthermore, irradiation duration and dose rate, a complex concept of dose and duration, are also important factors for induction of mutations. Previous reports on the effect of dose rate on mutation induction have provided conflicting results. A low dose rate was reported to be more effective to induce mutations than a high dose rate in barley and maize (Natarajan and Maric 1961). However, Mabuchi and Matsumura (1964) suggested that a high dose rate could induce a higher mutation

frequency than a low dose rate under an identical total dose in maize. In contrast, the mutation frequency is dependent on the total dose, not the dose rate, in chrysanthemum (Yamaguchi et al. 2008). Recently, Kim et al. (2016) proposed that a specific irradiation duration could induce a higher mutation frequency and broader spectrum of mutants in chrysanthemum. In the present study, I used the RD_{50} based on the multiplication and relative regeneration rates as a guide to construct mutant populations from two *Cymbidium* cultivars (Figure II-1).

Frequency and spectrum of induced leaf mutants

Luan et al. (2012) analyzed the LD_{50}, mutation frequency, and spectrum of mutants induced by γ-ray and 320 MeV $^{12}C^{6+}$ ion irradiations in two *Paphiopedilum* species. Several leaf-color (white margin and chlorophyll variegation) or -shape (large leaves, narrow leaves, and enormous shoot buds) mutants were observed with a mutation frequency of 3% in the two populations irradiated with 320 MeV $^{12}C^{6+}$ ions of 3 Gy, whereas no mutants were observed in the γ-irradiated populations. In addition, the proportions of leaf-color to leaf-shape mutants were 12:1 and 1:11 in the *P. delenatii* and *P. callosum* populations, respectively (Luan et al. 2012). In two *Dendrobium* species, a chlorophyll variegated mutant (induced by irradiation with 0.4 Gy) and leaf-shape mutants

(irradiation with 0.2–2.0 Gy) were identified in the $^{12}C^{6+}$ ion-irradiated *D. mirbellianum* and *D. crumenatum* populations, respectively (Abu Hassan et al. 2016). Ahmad et al. (2006) reported only leaf-shape mutants (narrow and pointed leaves, and abnormally shaped leaves) in an *Oncidium lanceanum* population irradiated with 220 MeV $^{12}C^{5+}$ ion of 1–2 Gy. However, compared with previous studies, I identified a relatively higher proportion of leaf-color mutants and a broader spectrum of mutants in the present study (Table II-1, Figure II-2). This finding may be due to the differences in plant species or radiation type used. Furthermore, Prina et al. (2012) reported that treatment of homozygous barley seeds with mutagens resulted in two types of chlorophyll variegations (light green, ~70%; and albino), whereas treatment of heterozygous seeds with mutagens dramatically changed the spectrum of somatic-sector mutations. In this respect, the high heterozygosity of the two *Cymbidium* cultivars, which are hybrids of *C. sinense* and *C. goeringii*, used in the current study also may be a cause of the broad mutation spectrum.

Effects of short-term irradiation and re-irradiation on mutation induction

Kim et al. (2016) reported that at an identical total γ-ray dose of 30 Gy, an irradiation duration of 4 h among durations of 1, 4, 8, 16, and 24 h induced the

highest frequency of flower-color mutations in chrysanthemum. Kodym et al. (2012) suggested that radiation-induced DNA damage is restored by a repair mechanism mainly in the S phase of the DNA replication cycle and that a long duration of irradiation reduces the effects of the radiation dose. In the present study, the mutation frequency increased with decrease in irradiation duration in the 50 Gy-irradiated RB003 populations and the mutation frequency of the RB012 population irradiated with 20 Gy/1 h was similar to that of the population γ-irradiated with 40 Gy/24 h. In addition, the highest mutation frequency was observed with irradiation durations of 4 h and 1 h in the RB003 and RB012 populations, respectively (Table II-1). These results indicate that short-term irradiation is more effective to induce mutations than long-term irradiation in *Cymbidium*. Kodym et al. (2012) reported that recurrent irradiation treatment was conducted to broaden the mutation spectrum and to increase the chances of obtaining desirable mutants in diverse plant species, but the experiments did not yield the expected results. However, several studies have reported the effectiveness of re-irradiation of ions in ornamental flower species (Yamaguchi 2018): e.g., cyclamen (Ishizaka 2018), *Osteospermum* spp. (Okada et al. 2012), and chrysanthemum (Sato et al. 2006). In the present study, the mutation spectrum was broadened by re-irradiation with γ-rays, although no increase in the mutation frequency was observed and the size of the re-irradiated population was

larger than that of single-irradiated population (Table II-1).

Stability of induced chimera mutants

The frequency of somatic mutations is extremely low and differs considerably among plant species. In Arabidopsis, the frequency of somatic mutations was calculated as approximately 1.6×10^{-10} mutations per base per cell division (Hoffman et al. 2004). Somaclonal variants were observed at frequencies of 0.6% and 0.05% from tissue culture of *Pelargonium* spp. and a *Cymbidium* hybrid, respectively (Kang et al. 2009, Skirvin and Janick, 1976). Mutagens such as γ-rays have been applied to increase the mutation rate and lead to genetically heterogeneous cells, which is a chimeric condition. Chimera types are determined by the mode of spread, spatial arrangement, and competitiveness of a mutated cell among the mutated and wild-type cells in the SAM layers (Geier 2012). In vegetatively propagated plants, Geier (2012) suggested several practical methods for chimera dissociation, such as mechanical wounding, application of plant hormones, lateral bud sprouting, *in vitro* shoot proliferation, adventitious shoot regeneration, and somatic embryogenesis. In the present study, periclinal chimera types [yellow marginal stripe (a mutation in the L2 layer) and yellow broad stripe (L3)] were more stable than mericlinal chimera types [yellow narrow stripe (L3)

and comb (L3)] (Table II-2), which is consistent with previous reports (Geier 2012). In a previous study, the stability of selected PLBs, which produced a somaclonal variant with a yellow marginal stripe, was 40% in a *Cymbidium* hybrid (Kang et al. 2009). Yamaguchi et al. (2009a) reported that the flower-color mutants induced by γ-rays were all identified as periclinal chimeras, but those induced by carbon-ion irradiations displayed a higher proportion of solid type mutants in chrysanthemum. Although with regard to chimera dissociation carbon ions are advantageous to γ-rays, with respect to horticultural potential γ-rays may be more useful than carbon ions account of the inducible phenotypic diversity. Prina et al. (2012) noted that positional variegation is caused by differential gene expression, which is not a chimeric condition. In the present study, the phenotype of mutants showing yellow large spots was unstable in the next generation, which may be a result of differential gene expression (Table II-2). I observed relatively higher stability of chimeras on the plant than the rhizome. However, I suggest that selection of stable mutant rhizomes through recurrent selection is more appropriate than selection of regenerated mutant plants, which may increase the risk of contamination or death during meristem culture, a long propagation period, and unintended rearrangement of cell layers. The present results provide useful information for mutation breeding of vegetatively propagated crops such as *Cymbidium* and for an improved understanding of chimerism in monocotyledons.

REFERENCES

Abu Hassan A, Ariffin S, Ahmad Z, Basiran MN, Oono Y, Hase Y, Shikazono N, Narumi I, Tanaka A. 2016. Mutation induction of orchid plants by ion beams. JAEA-Review 2015-037: 1–20.

Ahmad Z, Hassan AA, Idris NA, Basiran MN, Tanaka A, Shikazono N, Oono Y, Hase N. 2006. Effects of ion beam irradiation on *Oncidium lanceanum* orchids. J Nucl Relat Technol. 3: 1–8.

Chase MW, Cameron KM, Freudenstein JV, Pridgeon AM, Salazar G, van den Berg C, Schuiteman A. 2015. An updated classification of Orchidaceae. Bot J Linn Soc. 177: 151–174.

Chin DP, Mishiba K, Mii M. 2007. *Agrobacterium*-mediated transformation of protocorm-like bodies in *Cymbidium*. Plant Cell Rep. 26: 735–*743.*

Choi SH, Kim MJ, Lee JS, Ryu KH. 2006. Genetic diversity and phylogenetic relationships among and within species of oriental cymbidiums based on RAPD analysis. Sci Hortic. 108: 79–85.

Dehgahi R, Joniyasa A. 2017. Gamma irradiation-induced variation in *Dendrobium* Sonia-28 orchid protocorm-like bodies (PLBs). Fungal Genom Biol. 7: 151.

Filippis I, Lopez-Cobollo R, Abbott J, Butcher S, Bishop GJ. 2013. Using a periclinal chimera to unravel layer-specific gene expression in plants. Plant J. 75: 1039–1049.

Frank MH, Chitwood DH. 2016. Plant chimeras: The good, the bad, and the 'Bizzaria'. Dev Biol. 419: 41–53.

Geier T. 2012. Chimeras: Properties and dissociation in vegetatively propagated plants. *In*: Shu QY, Forster BP, Nakagawa H (eds.) Plant Mutation Breeding and Biotechnology, CAB International, Wallingford; FAO, Rome, pp. 191–202.

Hoffman PD, Leonard JM, Lindberg GE, Bollmann SR, Hays JB. 2004. Rapid accumulation of mutations during seed-to-seed propagation of

mismatch-repair-defective *Arabidopsis*. Genes Dev. 18: 2676–2685.

[IAEA] International Atomic Energy Agency. 2019. IAEA Mutant Variety Database [Dataset]. The joint FAO/IAEA Mutant Variety Database; [accessed 2019], https://mvd.iaea.org/#!Home.

Ishizaka H. 2018. Breeding of fragrant cyclamen by interspecific hybridization and ion-beam irradiation. Breed Sci. 68: 25–34.

Kang KW, Park KS, Mo SY, Kim DH, Kang SY. 2009. A new *Cymbidium* orchid variety "Daegook" bred by *in vitro* mutagenesis. Kor J Breed Sci. 41: 510–514.

Kim SH, Jo YD, Ryu J, Hong MJ, Kang BC, Kim JB. 2019. Effects of the total dose and duration of γ-irradiation on the growth responses and induced SNPs of a *Cymbidium* hybrid. Int J Radiat Biol. (In press)

Kim YS, Sung SY, Jo YD, Lee HJ, Kim SH. 2016. Effects of gamma ray dose rate and sucrose treatment on mutation induction in chrysanthemum. Eur J Hortic Sci. 81: 212–218.

Kodym A, Afza R, Forster BP, Ukai Y, Nakagawa H, Mba C. 2012. Methodology for physical and chemical mutagenic treatments. *In*: Shu QY, Forster BP, Nakagawa H (eds.) Plant Mutation Breeding and Biotechnology, CAB International, Wallingford; FAO, Rome, pp. 169–180.

Lee YM, Lee HJ, Kim YS, Kang SY, Kim DS, Kim JB, Ahn JW, Ha BK, Kim SH. 2016. Evaluation of the sensitivity to ionizing γ-radiation of a *Cymbidium* hybrid. J Hortic Sci Biotechnol. 91: 109–116.

Luan LQ, Uyen NHP, Ha VTT. 2012. In vitro mutation breeding of *Paphiopedilum* by ionizing radiation. Sci Hortic. 144: 1–9.

Mabuchi T, Matsumura S. 1964. Dose rate dependence of mutation rates from γ-irradiated pollen grains of maize. Jpn J Genet. 39: 131–135.

Natarajan AT, Maric MM. 1961. The time-intensity factor in dry seed irradiation. Radiat Bot. 1: 1–9.

Okada T, Iizuka M, Hase Y, Nozawa I, Narumi I, Sekiguchi M. 2012. Development of commercial variety of osteospermum by a stepwise mutagenesis by ion beam irradiation. Hort Res. (Japan) 11 (Suppl. 1): 428.

Okamura M, Hase Y, Furusawa Y, Tanaka A. 2015. Tissue-dependent somaclonal mutation frequencies and spectra enhanced by ion beam irradiation in chrysanthemum. Euphytica 202: 333–343.

Prina AR, Landau AM, Pacheco MG. 2012. Chimeras and mutant gene transmission. *In*: Shu QY, Forster BP, Nakagawa H (eds.) Plant Mutation Breeding and Biotechnology, CAB International, Wallingford; FAO, Rome, pp. 181–189.

Ryu J, So HS, Bae SH, Kang HS, Lee BC, Kang SY, Lee HY, Bae CH. 2013. Genetic diversity of *in vitro* cultured *Cymbidium* spp. irradiated with electron beam. Kor J Breed Sci. 45: 8–18.

Sarmah D, Kolukunde S, Sutradhar M, Singh BK, Mandal T, Mandal N. 2017. A review on: *In vitro* cloning of orchids. Int J Curr Microbiol Appl Sci. 6: 1909–1927.

Sato T, Ohya Y, Hase Y, Tanaka A. 2006. Studies on flower color and morphological mutations from chrysanthemum *in vitro* explants irradiated with ion beams. JAEA-Review 2005-001: 74–75.

Skirvin RM, Janick J. 1976. Tissue culture-induced variation in scented *Pelargonium* spp.. J Amer Soc Hort Sci. 101: 281–290.

Suprasanna P, Jain SM, Ochatt SJ, Kulkarni VM, Predieri S. 2012. Applications of *in vitro* techniques in mutation breeding of vegetatively propagated crops *In*: Shu QY, Forster BP, Nakagawa H (eds.) Plant Mutation Breeding and Biotechnology, CAB International, Wallingford; FAO, Rome, pp. 371–385.

Yamaguchi H. 2018. Mutation breeding of ornamental plants using ion beams. Breed Sci. 68: 71–78.

Yamaguchi H, Shimizu A, Degi K, Morishita T. 2008. Effects of dose and dose rate of gamma ray irradiation on mutation induction and nuclear DNA content in chrysanthemum. Breed Sci. 58: 331–335.

Yamaguchi H, Shimizu A, Hase Y, Degi K, Tanaka A, Morishita T. 2009a. Mutation induction with ion beam irradiation of lateral buds of chrysanthemum and analysis of chimeric structure of induced mutants. Euphytica 165: 97–103.

Yamaguchi H, Hase Y, Tanaka A, Shikazono N, Degi K, Shimizu A, Morishita T. 2009b. Mutagenic effects of ion beam irradiation on rice. Breed Sci. 59: 169–177.

CHAPTER III

Transcriptome analysis to identify candidate genes associated with the yellow-leaf phenotype of a *Cymbidium* mutant generated by γ-irradiation

This research has been published in *PLoS ONE* [2020; doi: 10.1371/journal.pone.0228078].

ABSTRACT

Leaf color is an important agronomic trait in flowering plants, including orchids. However, factors underlying leaf phenotypes in plants remain largely unclear. A mutant displaying yellow leaves was obtained by the γ-ray-based mutagenesis of a *Cymbidium* orchid and characterized using RNA sequencing. A total of 144,918 unigenes obtained from over 25 million reads were assigned to 22 metabolic pathways in the Kyoto Encyclopedia of Genes and Genomes database. In addition, gene ontology was used to classify the predicted functions of transcripts into 73 functional groups. The RNA sequencing analysis identified 2,267 differentially expressed genes between wild-type and mutant *Cymbidium* sp. Genes involved in chlorophyll biosynthesis and degradation as well as ion transport were identified and assayed for their expression levels in wild-type and mutant plants using quantitative real-time profiling. No critical expression changes were detected in genes involved in chlorophyll biosynthesis. In contrast, seven genes involved in ion transport, including two metal ion transporters, were down-regulated, and chlorophyllase 2, associated with chlorophyll degradation was up-regulated. Together, these results suggest that alterations in chlorophyll metabolism and/or ion transport might contribute to leaf color in *Cymbidium* orchids.

INTRODUCTION

Orchids such as *Cymbidium*, *Dendrobium*, *Oncidium*, and *Phalaenopsis* are important cash crops worldwide, and the orchid industry has contributed substantially to the economy of many Southeast Asian countries (Cheamuangphan et al. 2013; Sarmah et al. 2017). Because of its fragrant flowers and straight leaves, *Cymbidium* is a popular orchid in China, Korea, and Japan (Choi et al. 2006; Xu et al. 2006; Aceto and Gaudio 2011). In addition to its floral diversity, the color and pattern of *Cymbidium* leaves is an important marketable feature (Yukawa and Stern 2002; Li et al. 2004; Zhang et al. 2013) and the focus of *Cymbidium* breeding programs (Chugh et al. 2009).

Although the biological significance and bio-diversity of genome sizes in angiosperms have received considerable attention in recent years (Bennett et al. 2005; Leitch et al. 2007), the genomic organization of Orchidaceae remains poorly characterized. This could be largely owing to the poor genome representation of Orchidaceae, which contains over 28,000 species distributed in 763 genera (Christenhusz and Byng 2016). Thus far, the genomes of four orchids, *Phalaenopsis equestris*, *Dendrobium catenatum*, *Dendrobium officinale*, and *Apostaceae shengen*, have been sequenced (Tsai et al. 2017). The genome

sequences revealed that genome sizes in Orchidaceae have a 168-fold, making them the most diverse among angiosperms (Leitch et al. 2009). The assembled sequenced genomes of orchids have predicted gene numbers ranging from 28,910 in *P. equestris* to 35,567 in *D. officinale* (Cai et al. 2015; Yan et al. 2015).

Recent advances in orchid genome research have facilitated conventional and mutagenesis-based breeding approaches designed to generate varieties with unique flower and leaf phenotypes (Ulukapi and Nasircilar 2015). Leaf yellowing is generally associated with chlorophyll (Chl) biosynthesis or degradation pathways, both of which are mediated by multiple enzymatic steps. Thus, a block in any of the step leading to Chl synthesis can potentially result in low Chl content and thereby altered leaf color (Nagata et al. 2005; Adhikari et al. 2011). The leaf color phenotype has been extensively studied in rice and has provided insights into the steps involved in Chl biosynthesis and degradation, chloroplast developments, tetrapyrrole synthesis, and photosynthesis (Deng et al. 2014). These studies have led to the isolation of diverse leaf colors and patterns including albino, light and purple green leaves, as well as striped and zebra-patterned leaves (Deng et al. 2012). Thus far, over 50 genes contributing to leaf color have been characterized in rice and 13 of these function in Chl biosynthesis (Jung et al. 2003; Lee et al. 2005; Zhang et al. 2006; Liu et al. 2007; Wu et al. 2007; Wang et al. 2010; Huang et al. 2013; Sakuraba et al. 2013; Tian et al. 2013;

Zhou et al. 2013; Ma et al. 2017; Qin et al. 2017). These studies suggest that genes regulating leaf color can, directly or indirectly, contribute to Chl biosynthesis and/or structure of the chloroplast and that Chl and anthocyanin content are major contributors to the leaf color. The biosynthesis of Chl is also dependent on biochemical processes that regulate uptake and transport of macronutrients including metals and cofactors. The uptake, chelation, trafficking, and storage of metal ions is tightly regulated to maintain an optimal intracellular concentration of metal ions for Chl biosynthesis. Metal ions also play essential roles in photosynthetic and metabolic processes associated with leaf color (Burkhead et al. 2009; Pilon et al. 2009; Yruela 2009; Nouet et al. 2011). For example, a mutation in iron-regulated transporter 1 alters composition and abundance of the photosynthetic apparatus in Arabidopsis and causes drastic reduction in growth rate and fertility (Varotto et al. 2002; Vert et al. 2002). In this study, I used a γ-ray-based mutagenetic procedure to isolate a leaf-color mutant in *Cymbidium*, and I show that the mutant's yellow leaf-color is likely associated with Chl degradation and/or ion transport.

MATERIALS AND METHODS

Plant materials

The wild-type (WT) *Cymbidium* hybrid, RB003 was derived from a cross between *C. sinense* × *C. goeringii*. A yellow leaf-color mutant, designated as S12, was derived from RB003 by γ-ray mutagenesis, which was carried out at the Korea Atomic Energy Research Institute. All plants were grown in a greenhouse under natural light and photoperiod.

RNA extraction

Extraction of total RNA from six-month old leaves of the WT and the S12 mutants was carried out using a RNease Plant Mini kit (Qiagen, Hilden, Germany), following the manufacturer's instructions. RNA quality and concentration were determined using on a Nanodrop 2000 spectrophotometer (Thermo Fisher Scientific, Waltham, MA, USA).

Quantitative real-time PCR (qRT-PCR) analysis

Reverse transcription (RT) and first-strand cDNA synthesis were carried out using a ReverTra Ace-α- kit (Toyobo Co. Ltd, Osaka, Japan). Quantitative RT-PCR was carried out with iQ SYBR Green Supermix (Bio-Rad, Hercules, CA, USA). Quantitative PCR was performed using CFX96 Touch Real-Time PCR Detection System (Bio-Rad, Hercules, USA). The PCR conditions included and initial denaturation step of 95°C for 10 min followed by 35 cycles of 95°C for 15 s, 56–62°C for 15 s and 72°C for 30 s. Each sample was run in triplicates and *ACTIN* was used as an internal control. Cycle threshold values were calculated using Bio-Rad CFX Manager 3.1 software (Bio-Rad, Hercules, USA). Gene-specific primers used for quantitative RT-PCR are described in S1 Table.

Chl and carotenoid content assay

Six-month-old leaves of the WT and the S12 mutants were sampled for Chl and carotenoid determination. Amounts of Chls *a* and *b* and carotenoids were estimated following the method of Lichtenthaler (1987). The fresh leaf samples were ground using liquid nitrogen and suspended in 96% ethanol (Sigma, St. Louis, MO, USA). This extract was vortexed and placed at room temperature in dark for 24 h. The absorption spectra of the extract was measured at 470, 648.6, and 664.2 nm using a UV-1800 spectrophotometer (Shimadzu, Kyoto, Japan).

RNA sequencing and *de novo* assembly

The cDNA libraries were prepared from both the WT and the S12 leaves. Raw reads were trimmed by filtering out adaptor-only nucleotides that were smaller than 75 bp using Trimmomatic (v.0.32) (Bolger et al. 2014). *De novo* assembler Trinity (v.2.2.0) was used to construct large contigs from the filtered reads (Grabherr et al. 2011). Trinity is a representative RNA assembler based on the de Bruijn graph algorithm. The assembly pipeline of Trinity consists of three consecutive modules: Inchworm, Chrysalis, and Butterfly. Protein coding sequences (CDSs) were extracted from the reconstructed transcripts using TransDecoder (v.3.0.1), a utility included with Trinity to assist with the identification of potential coding region (Haas et al. 2013). The prediction of coding regions is based on search of all possible CDSs, verification of the predicted CDSs by GENEID (Blanco et al. 2007), and selecting the region that has the highest score among candidate sequences.

Functional annotation

The trimmed read were annotated with protein databases including Gene Ontology (GO), database for annotation, visualization, and integrated discovery

(DAVID) (Huang et al. 2007), Kyoto Encyclopedia of Genes and Genomes (KEGG), and eukaryotic clusters of orthologous genes (KOG) databases. GO includes biological processes (BP), cellular component (CC), and molecular function (MF). KEGG is a major recognized pathway-related database that integrates genomic, biochemical, and systemic information. DAVID is a web-accessible program that integrates functional genomic annotations with intuitive graphical displays, which highlights pathway members within the biochemical pathways provided by KEGG. KOG categories were obtained via comparisons to the KOG database using RPS-BLAST (included with BLAST v2.2.26) (Tatusov et al. 2003).

Identification of differentially expressed genes between wild-type and S12 mutant

Gene expression profiles were analyzed using the method of RNA-Seq following Expectation Maximization (RSEM) (Li and Dewey 2011). The unique feature of RSEM is that it does not rely on a reference genome. RSEM uses the Bowtie alignment program to align transcripts. Differentially expressed genes (DEGs) were identified using edgeR (Robinson et al. 2010), a Bioconductor package based one the generalized linear model that analyzes RNA-Seq data by

considering gene expression as a negative binomial. I used a false discovery rate (FDR) < 0.05 significance cut-off for multiple testing adjustments (Benjamini and Hochberg 1995).

RESULTS

Reduced accumulation of Chls and carotenoids in the S12 mutant

The S12 mutant developed yellow-colored leaves from the seedling stage to maturity (Figure III-1). To determine if this was associated with reduced in Chl or carotenoid content, we quantified Chl *a* and Chl *b* as well as total carotenoids. A significant reduction in Chl and carotenoid contents was observed in S12 mutant leaves; Chl *a*, Chl *b*, and carotenoid levels were reduced by 85%, 78%, and 65%, respectively (Figure III-2A, C). The ratio between Chl *a* and Chl *b* also differed nominally but significant difference between the WT and the S12 mutants. The Chl *a*/*b* ratio serves as a useful indicator of plant response to shading (Hendry and Price 1995) (Figure III-2B).

To determine molecular changes underlying the S12 mutation, I assayed changes in genome-wide transcript levels using RNA-Seq. To this end, equal amount of RNAs from the WT and the S12 mutants were used to construct cDNA libraries, and then sequenced by Trimmomatic (v0.32) platform. The average length of clean reads was 308–315 bp and a total of 30.83 million (99.92%) and 27.45 million (99.94%) clean reads were generated from the WT and the S12 mutant, respectively. A total of 225,694 transcripts were assembled into 144,918 unigenes with an average

length of 1,257 bp (Table III-1). I used gene ontology (GO) classification to classify the predicted functions of unigenes, which were categorized into 73 functional groups (FDR < 0.05). GO assignments were divided into three categories including biological process (BP), cellular component (CC), and molecular function (MF). Integral component of membrane (15.83%), plasma membrane (13.07%), and cytoplasm (12.36%) were dominant groups in the CC category followed by chloroplast (11.93%), cytosol (8.21%), and membrane (6.07%). Predicted proteins assigned to BP category were mainly associated with transcription (6.52%), protein phosphorylation (3.51%), protein ubiquitination (2.21%), and embryo development (1.87%). In the MF category, the most heavily represented groups were linked to ATP binding (9.99%), protein binding (9.09%), metal ion binding (5.74%), and protein serine/threonine kinase activity (3.84%) (Figure III-3).

Next, I mapped the assembled unigenes to the reference canonical pathway in the KEGG, including metabolism, genetic information processing, environmental information processing, and cellular processes (http://www.kegg.jp/kegg/pathway.html). The 144,918 unigenes were assigned to 22 KEGG sub-pathways (Figure III-4). Theses pathways included KEGG orthology (KO) entries for metabolism (734 KOs), genetic information processing (69 KOs), environmental information processing (14 KOs), and cellular processes (108 KOs) (Table III-2).

Table III-1. Summary of RNA sequencing and *de novo* transcriptome assembly results.

	Wild type	S12 mutant
Number of raw reads	30,860,529	27,468,828
Average length of raw reads (bp)	101	101
Number of trimmed reads	30,836,504	27,452,350
Number of transcripts	225,694	
Number of unigenes	144,918	
Contig N50 (bp)	1,257	
Number of DEGs with significant expression differences (FDR < 0.05)	2,267	

Table III-2. Functional categorization of assembled unigenes in KEGG pathways.

KEGG sub-pathways	Count
Metabolism	
1.0 Global and overview maps	**343**
01130 Biosynthesis of antibiotics	152
01200 Carbon metabolism	102
01230 Biosynthesis of amino acids	89
1.1 Carbohydrate metabolism	**179**
00020 Citrate cycle (TCA cycle)	26
00520 Amino sugar and nucleotide sugar metabolism	50
00620 Pyruvate metabolism	35
00630 Glyoxylate and dicarboxylate metabolism	29
00640 Propanoate metabolism	12
00562 Inositol phosphate metabolism	27
1.3 Lipid metabolism	**102**
00071 Fatty acid degradation	22
00561 Glycerolipid metabolism	29
00564 Glycerophospholipid metabolism	38
00565 Ether lipid metabolism	13
1.5 Amino acid metabolism	**81**
00260 Glycine, serine and threonine metabolism	33
00280 Valine, leucine and isoleucine degradation	26
00330 Arginine and proline metabolism	22
1.6 Metabolism of other amino acids	**21**
00410 Beta-alanine metabolism	21
1.10 Biosynthesis of other secondary metabolites	**8**
00261 Monobactam biosynthesis	8

Table III-2. Continued.

KEGG sub-pathways	Count
Genetic Information Processing	
2.1 Transcription	**69**
03040 Spliceosome	69
Environmental Information Processing	
3.1 Membrane transport	**14**
02010 ABC transporters	14
Cellular Processes	
4.1 Transport and catabolism	**108**
04144 Endocytosis	69
04146 Peroxisome	39

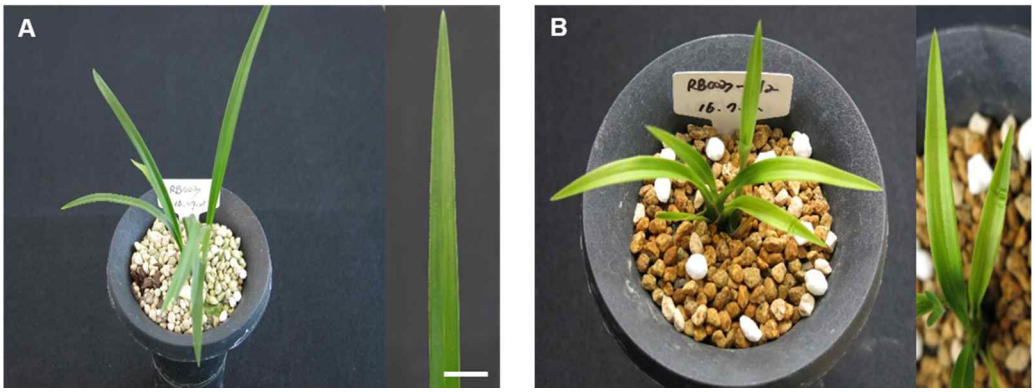

Figure III-1. Morphological phenotypes of typical wild-type and S12 mutant plants of *Cymbidium* hybrid RB003. (A) Wild-type plants, (B) The yellow leaved S12 mutant. Scale bar: 1 cm.

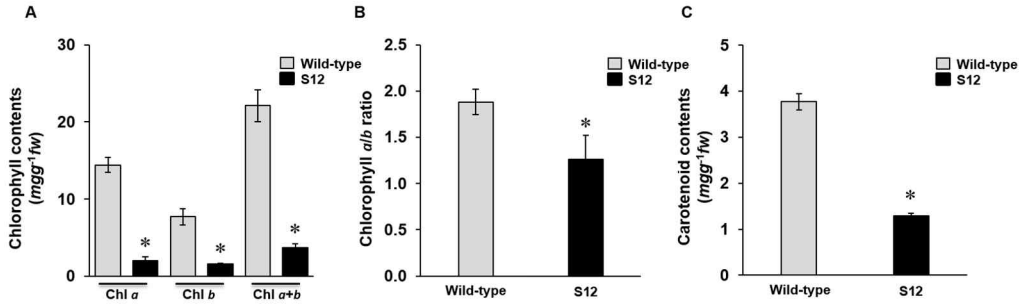

Figure III-2. Relative levels of chlorophylls *a* and *b* and carotenoids in the wild-type and S12 mutant. (A) Total chlorophyll content, (B) chlorophyll *a*/*b* ratio, and (C) carotenoid contents of wild-type and S12 mutant leaves. Error bars represent standard deviation (n = 3). The experiment was repeated three times with similar results.

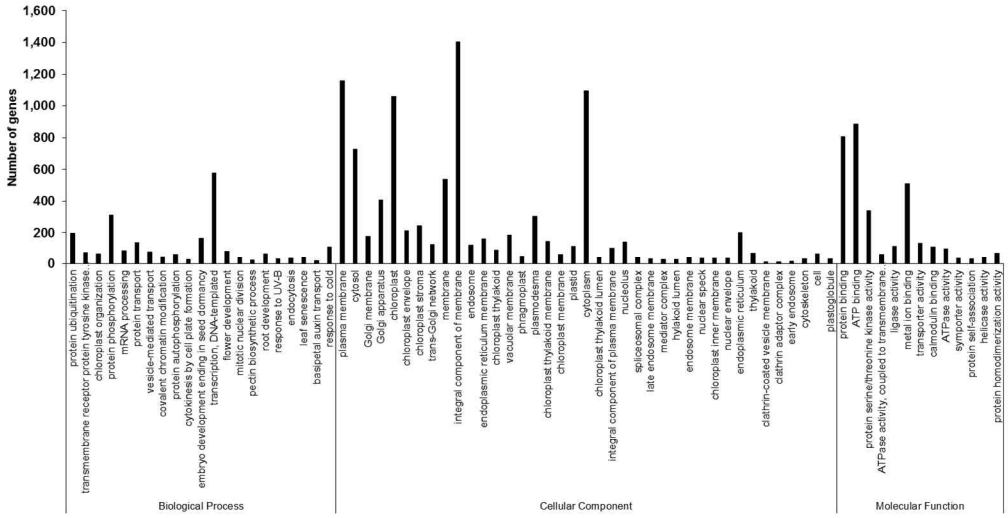

Figure III-3. Distribution of annotated sequences based on Gene Ontology (GO) analysis. GO functional classification assigned 144,918 unigenes to 73 subcategories under the three main GO categories of biological process, cellular component, and molecular function. The *x*-axis indicates the subcategories, and the *y*-axis indicates the number of genes in each category.

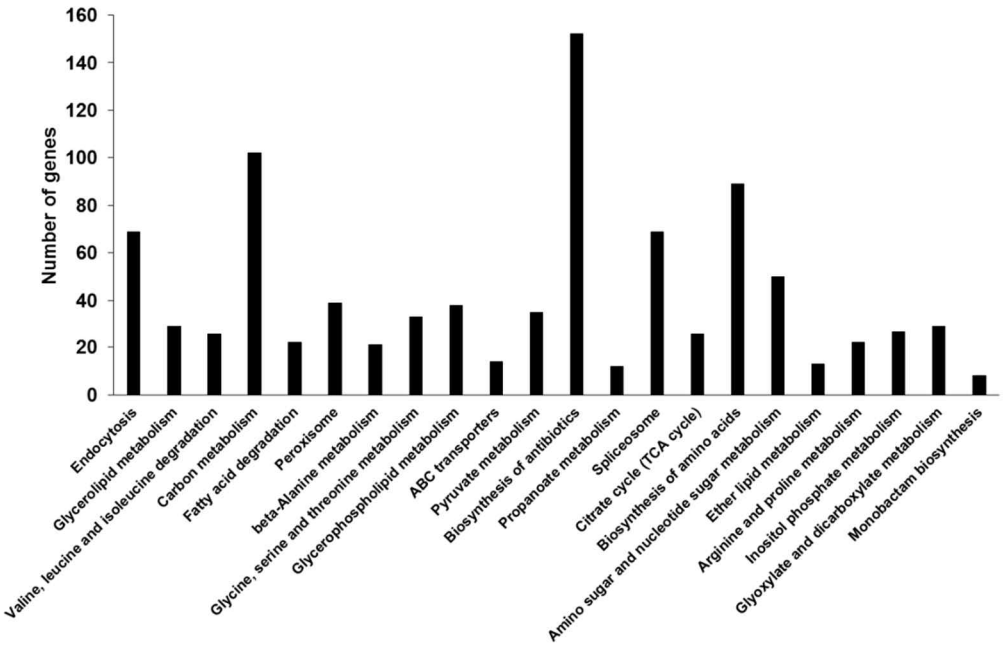

Figure III-4. Distribution of annotated sequences based on Kyoto Encyclopedia of Genes and Genomes (KEGG) pathway analysis. The *x*-axis indicates enriched KEGG pathways, and the *y*-axis represents the number of genes within each KEGG pathway.

The implicated role of ion transport and Chl catabolism in the S12 phenotype according to DEG analysis

Gene expression analysis identified a total of 2,267 DEGs (FDR < 0.05) between the WT and the S12 mutant. Among these genes, 724 genes were up-regulated and 529 were down-regulated (Figure III-5). The DEGs were categorized into 27 functional groups in GO classification (FDR < 0.05). Predicted proteins assigned to biological process (BP) were mainly associated with single-organism process, which corresponded to the largest group. Cell and membrane terms were dominant among cellular components (CC). Those assigned to molecular function (MF) were mainly linked to ATP binding and transport activity (Figure III-6). Especially, when DEG GO and total GO were compared in CC and MF, percentage of membrane group and transporter activity group were higher in DEG GO.

The DEGs were further classified into 22 functional categories using the KOG system. The largest KOG cluster was carbohydrate transport and metabolism (G), followed by secondary metabolites biosynthesis, transport and catabolism (Q), post-translational modification (O), energy production and conversion (C), and general function (R) (Figure III-7). The KOG categories were further divided into multiple classes including cellular processes and

signaling (273), information storage and processing (90), metabolism (705), and poorly characterized (135) classes (Table III-7). Next, I analyzed gene pathway assignment of DEGs to KEGG pathway. As a result, DEGs were assigned to seven sub-pathways (Figure III-8), which in turn served as a template for assaying specific metabolic processes associated with the S12 mutant. To understand the biological roles of the screened major targets, I used DAVID to perform the GO biological process enrichment analysis. The DAVID, the most widely used on-line tool for functional classification and relies on a partitioning approach that groups genes together on the basis of their functional similarities. As predicted, a major category of DEGs was involved in membrane and chloroplast functions (Table III-3). These DEGs included ABC transporters that were up-regulated in the S12 mutant and genes associated with ion transport were down-regulated (Table III-4, 5). Interestingly, the metal ion transporters have been associated with leaf color and photosynthesis (Yruela 2013; López-Millán et al. 2016); their encoding genes were thus considered as candidates for the genes responsible for the phenotype seen in the S12 mutant.

Table III-3. Functional annotation of differentially expressed genes based on DAVID.

Database	Keyword	Count	*P*-value
Cluster 1	**Enrichment score: 7.43**		
UP_KEYWORDS	Membrane	232	1.00×10^{-13}
UP_KEYWORDS	Transmembrane helix	185	3.50×10^{-8}
UP_KEYWORDS	Transmembrane	185	5.30×10^{-8}
GOTERM_CC_DIRECT	Integral component of membrane	177	9.70×10^{-6}
UP_SEQ_FEATURE	Transmembrane region	89	3.90×10^{-5}
Cluster 2	**Enrichment score: 3.91**		
UP_KEYWORDS	Nucleus	132	9.60×10^{-10}
UP_KEYWORDS	Transcription regulation	79	9.50×10^{-7}
UP_KEYWORDS	Transcription	80	1.20×10^{-6}
UP_KEYWORDS	DNA-binding	70	1.30×10^{-5}
GOTERM_MF_DIRECT	Sequence-specific DNA binding	35	1.80×10^{-3}
GOTERM_MF_DIRECT	Transcription factor activity, sequence-specific DNA binding	69	6.50×10^{-3}
GOTERM_BP_DIRECT	Transcription, DNA-templated	75	7.40×10^{-3}
GOTERM_BP_DIRECT	Regulation of transcription, DNA-templated	76	5.80×10^{-2}
GOTERM_MF_DIRECT	DNA binding	71	1.00×10^{-1}
Cluster 3	**Enrichment Score: 3.8**		
UP_KEYWORDS	Chloroplast	64	1.30×10^{-6}
UP_KEYWORDS	Plastid	64	1.50×10^{-6}
UP_KEYWORDS	Transit peptide	73	2.90×10^{-6}
GOTERM_CC_DIRECT	Chloroplast	109	5.20×10^{-2}
UP_SEQ_FEATURE	Transit peptide:chloroplast	25	3.50×10^{-1}

Table III-4. Differentially expressed genes with increased expression levels that likely lead to higher enzymatic activities.

Trinity ID	Uniprot accession	Gene symbol	Gene	logFC	FDR
TRINITY_DN71117_c0_g1	Q9SYI2	AB3B	ABC transporter B family member 3	1.028443	0.008577
TRINITY_DN85004_c0_g1	Q9LK64	AB3C	ABC transporter C family member 3	1.787229	0.013526
TRINITY_DN87313_c1_g1	Q8LGU1	AB8C	ABC transporter C family member 8	2.204471	8.69×10^{-9}
TRINITY_DN81240_c2_g1	Q9M1C7	AB9C	ABC transporter C family member 9	2.136759	5.38×10^{-11}
TRINITY_DN86578_c4_g1	Q9SKX0	AB13C	ABC transporter C family member 13	1.091064	0.0379
TRINITY_DN63855_c0_g2	Q9FF46	AB28G	ABC transporter G family member 28	3.192968	8.98×10^{-5}
TRINITY_DN84784_c2_g1	Q8GU89	AB37G	ABC transporter G family member 37	1.53448	0.020845
TRINITY_DN85702_c1_g3	Q8GU88	AB39G	ABC transporter G family member 39	1.097948	0.00171
TRINITY_DN75921_c1_g1	Q94AH3	NIPA4	Magnesium transporter NIPA4	1.313692	0.00298
TRINITY_DN76502_c0_g1	Q8GYH8	SUT42	Sulfate transporter 4;2	2.36809	1.72×10^{-17}
TRINITY_DN85119_c0_g1	Q9LHN7	PHSC	Polyamine transporter	0.856779	0.038716
TRINITY_DN81780_c0_g1	Q9SQZ0	CAAT7	Cationic amino acid transporter 7	2.018167	8×10^{-5}
TRINITY_DN75271_c0_g1	Q10Q65	NRAM2	Metal transporter Nramp2	2.881755	7.46×10^{-19}
TRINITY_DN74882_c1_g1	Q9M7I7	CLH2	Chlorophyllase-2	1.490092	0.0010
TRINITY_DN78535_c3_g1	Q84ST4	NOL	Chlorophyll(ide) b reductase	0.400089	0.5953
TRINITY_DN77744_c2_g1	Q9FYC2	PAO	Pheophorbide a oxygenase	0.534353	0.6442
TRINITY_DN81301_c1_g1	Q9MTQ6	RCCR	Red chlorophyll catabolite reductase	0.114782	0.9641

Table III-5. Differentially expressed genes with decreased expression levels that likely lead to lower enzymatic activities.

Trinity ID	Uniprot accession	Gene symbol	Gene	logFC	FDR
TRINITY_DN74817_c0_g1	Q8L4S2	MRS2F	Magnesium transporter MRS2-F	–2.53315	0.001367
TRINITY_DN80302_c2_g1	Q058N4	MRS2B	Magnesium transporter MRS2-11	–1.10454	0.014623
TRINITY_DN35346_c0_g1	Q5JK32	HAK5	Potassium transporter 5	–7.80167	1.45×10^{-11}
TRINITY_DN86452_c2_g1	Q67UC7	HAK17	Potassium transporter 17	–2.28674	0.000628
TRINITY_DN82926_c0_g1	O82089	CCH	Copper transport protein CCH	–2.84536	0.009691
TRINITY_DN82149_c4_g1	Q94LW6	SUT35	Sulfate transporter 3;5	–1.33172	0.018302
TRINITY_DN86390_c5_g1	Q8VZ80	PLT5	Polyol transporter	–1.74481	0.010401
TRINITY_DN81484_c2_g1	Q93ZF5	PHO11	Phosphate transporter PHO1 homolog 1	–11.8706	1.8×10^{-17}
TRINITY_DN82844_c0_g1	Q9C9Z1	ZTP50	Zinc transporter 50	–1.51218	8.95×10^{-5}
TRINITY_DN85192_c3_g1	Q9M1P7	BOR2	Boron transporter 2	–10.5916	2.93×10^{-8}
TRINITY_DN55717_c0_g1	Q84KJ6	AMT31	Ammonium transporter 3 member 1	–7.6494	2.67×10^{-7}
TRINITY_DN83319_c2_g1	Q9LS46	ALMT9	Aluminum-activated malate transporter 9	–11.5069	0.032332
TRINITY_DN82053_c3_g1	Q7XUJ2	YSL9	Metal-nicotianamine transporter YSL9	–2.88577	7.76×10^{-13}
TRINITY_DN59808_c0_g2	P27489	CAB13	Chlorophyll a-b binding protein 13	–3.77677	0.006663
TRINITY_DN74933_c1_g1	Q9SW18	CHLM	Magnesium protoporphyrin IX methyltransferase	–1.00694	0.382536
TRINITY_DN83083_c8_g2	Q9M591	CRD1	Magnesium-protoporphyrin IX monomethylester cyclase	–0.46194	0.787932
TRINITY_DN76234_c0_g1	Q5W6H5	CHLG	Chlorophyll synthase	–1.10377	0.092632
TRINITY_DN80530_c2_g1	Q41249	PORA	Protochlorophyllide a reductase	–4.57080	0.491924
TRINITY_DN80260_c3_g15	Q5N800	NYC1	Probable chlorophyll(ide) b reductase	–2.70738	0.002168

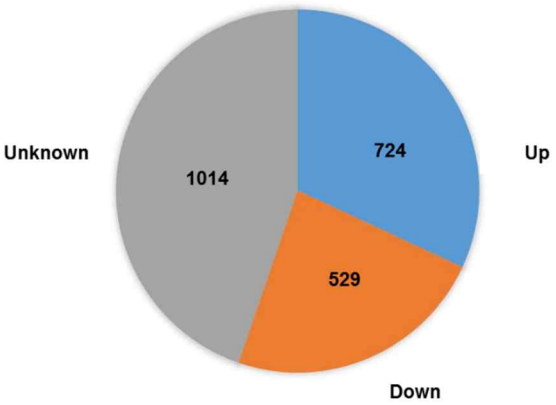

Figure III-5. Venn diagram showing numbers of genes with altered expressions in the S12 mutant compared with wild-type. Genes were categorized on the basis of their biological functions. Genes not showing homology to genes of any known function are listed as unknown.

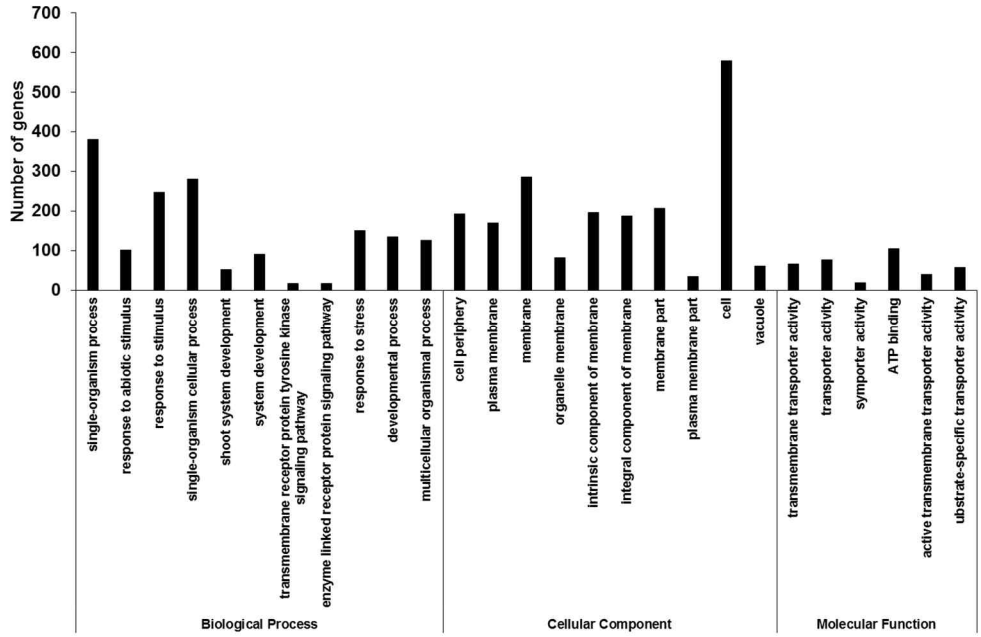

Figure III-6. Gene Ontology (GO) functional classification of differentially expressed genes (DEGs). GO classification assigned 2,267 DEGs to 27 functional groups based on their biological functions.

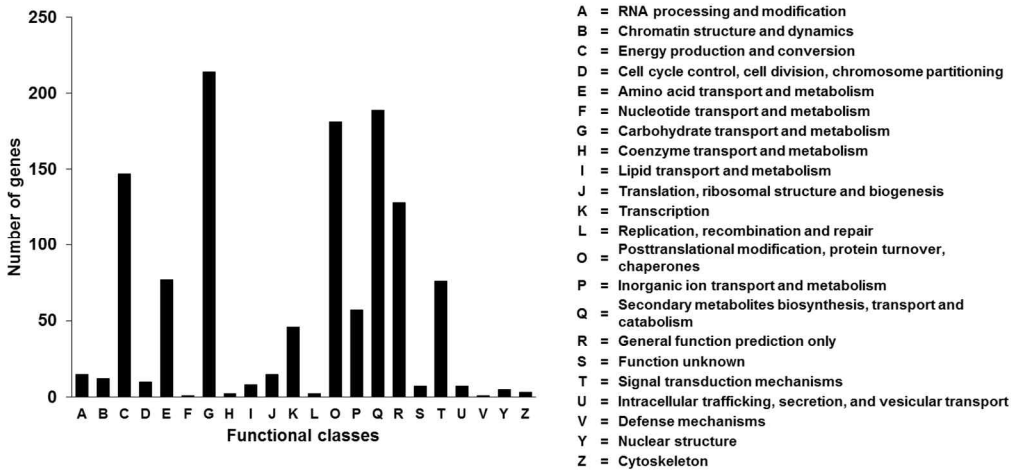

Figure III-7. Eukaryotic clusters of orthologous genes (KOG) annotations of differentially expressed genes (DEGs). The 2,267 DEGs were aligned with the KOG database and classified into 22 molecular families**.** Letters on the *x*-axis refer to categories on the right. The *y*-axis indicates the number of DEGs in the corresponding KOG category.

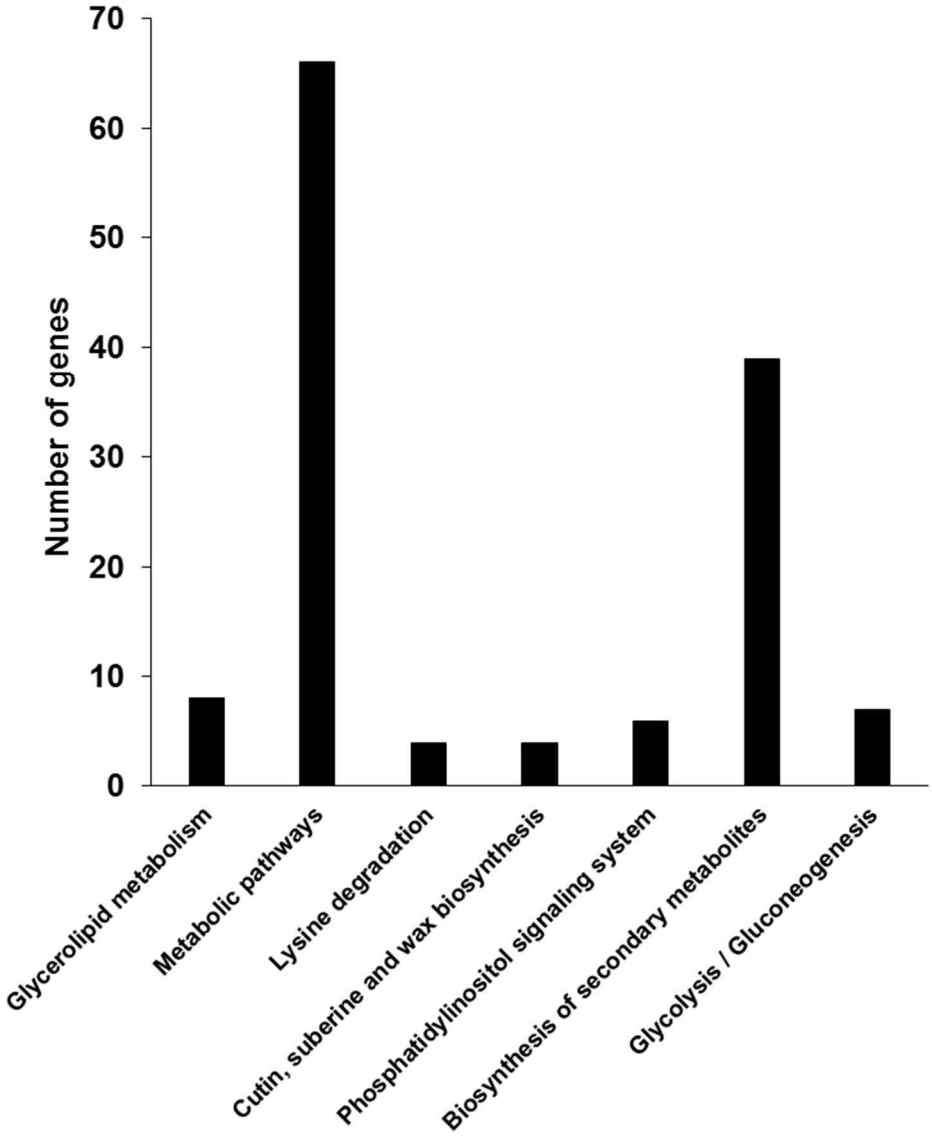

Figure III-8. KEGG pathway representation of differentially expressed genes (DEGs) in the S12 mutant.

I next identified genes associated with Chl metabolism to assay association between transcript and Chl levels. A previous study in the model plant Arabidopsis revealed that 16 genes are involved in the conversion of glutamyl-tRNA to Chl (Hörtensteiner and Kräutler 2011). In addition, genes associated with several major Chl catabolites have been identified, including Chlorophyll *a-b* binding protein 13 (*CAB13*), non-yellow coloring 1 (*NYC1*), NYC1-like (*NOL)*, chlorophyllases *(CLHs)*, pheophorbide oxygenase (*PAO)*, and red Chl catabolite reductase (*RCCR*) (Eckhardt et al. 2004). No significant differences in expression levels were observed between the WT and the S12 mutant for genes involved in Chl biosynthesis. However, elevated expression levels of *CLH2*, a gene involved in Chl degradation, was observed in the S12 mutant (Figure III-9). To validate the RNA-Seq data, I used qRT-PCR to measure the expression levels of 16 genes, including genes associated with ion transport and Chl biosynthesis and degradation. The qRT-PCR analysis confirmed ~18 fold higher levels of *CLH2* in the S12 mutant. In comparison, *CAB13* and seven ion transporters, including two metal ion transporters were down-regulated in the S12 mutants, by 1.65- and 1.3–4.05-fold, respectively (Figure III-10O, A–I). The expression levels of five other ion transporter genes were ~4.5–52.3-fold higher in the S12 mutants (Figure III-10J–N). Together, these results suggest that the reduced levels of Chl in the S12 mutant could be a result of increased Chl degradation and/or impaired ion transport associated with Chl biosynthesis.

Table III-6. Primers used for qRT-PCR analysis.

Trinity ID	Primer Name	Sequence
TRINITY_DN35346_c0_g1	HAK5-F	TTG CAA GTT GGG CTC TTT CT
	HAK5-R	GAA CCA CAG CAC AAT GAT GG
TRINITY_DN86452_c2_g1	HAK17-F	GCA ATT GCT TGG GGG TAC TA
	HAK17-R	AAA TGG GCC AGT AGA CAT CG
TRINITY_DN82926_c0_g1	CCH-F	CGT TTC CGA CCA CGT ATT CT
	CCH-R	CCC TCT TAA CGG AAC CAA CA
TRINITY_DN82149_c4_g1	SUT35-F	CAG TTC AAG GGC TTG CTA GG
	SUT35-R	CGC AAA GGC AAT TAC TCC TC
TRINITY_DN81484_c2_g1	PHO11-F2	TTT GTG GAG AGG GGT GAG TC
	PHO11-R2	CTA ACG CCG AAC TCT CTT GG
TRINITY_DN82844_c0_g1	ZTP50-F	ATT CCT TTG GCG AAG GTT CT
	ZTP50-R	CTT TGT GGA AAG CAT CAG CA
TRINITY_DN55717_c0_g1	AMT31-F2	TAT AAG GGC GTG GAT GGT GT
	AMT31-R2	ACC AGC ATG AGA AGC AGG TT
TRINITY_DN82053_c3_g1	YSL9-F	CTG TGG CGT CAG ATC TCA AA
	YSL9-R	CGA GGA CTT TGG TCC ATG TT
TRINITY_DN86390_c5_g1	PLT5-F	AAG TAG TTG CCG AGG AAG CA
	PLT5-R	ACG TCG CTT ATG TCG AGG TC
TRINITY_DN59808_c0_g2	CAB13-F	TCT GCC CAG ACA CCA TCA TA
	CAB13-R	CTC CTT CGC TGA AGA TTT G
TRINITY_DN80260_c3_g15	NYC1-F	TTT GCT GTG AAT GAG CTT GG
	NYC1-R	GCC CCA TCC ATA TTG AAC AC
TRINITY_DN74882_c1_g1	CLH2-F	GCC CTT GCT TGT CTC AAC TC
	CLH2-R	GAA TCA GGT CCT GCA ATG GT
Genebank: GU181353	ACTIN-F	AAT CCC AAG GCA AAC AGA
	ACTIN-R	CCA TCA CCA GAA TCC AG

Table III-7. Functional classification of differentially expressed genes identified by KEGG clusters of orthologous genes (KOG) analysis.

Term	nseqs	pval	padj	Total_Number_of_KOG
KOG0224_Aquaporin (major intrinsic proteinfamily)[Carbohydratetransportandmetabolism]	8	5.61E-05	0.13957919	18
KOG3467_Histone H4 [Chromatin structure anddynamics]	6	0.00024576	0.30548493	11
KOG1339_Aspartyl protease [Posttranslationalmodification,proteinturnover,chaperones]	25	0.00084472	0.69998734	48
KOG4626_O-linked N-acetylglucosamine transferaseOGT[Carbohydratetransportandmetabolism,Posttranslationalmodification,proteinturnover,chaperones,Signaltransductionmechanisms]	15	0.00204894	1	23
KOG0927_Predicted transporter (ABC superfamily)[Generalfunctionpredictiononly]	5	0.00253318	1	11
KOG1283_Serine carboxypeptidases[Posttranslationalmodification,proteinturnover,chaperones]	11	0.00415058	1	28
KOG0051_RNA polymerase I termination factorsuperfamily[Transcription]	11	0.00415058	1	22
KOG2051_Nonsense-mediated mRNA decay 2 protein[RNAprocessingandmodification]	2	0.0042895	1	3
KOG1318_Helix loop helix transcription factor EB[Transcription]	7	0.00802821	1	15
KOG3207_Beta-tubulin folding cofactor E[Posttranslationalmodification,proteinturnover,chaperones]	8	0.01222629	1	13
KOG3070_Predicted RNA-binding protein containingPINdomainandinvovledintranslationorRNAprocessing[Translation,ribosomalstructureandbiogenesis]	3	0.01230859	1	3
KOG1604_Predicted mutarotase [Carbohydratetransportandmetabolism]	3	0.01230859	1	4
KOG0525_Branched chain alpha-keto aciddehydrogenaseE1,betasubunit[Energyproductionandconversion]	3	0.01230859	1	3
KOG0460_Mitochondrial translation elongationfactorTu[Translation,ribosomalstructureandbiogenesis]	3	0.01230859	1	6
KOG4194_Membrane glycoprotein LIG-1 [Signaltransductionmechanisms]	4	0.02355206	1	12
KOG4656_Copper chaperone for superoxidedismutase[Inorganiciontransportandmetabolism]	10	0.02374824	1	22
KOG1237_H+/oligopeptide symporter [Amino acidtransportandmetabolism]	36	0.0278775	1	61
KOG1114_Tripeptidyl peptidase II[Posttranslationalmodification,proteinturnover,chaperones]	5	0.03756465	1	16
KOG1571_Predicted E3 ubiquitin ligase[Posttranslationalmodification,proteinturnover,chaperones]	5	0.03756465	1	6
KOG0501_K+-channel KCNQ [Inorganic ion transportandmetabolism]	5	0.03756465	1	16
KOG0143_Iron/ascorbate family oxidoreductases[Secondarymetabolitesbiosynthesis,transportandcatabolism,Generalfunctionpredictiononly]	41	0.04899636	1	87
KOG0039_Ferric reductaserelatedproteins[Inorganiciontransportandmetabolism,Secondarymetabolitesbiosynthesis,transportandcatabolism]	6	0.05393668	1	8
KOG4198_RNA-binding Ran Zn-finger protein andrelatedproteins[Generalfunctionpredictiononly]	6	0.05393668	1	10
KOG0684_Cytochrome P450 [Secondary metabolitesbiosynthesis,transportandcatabolism]	42	0.05414415	1	94
KOG0724_Zuotin and related molecular chaperones(DnaJsuperfamily),containsDNA-bindingdomains[Posttranslationalmodification,proteinturnover,chaperones]	14	0.05931852	1	24
KOG0977_Nuclear envelope protein lamininintermediatefilamentsuperfamily[Cellcyclecontrol,celldivision,chromosomepartitioning,Nuclearstructure]	1	0.06557108	1	5

Table III-7. Continued.

Term	nseqs	pval	padj	Total_Number_of_KOG
KOG4795_Protein associated with transcriptionalelongationfactorELL[Transcription]	1	0.06557108	1	1
KOG4160_BPI/LBP/CETP family protein [Defensemechanisms]	1	0.06557108	1	1
KOG4582_Uncharacterized conserved proteincontainsZZ-typeZn-finger[Generalfunctionpredictiononly]	1	0.06557108	1	1
KOG2558_Negative regulator of histones[Transcription]	1	0.06557108	1	1
KOG4696_Uncharacterized conserved protein[Functionunknown]	1	0.06557108	1	1
KOG1475_Ribosomal protein RPL1/RPL2/RL4L4 [RNAprocessingandmodification]	1	0.06557108	1	6
KOG0816_Protein involved in mRNA turnover [RNAprocessingandmodification]	1	0.06557108	1	3
KOG2368_Hydroxymethylglutaryl-CoA lyase [Energyproductionandconversion,Aminoacidtransportandmetabolism]	1	0.06557108	1	1
KOG1335_Dihydrolipoamide dehydrogenase [Energyproductionandconversion]	1	0.06557108	1	3
KOG3327_Thymidylate kinase/adenylate kinase[Nucleotidetransportandmetabolism]	1	0.06557108	1	1
KOG1446_Histone H3 (Lys4) methyltransferasecomplexandRNAcleavagefactorIIcomplex, subunitSWD2[RNAprocessingandmodification,Chromatinstructureanddynamics,Posttranslationalmodification,proteinturnover,chaperones]	1	0.06557108	1	1
KOG1450_Predicted Rho GTPase-activating protein[Signaltransductionmechanisms]	1	0.06557108	1	1
KOG4321_Predicted phosphate acyltransferases[Lipidtransportandmetabolism]	1	0.06557108	1	1
KOG0836_F-actin capping protein[Cytoskeleton]	1	0.06557108	1	2
KOG4413_26S proteasome regulatory complexsubunitPSMD5[Posttranslationalmodification,proteinturnover,chaperones]	1	0.06557108	1	1
KOG0766_Predicted mitochondrial carrier protein[Energyproductionandconversion]	1	0.06557108	1	3
KOG2154_Predicted nucleolar protein involved inribosomebiogenesis[Translation,ribosomalstructureandbiogenesis]	1	0.06557108	1	1
KOG1046_Puromycin-sensitive aminopeptidase andrelatedaminopeptidases[Aminoacidtransportandmetabolism,Posttranslationalmodification,proteinturnover,chaperones]	1	0.06557108	1	4
KOG2111_Uncharacterized conserved proteincontainsWD40repeats[Functionunknown]	1	0.06557108	1	4
KOG0388_SNF2 family DNA-dependent ATPase[Replication,recombinationandrepair]	1	0.06557108	1	1
KOG2681_Metal-dependent phosphohydrolase[Functionunknown]	1	0.06557108	1	1
KOG0904_Phosphatidylinositol 3-kinase catalyticsubunit(p110)[Signaltransductionmechanisms]	1	0.06557108	1	2
KOG1161_Protein involved in vacuolarpolyphosphateaccumulation,containsSPXdomain[Inorganiciontransportandmetabolism]	1	0.06557108	1	3

Table III-7. Continued.

Term	nseqs	pval	padj	Total_Number_of_KOG
KOG2458_Endoplasmic reticulum protein EP58containsfilaminroddomainandKDELmotif[Generalfunctionpredictiononly]	1	0.06557108	1	3
KOG2697_Histidinol dehydrogenase [Amino acidtransportandmetabolism]	1	0.06557108	1	1
KOG4166_Thiamine pyrophosphate-requiring enzyme[Aminoacidtransportandmetabolism,Coenzymetransportandmetabolism]	1	0.06557108	1	1
KOG1440_CDP-diacylglycerol synthase [Lipidtransportandmetabolism]	1	0.06557108	1	2
KOG0266_WD40 repeat-containing protein [Generalfunctionpredictiononly]	1	0.06557108	1	4
KOG3440_Ubiquinol cytochrome c reductasesubunitQCR7[Energyproductionandconversion]	1	0.06557108	1	2
KOG2664_Small nuclear RNA activating proteincomplex-50kDsubunit(SNAP50)[Transcription]	1	0.06557108	1	1
KOG2642_Alpha-1glucosyltransferase/transcriptionalactivator[Posttranslationalmodification,proteinturnover,chaperones,Transcription,Lipidtransportandmetabolism,Signaltransductionmechanisms]	1	0.06557108	1	1
KOG2306_Uncharacterized conserved protein[Functionunknown]	1	0.06557108	1	1
KOG0573_Asparagine synthase [Amino acidtransportandmetabolism]	1	0.06557108	1	1
KOG1273_WD40 repeat protein [General functionpredictiononly]	1	0.06557108	1	2
KOG3599_Ca2+-modulated nonselective cationchannelpolycystin[Inorganiciontransportandmetabolism,Signaltransductionmechanisms]	1	0.06557108	1	1
KOG0465_Mitochondrial elongation factor[Translation,ribosomalstructureandbiogenesis]	1	0.06557108	1	2
KOG0484_Transcription factor PHOX2/ARIXcontainsHOXdomain[Transcription]	1	0.06557108	1	1
KOG2906_RNA polymerase III subunit C11[Transcription]	1	0.06557108	1	2
KOG3784_Sorting nexin protein SNX27 [Generalfunctionpredictiononly,Signaltransductionmechanisms,Intracellulartrafficking,secretion,andvesiculartransport]	1	0.06557108	1	3
KOG0825_PHD Zn-finger protein [General functionpredictiononly]	1	0.06557108	1	3
KOG0951_RNA helicase BRR2[RNAprocessingandmodification]	1	0.06557108	1	1
KOG3110_Riboflavin kinase [Coenzyme transportandmetabolism]	1	0.06557108	1	1
KOG0186_Proline oxidase [Amino acid transportandmetabolism]	1	0.06557108	1	4
KOG1525_Sister chromatid cohesion complex CohesinsubunitPDS5[Cellcyclecontrol,celldivision,chromosomepartitioning]	1	0.06557108	1	5
KOG4635_Vacuolar import and degradation protein[Intracellulartrafficking,secretion,andvesiculartransport]	1	0.06557108	1	1
KOG2962_Prohibitin-related membrane proteasesubunits[Generalfunctionpredictiononly]	1	0.06557108	1	1

Table III-7. Continued.

Term	nseqs	pval	padj	Total_Number_of_KOG
KOG3636_Uncharacterized conserved proteincontainsTBCandRhodanesedomains[Generalfunction predictiononly]	1	0.06557108	1	2
KOG4573_Phosphoprotein involved in cytoplasm tovacuoletargetingandautophagy[Intracellulartrafficking,secretion,andvesiculartransport]	1	0.06557108	1	2
KOG0540_3-Methylcrotonyl-CoA carboxylasenon-biotincontainingsubunit/Acetyl-CoAcarboxylasecarboxyltransferase,subunitbeta[Aminoacidtransportandmetabolism,Lipidtransportandmetabolism]	1	0.06557108	1	4
KOG4218_Nuclear hormone receptor betaFTZ-F1[Transcription]	1	0.06557108	1	1
KOG3148_Glucosamine-6-phosphate isomerase[Carbohydratetransportandmetabolism]	1	0.06557108	1	1
KOG2332_Ferritin [Inorganic ion transport andmetabolism]	1	0.06557108	1	7
KOG3121_Dynactin	1	0.06557108	1	1
KOG1967_DNA repair/transcription protein Mms19[Replication,recombinationandrepair,Transcription]	1	0.06557108	1	1
KOG3198_Signal recognition particleSrp19[Intracellulartrafficking,secretion,andvesiculartransport]	1	0.06557108	1	1
KOG0170_E3 ubiquitin protein ligase[Posttranslationalmodification,proteinturnover,chaperones]	1	0.06557108	1	1
KOG1963_WD40 repeat protein [General functionpredictiononly]	1	0.06557108	1	1
KOG0719_Molecular chaperone (DnaJ superfamily)[Posttranslationalmodification,proteinturnover,chaperones]	1	0.06557108	1	2
KOG1628_40S ribosomal protein S3A [Translationribosomalstructureandbiogenesis]	1	0.06557108	1	3
KOG0105_Alternative splicing factor ASF/SF2(RRMsuperfamily)[RNAprocessingandmodification]	1	0.06557108	1	1
KOG0195_Integrin-linked kinase [Signaltransductionmechanisms]	15	0.07066646	1	24
KOG0626_Beta-glucosidasephlorizinhydrolase,andrelatedproteins[Carbohydratetransportandmetabolism]	7	0.07230006	1	16
KOG1150_Predicted molecular chaperone (DnaJsuperfamily)[Posttranslationalmodification,proteinturnover,chaperones]	7	0.07230006	1	13
KOG1050_Trehalose-6-phosphate synthase componentTPS1andrelatedsubunits[Carbohydratetransportandmetabolism]	7	0.07230006	1	17
KOG1192_UDP-glucuronosyl and UDP-glucosyltransferase[Carbohydratetransportandmetabolism,Energyproductionandconversion]	59	0.08934989	1	135
KOG0905_Phosphoinositide 3-kinase [Signaltransductionmechanisms]	8	0.09232465	1	9

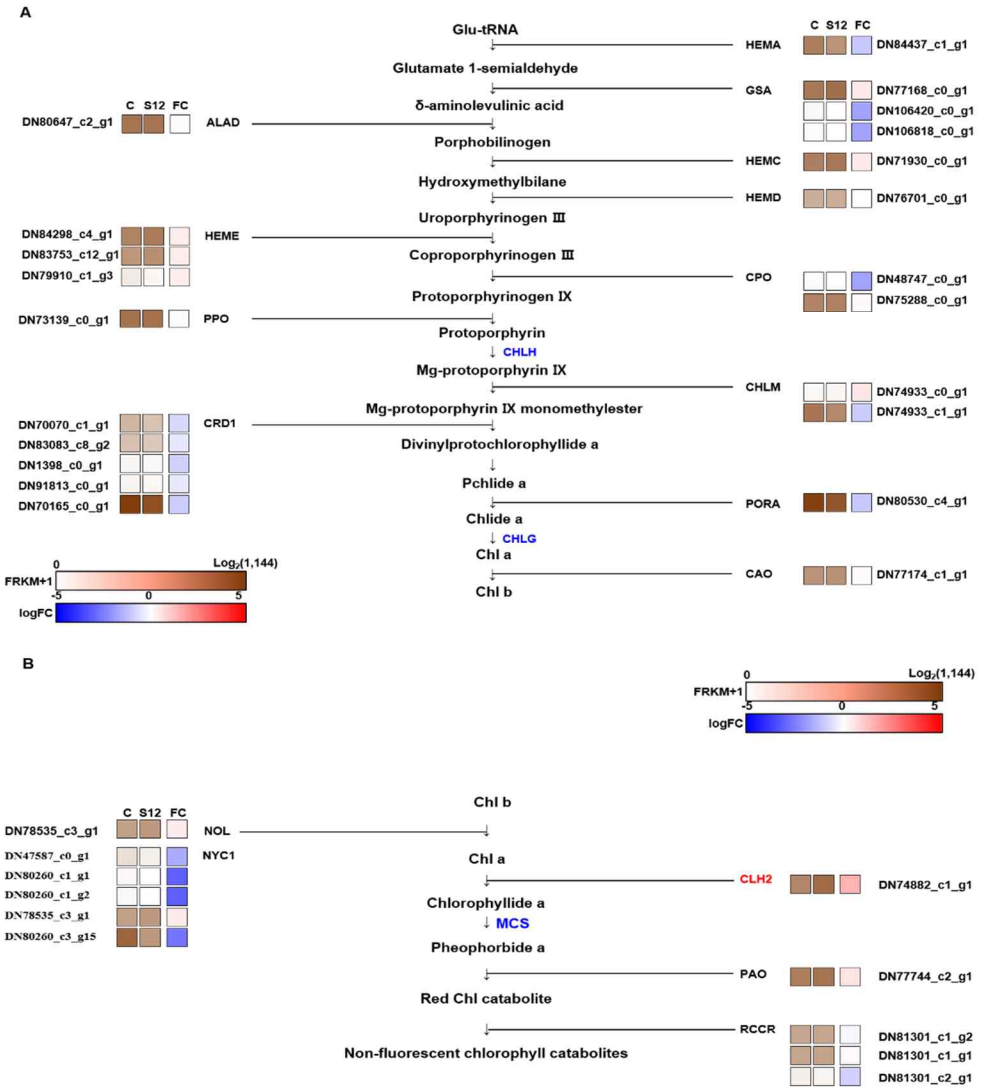

Figure III-9. Schematic diagram of reads mapped to genes encoding proteins involved in chlorophyll biosynthesis and degradation. (**A**) Chlorophyll biosynthetic pathway. (**B**) Chlorophyll degradation pathway. C, S12, and FC stand for wild-type, S12 mutant, and fold change, respectively. In both (**A**) and (**B**), the logarithm of the FPKM (fragments per kilobase of exon per million fragments mapped) +1 value of each sample and the logarithm of the ratio of the FPKM+1 values of two samples are represented by the color scales in the bottom right-hand corner of the figure.

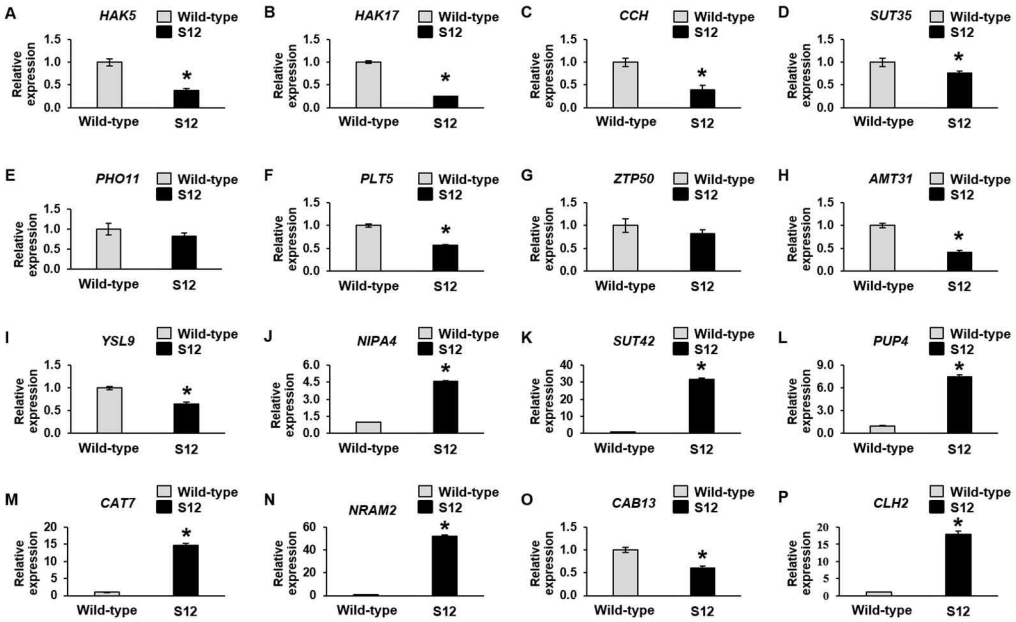

Figure III-10. Quantitative real-time PCR analysis of 16 genes showing altered expression in the RNA-Seq analysis. The genes were associated with ion transporters (**A–N**), chlorophyll biosynthesis (**O**), and chlorophyll degradation (**P**). More specifically, **A–P** indicate the relative expression levels of Potassium transporter 5 (*HAK5*), Potassium transporter 17 (*HAK17*), Copper transport protein CCH (*CCH*), Sulfate transporter 3;5 (*SUT35*), Phosphate transporter PHO1 homolog 1 (*PHO11*), Polyol transporter (*PLT5*), Zinc transporter 50 (*ZTP50*), Ammonium transporter 3 member 1 (*AMT31*), Metal-nicotianamine transporter (*YSL9*), Magnesium transporter (*NIPA4*), Sulfate transporter 4;2 (*SUT42*), Amino acid permease family protein (*PUT4*), Cationic amino acid transporter 7 (*CAT7*), Metal transporter Nramp2 (*NRAM2*), Chlorophyll *a-b* binding protein 13 (*CAB13*), and Chlorophyllase-2 (*CLH2*), respectively. The *ACTIN* gene served as an internal control. Error bars indicate standard deviation (n = 3). The experiment was repeated three times with similar results.

DISCUSSION

In this study, I used a γ-ray-based mutagenesis procedure to isolate a leaf-color mutant in C*ymbidium*, which showed a notable decreases in Chl and carotenoid levels. The RNA-Seq analysis identified 2,267 DEGs, including 724 up-regulated and 529 down-regulated in the S12 mutant. A functional classification of these genes allowed us to identify the chlorophyllase gene, *CLH2*, which was induced ~18-fold in the S12 mutants. The *CLH2*-encoded enzyme facilitates Chl catabolism, and increased levels of *CLH2* have been associated with reduced Chl contents in a number of plants (Rodriguez et al. 1987; Mınguez-Mosquera et al. 1994; Almela et al. 1996; Todorov et al. 2003; Ben-Yaakov et al. 2006; Aiamla-or et al. 2010; Chen et al. 2012; Kraj 2015). These results are consistent with a previous study (Zhu et al. 2015), which suggested that the yellow-striped leaves of *C. sinense* variants were associated with increased Chl degradation. Notably, *C. sinense* variants characterized by Zhu et al. (2015) showed ~1–3-fold higher expression levels of *CLH2* compared with the ~18-fold increase seen in the S12 mutant. Zhu et al. also observed a ~1–3-fold increase in the expression levels of *RCCR*, which acts downstream of *CLH2* in the Chl degradation pathway (Zhu et al. 2015). However, unlike the *C. sinense*

variants characterized by Zhu et al. (2015), the S12 mutant showed normal expression levels of *RCCR*. Consistent with previous studies (Jung et al. 2003; Nagata et al. 2005; Sakuraba et al. 2013; Zhu et al. 2015; Ma et al. 2017; Qin et al. 2017), the S12 mutant also showed reduced levels of carotenoids, a phenotype commonly observed in Chl-deficient mutants. The S12 mutant also contained an altered Chl *a* to Chl *b* ratio, in which Chl *b* is required to stabilize the light-harvesting protein complex (Huang et al. 2013). This, in turn, correlated with a reduced expression level of *NYC1* in the S12 mutant, which encodes a chlorophyll *b* reductase that catalyzes the conversion of Chl *b* to Chl *a*. Thus, a reduced Chl content and decreased Chl *a/b* ratio in the S12 mutant may be associated with fewer light-harvesting antenna complexes. In contrast, the S12 mutant showed normal expression levels of all 16 genes associated with Chl biosynthesis. This further suggests that the reduced Chl content in S12 leaves was likely associated with Chl catabolism and not biosynthesis.

Metals such as iron (Fe), copper (Cu), manganese (Mn), zinc (Zn), and magnesium (Mg) play key roles as cofactors in photosynthesis: Fe, as a cofactor for three photosynthetic electron transfer chain complexes; Cu, as a cofactor for thylakoid lumen electron transport protein plastocyanin; Mn, for photosystem II functions; Zn, plays a key role in the catalysis of chloroplastic ß-carbonic anhydrase enzyme; and Mg, in the center of the Chl ring (Shcolnick and Keren

2006; Pilon et al. 2009; Yruela 2013). The transitions of these metal ions are regulated to maintain cellular homeostasis, and excess metal ions cause oxidative stress because of their deleterious interactions with oxygen (Shcolnick and Keren 2006; Pilon et al. 2009). In this study, I identified diverse metal ion transporters among down-regulated DEGs. In particular, the down-regulated expression levels of *CCH* (Cu-ion transporter) and *YSL9* (Fe-ion transporter) were confirmed by qRT-PCR (Table III-5). The Arabidopsis *CCH* gene is a functional homolog of the yeast (*Saccharomyces cerevisiae*) gene *Anti-oxidant 1*, which, when mutated, results in a reduced Fe-uptake capability (Himelblau et al. 1998). Senoura et al. (2017) reported that *OsYSL9* mainly localizes in the plasma membrane and transports Fe(II)-nicotianamine and Fe(III)-deoxymugineic acid. The expression of *OsYSL9* is repressed in the leaves under Fe-starvation conditions. The down-regulated expressions of *CCH* and *YSL9* could affect the Fe ion transition in the cell, which could be correlated with the reduced Chl content in the S12 mutant. NRAMP proteins are involved in Fe homeostasis (Varotto et al. 2002), and the expression levels of *AtNRAMP1*, *3*, and *4* are up-regulated in response to Fe deficiency (Curie et al. 2000; Thomine et al. 2000). Additionally, *AtNRAMP3* and *4* remobilize vacuolar Mn in leaves and have important roles in photosystem II functions (Lanquar et al. 2010). In cyanobacteria, the ABC-type Mn transport complex is induced under Mn-

starvation conditions (Bartsevich et al. 1995). In the S12 mutant, the reduced Fe content is expected because of the down-regulated expression levels of *CCH* and *YSL9* (Table III-5). Additionally, the up-regulated expression levels of *NRAM2* and the ABC transporter family were identified (Table III-4), which was consistent with previous reports (Bartsevich et al. 1995; Curie et al. 2000; Thomine et al. 2000; Lanquar et al. 2010).

In the present study, I found that seven genes involved in ion transport, including two metal ion transporters (*CCH* and *YSL9*), were down-regulated, and *CLH2*, associated with Chl degradation, was up-regulated in the yellow leaf-color mutant, S12. This provides useful information for understanding Chl biosynthesis and degradation in *Cymbidium*. In addition, these results show that γ-ray-based mutagenesis can be employed as a useful tool to generate genetic diversity among orchid species.

REFERENCES

Aceto S, Gaudio L. 2011. The MADS and the beauty: genes involved in the development of orchid flowers. Curr Genomics. 12(5): 342–356.

Adhikari ND, Froehlich JE, Strand DD, Buck SM, Kramer DM, Larkin RM. 2011. GUN4-porphyrin complexes bind the ChlH/GUN5 subunit of Mg-Chelatase and promote chlorophyll biosynthesis in *Arabidopsis*. Plant Cell. 23(4): 1449–1467.

Aiamla-or S, Kaewsuksaeng S, Shigyo M, Yamauchi N. 2010. Impact of UV-B irradiation on chlorophyll degradation and chlorophyll-degrading enzyme activities in stored broccoli (*Brassica oleracea* L. Italica Group) florets. Food Chem. 120(3): 645–651.

Almela L, Javaloy S, Fernández-López JA, López-Roca JM. 1996. Varietal classification of young red wines in terms of chemical and colour parameters. J Sci Food Agric. 70(2): 173–180.

Bartsevich VV, Pakrasi HB. 1995. Molecular identification of an ABC transporter complex for manganese: analysis of a cyanobacterial mutant strain impaired in the photosynthetic oxygen evolution process. EMBO J. 14(9): 1845-53.

Benjamini Y, Hochberg Y. 1995. Controlling the false discovery rate: a practical and powerful approach to multiple testing. J R Stat Soc Series B Stat Methodol. 57(1): 289–300.

Bennett MD, Leitch IJ. 2005. Nuclear DNA amounts in angiosperms: progress, problems and prospects. Ann Bot. 95(1):45–90.

Ben-Yaakov E, Harpaz-Saad S, Galili D, Eyal Y, Goldschmidt E. 2006. The relationship between chlorophyllase activity and chlorophyll degradation during the course of leaf senescence in various plant species. Isr J Plant Sci. 54(2): 129–135.

Blanco E, Parra G, Guigó R. Using geneid to identify genes. 2007. Curr Protoc Bioinformatics. 18(1): 4.3.1–4.3.28.

Bolger AM, Lohse M, Usadel B. 2014. Trimmomatic: a flexible trimmer for

Illumina sequence data. Bioinformatics. 30(15): 2114–2120.

Burkhead JL, Gogolin Reynolds KA, Abdel-Ghany SE, Cohu CM, Pilon M. 2009. Copper homeostasis. New Phytol. 182(4): 799–816.

Cheamuangphan A, Panmanee C, Tansuchat R. 2013. Value chain analysis for orchid cut flower business in Chiang Mai. Business and Information. pp. 7–9.

Cai J, Liu X, Vanneste K, Proost S, Tsai WC, Liu KW, et al. 2015. The genome sequence of the orchid *Phalaenopsis equestris*. Nat Genet. 47:65–72.

Chen W, Zheng J, Li Y, Guo W. 2010. Effects of high temperature on photosynthesis, chlorophyll fluorescence, chloroplast ultrastructure, and antioxidant activities in fingered citron. Russ J Plant Physiol. 59(6): 732–740.

Choi S, Kim M, Lee J, Ryu K. 2006. Genetic diversity and phylogenetic relationships among and within species of oriental cymbidiums based on RAPD analysis. Sci Hortic. 108(1): 79–85.

Christenhusz MJ, Byng JW. 2016. The number of known plants species in the world and its annual increase. Phytotaxa. 261(3): 201–217.

Chugh S, Guha S, Rao IU. 2009. Micropropagation of orchids: a review on the potential of different explants. Sci Hortic. 122(4): 507–520.

Curie C, Alonso JM, Le Jean M, Ecker JR, Briat JF. 2000. Involvement of NRAMP1 from Arabidopsis thaliana in iron transport. Biochem J. 347: 749–55.

Deng X, Zhang H, Wang Y, Shu Z, Wang G, Wang G. 2012. Research advances on rice leaf-color mutant genes. Hybrid Rice. 27(5): 9–14.

Deng X-J, Zhang H-Q, Wang Y, He F, Liu J-L, Xiao X, et al. 2014. Mapped clone and functional analysis of leaf-color gene *Ygl7* in a rice hybrid (*Oryza sativa* L. ssp. *indica*). PLoS ONE. 9(6): e99564.

Eckhardt U, Grimm B, Hörtensteiner S. 2004. Recent advances in chlorophyll biosynthesis and breakdown in higher plants. Plant Mol Biol. 56(1): 1–14.

Grabherr MG, Haas BJ, Yassour M, Levin JZ, Thompson DA, Amit I, et al. 2011. Full-length transcriptome assembly from RNA-Seq data without a reference genome. Nat Biotechnol. 29(7): 644.

Haas BJ, Papanicolaou A, Yassour M, Grabherr M, Blood PD, Bowden J, et al. 2013. *De novo* transcript sequence reconstruction from RNA-seq using the Trinity platform for reference generation and analysis. Nat Protoc. 8(8): 1494.

Hendry GAF, Price AH. 1993. Stress indicators: chlorophylls and carotenoids. *In*: Hendry GAF, Grime JP (eds) Methods in comparative plant ecology. Chapman & Hall, London, pp. 148–152.

Himelblau E, Mira H, Lin S-J, Culotta VC, Peñarrubia L, Amasino RM. 1998. Identification of a functional homolog of the yeast copper homeostasis gene *ATX1* from Arabidopsis. Plant Physiol. 117: 1227–34.

Hörtensteiner S, Kräutler B. 2011. Chlorophyll breakdown in higher plants. Biochim Biophys Acta Bioenerg. 1807(8): 977–988.

Huang DW, Sherman BT, Tan Q, Collins JR, Alvord WG, Roayaei J, et al. 2007. The DAVID gene functional classification tool: a novel biological module-centric algorithm to functionally analyze large gene lists. Genome Biol. 8(9): R183.

Huang J, Qin F, Zang G, Kang Z, Zou H, Hu F, et al. 2013. Mutation of *OsDET1* increases chlorophyll content in rice. Plant Sci. 210: 241–249.

Huang W, Chen Q, Zhu Y, Hu F, Zhang L, Ma Z, He Z, Huang J. 2013. *Arabidopsis* thylakoid formation 1 is a critical regulator for dynamics of PSII-LHCII complexes in leaf senescence and excess light. Mol Plant. 6:1673–91.

Jung K-H, Hur J, Ryu C-H, Choi Y, Chung Y-Y, Miyao A, et al. 2003. Characterization of a rice chlorophyll-deficient mutant using the T-DNA gene-trap system. Plant Cell Physiol. 44(5): 463–472.

Kraj W. 2015. Chlorophyll degradation and the activity of chlorophyllase and Mg-dechelatase during leaf senescence in *Fagus sylvatica*. Dendrobiol. 74: 43–57.

Lanquar V, Ramos MS, Lelièvre F, Barbier-Brygoo H, Krieger-Liszkay A, Krämer U, et al. 2010. Export of vacuolar manganese by *At*NRAMP3 and *At*NRAMP4 is required for optimal photosynthesis and growth under manganese deficiency. Plant Physiol. 152(4): 1986-99.

Lee S, Kim J-H, Yoo ES, Lee C-H, Hirochika H, An G. 2005. Differential regulation of *chlorophyll a oxygenase* genes in rice. Plant Mol Biol.

57(6): 805–818.

Leitch IJ, Bennett MD. 2007. Genome size and its uses: The impact of flow cytometry. *In*: Dolezel J, Greilhuber J, Suda J, (eds) Flow cytometry with plant cells: Analysis of genes, chromosomes and genomes.

Leitch IJ, Kahandawala I, Suda J, Hanson L, Ingrouille MJ, Chase MW, Fay MF. 2009. Genome size diversity in orchids: consequences and evolution. Ann Bot. 104:469–481.

Li B, Dewey CN. 2011. RSEM: accurate transcript quantification from RNA-Seq data with or without a reference genome. BMC Bioinformatics. 12(1): 323.

Li Y, Imai K, Ohno H, Matsui S. 2004. Effects of acclimatization temperatures on antioxidant enzyme activities in mericlones of a cattleya hybrid. J Jap Soc Hort Sci. 73(4): 386–392.

Liu W, Fu Y, Hu G, Si H, Zhu L, Wu C, et al. 2007. Identification and fine mapping of a thermo-sensitive chlorophyll deficient mutant in rice (*Oryza sativa* L.). Planta. 226(3): 785–795.

López-Millán AF, Duy D, Philippar K. 2016. Chloroplast iron transport proteins–function and impact on plant physiology. Front Plant Sci. 7: 178.

Ma X, Sun X, Li C, Huan R, Sun C, Wang Y, et al. 2017. Map-based cloning and characterization of the novel yellow-green leaf gene *ys83* in rice (*Oryza sativa*). Plant Physiol Biochem. 111: 1–9.

Mınguez-Mosquera M, Hornero-Méndez D. 1994. Formation and transformation of pigments during the fruit ripening of *Capsicum annuum* cv. *Bola* and *Agridulce*. J Agric Food Chem. 42: 38–44.

Nagata N, Tanaka R, Satoh S, Tanaka A. 2005. Identification of a vinyl reductase gene for chlorophyll synthesis in *Arabidopsis thaliana* and implications for the evolution of Prochlorococcus species. Plant Cell. 17(1): 233–240.

Nouet C, Motte P, Hanikenne M. 2011. Chloroplastic and mitochondrial metal homeostasis. Trends Plant Sci. 16(7): 395–404.

Pilon M, Cohu CM, Ravet K, Abdel-Ghany SE, Gaymard F. 2009. Essential transition metal homeostasis in plants. Curr Opin Plant Biol. 12(3): 347–357.

Qin R, Zeng D, Liang R, Yang C, Akhter D, Alamin M, et al. 2017. Rice gene

SDL/*RNRS1*, encoding the small subunit of ribonucleotide reductase, is required for chlorophyll synthesis and plant growth development. Gene. 627: 351–362.

Robinson MD, McCarthy DJ, Smyth GK. 2010. edgeR: a Bioconductor package for differential expression analysis of digital gene expression data. Bioinformatics. 26(1): 139–140.

Rodriguez M, Gonzélez M, Linares J. 1987. Degradation of chlorophyll and chlorophyllase activity in senescing barley leaves. J Plant Physiol. 129(3-4): 369–374.

Sakuraba Y, Rahman ML, Cho SH, Kim YS, Koh HJ, Yoo SC, et al. 2013. The rice *faded green leaf* locus encodes protochlorophyllide oxidoreductase B and is essential for chlorophyll synthesis under high light conditions. Plant J. 74(1): 122–133.

Sarmah D, Kolukunde S, Sutradhar M, Singh BK, Mandal T, Mandal N. 2017. A review on: *in vitro* cloning of orchids. Int J Curr Microbiol Appl Sci. 6(9): 1909–1927.

Senoura T, Sakashita E, Kobayashi T, Takahashi M, Aung MS, Masuda H, et al. 2017. The iron-chelate transporter OsYSL9 plays a role in iron distribution in developing rice grains. Plant Mol Biol. 95: 375–87.

Shcolnick S, Keren N. 2006. Metal homeostasis in cyanobacteria and chloroplasts. Balancing benefits and risks to the photosynthetic apparatus. Plant Physiol. 141: 805–10.

Tatusov RL, Fedorova ND, Jackson JD, Jacobs AR, Kiryutin B, Koonin EV, et al. 2003. The COG database: an updated version includes eukaryotes. BMC Bioinformatics. 4(1): 41.

Thomine S, Wang R, Ward JM, Crawford NM, Schroeder JI. 2000. Cadmium and iron transport by members of a plant metal transporter family in *Arabidopsis* with homology to *Nramp* genes. Proc Natl Acad Sci U S A. 97(9): 4991–6.

Tian X, Ling Y, Fang L, Du P, Sang X, Zhao F, et al. 2013. Gene cloning and functional analysis of yellow green leaf3 (*ygl3*) gene during the whole-plant growth stage in rice. Genes Genomics. 35(1): 87–93.

Todorov D, Karanov E, Smith AR, Hall M. 2003. Chlorophyllase activity and chlorophyll content in wild type and *eti 5* mutant of *Arabidopsis*

thaliana subjected to low and high temperatures. Biol Plant. 46(4): 633–636.

Tsai W, Dievart A, Hsu C, Hsiao Y, Chiou S, Huang H, Chen H. 2017. Post genomics era for orchid research. Bot Stud. 58:61.

Ulukapi K, Nasircilar AG. 2015. Developments of gamma ray application on mutation breeding studies in recent years. International Conference on Advances in Agricultural, Biological & Environmental Sciences (AABES-2015), London, United Kingdom. pp. 31-34.

Varotto C, Maiwald D, Pesaresi P, Jahns P, Salamini F, Leister D. 2002. The metal ion transporter IRT1 is necessary for iron homeostasis and efficient photosynthesis in *Arabidopsis thaliana*. Plant J. 31(5): 589–599.

Vert G, Grotz N, Dédaldéchamp F, Gaymard F, Guerinot ML, Briat J-F, et al. 2002. IRT1, an Arabidopsis transporter essential for iron uptake from the soil and for plant growth. Plant Cell. 14(6): 1223–1233.

Wang P, Gao J, Wan C, Zhang F, Xu Z, Huang X, et al. 2010. Divinyl chlorophyll(ide) *a* can be converted to monovinyl chlorophyll(ide) *a* by a divinyl reductase in rice. Plant Physiol. 153(3): 994–1003.

Wu Z, Zhang X, He B, Diao L, Sheng S, Wang J, et al. 2007. A chlorophyll-deficient rice mutant with impaired chlorophyllide esterification in chlorophyll biosynthesis. Plant Physiol. 145(1): 29–40.

Xu Y, Teo LL, Zhou J, Kumar PP, Yu H. 2006. Floral organ identity genes in the orchid *Dendrobium crumenatum*. Plant J. 46(1): 54–68.

Yan L, Wang X, Liu H, Tian Y, Lian J, Yang R, et al. 2015. The genome of *Dendrobium officinale* illuminates the biology of the important traditional Chinese orchid herb. Mol Plant. 8:922–934.

Yruela I. 2009. Copper in plants: acquisition, transport and interactions. Funct Plant Biol. 36(5): 409–430.

Yruela I. 2013. Transition metals in plant photosynthesis. Metallomics. 5(9): 1090–1109.

Yukawa T, Stern WL. 2002. Comparative vegetative anatomy and systematics of *Cymbidium* (Cymbidieae: Orchidaceae). Bot J Linn Soc. 138(4): 383–419.

Zhang J, Wu K, Zeng S, da Silva JAT, Zhao X, Tian C-E, et al. 2013.

Transcriptome analysis of *Cymbidium sinense* and its application to the identification of genes associated with floral development. BMC Genomics. 14(1): 279.

Zhang H, Li J, Yoo J-H, Yoo S-C, Cho S-H, Koh H-J, et al. 2006. Rice *Chlorina-1* and *Chlorina-9* encode ChlD and ChlI subunits of Mg-chelatase, a key enzyme for chlorophyll synthesis and chloroplast development. Plant Mol Biol. 62(3): 325–337.

Zhou K, Ren Y, Lv J, Wang Y, Liu F, Zhou F, et al. 2013. *Young Leaf Chlorosis 1*, a chloroplast-localized gene required for chlorophyll and lutein accumulation during early leaf development in rice. Planta. 237(1): 279–292.

Zhu G, Yang F, Shi S, Li D, Wang Z, Liu H, et al. 2015. Transcriptome characterization of *Cymbidium sinense* 'Dharma' using 454 pyrosequencing and its application in the identification of genes associated with leaf color variation. PLoS ONE. 10(6): e0128592.

CHAPTER IV

γ-irradiation combined with light modulation increases the frequency of leaf-color mutation in *Cymbidium*

This research has been submitted in *Plants*.

ABSTRACT

Radiation randomly induces chromosomal mutations in plants. However, it was recently found that the rate of flower-color mutation could be specifically increased by up-regulating anthocyanin pathway gene expression before conducting radiation treatments. The mechanisms of chlorophyll biosynthesis and degradation are active areas of plant study because chlorophyll metabolism is closely connected to photosynthesis. In this study, I determined the optimal light modulation for up-regulating the expression of six chlorophyll pathway genes and measured effects of light modulation on the γ-irradiation-induced frequency of leaf-color mutation in two *Cymbidium* cultivars. To degrade chlorophylls in rhizomes, 60–75 days of dark treatment was required. To up-regulate the expression of chlorophyll pathway genes, 10 days of light treatment was found to be optimal. Light modulation followed by γ-irradiation increased chlorophyll-related leaf mutants by 1.4- to 2.0-fold compared with γ-ray treatment alone. Light modulation combined with γ-irradiation increased the frequency of leaf-color mutants in *Cymbidium*, supporting wider implementation of plant breeding methodology that increases the mutation frequency of a target trait by controlling the expression of genes related to the target trait.

INTRODUCTION

Physical mutagens, such as X-rays (Howden et al. 1995; Roman et al. 1995; Shirley et al. 1995), γ-rays (Mandal et al. 2000; Yamaguchi et al. 2008; Pestanana et al. 2011), and ion particles (Roman et al. 1995; Shirley et al. 1995; Shikazono et al. 2003; Hase et al. 2012; Kim et al. 2019), and chemical mutagens, such as ethyl methanesulfonate (Roman et al. 1995; Shirley et al. 1995; Gady et al. 2009; Garcia et al. 2016; Shirasawa et al. 2016), *N*-nitroso-*N*-methylurea (Yang et al. 2016; Huang et al. 2017; Coe et al. 2018), and colchicine (Chen et al. 2011; Blasco et al. 2015; Cai et al. 2015), have been widely used to induce mutations in various plants. In plant mutation breeding, researchers have focused on developing methods to increase mutation frequency and broaden the mutation spectrum. Three strategies have been explored to achieve these objectives: firstly, controlling irradiation conditions, such as total dose (Yamaguchi et al. 2008, 2009; Kodym et al. 2012; Lee et al. 2016), dose rate (Natarajan and Maric 1961; Mabuchi and Matsumura 1964; Nishiyama et al. 1966; Dewey 1969; Killion and Constantin 1971; Bottino et al. 1975), and irradiation duration (Kim et al. 2016, 2019); secondly, controlling the material condition, such as developmental stage (Kowyama et al. 1994) and plant tissues (Okamura et al. 2015; Hase et al. 2018);

and finally, using different radiation types, such as aerospace environment (Liu et al. 2007; Yu et al. 2013), heavy ion particles (Shikazono et al. 2005; Yamaguchi et al. 2009; Tanaka et al. 2010), and proton ion particles (Lee et al. 2015; Kim et al. 2019). Generally, radiation induces mutations randomly in plant chromosomes.

Recently, it was reported that in human cells the sensitivity of DNA to γ-irradiation varied with the chromatin status (Takata et al. 2013; Venkatesh et al. 2016). Takata et al. (2013) reported that the ratio of DNA double-strand breaks to γ-irradiation was higher in decondensed chromatin than in condensed chromatin, and Venkatesh et al. (2016) verified that sensitivity to γ-irradiation, in terms of DNA double-strand breaks, was higher in euchromatin than heterochromatin regions. In addition, Hase et al. (2010) suggested that radiation could increase the mutation frequency for flower color when the genes involved in flower-color synthesis are highly expressed. The effect of sucrose treatment on the expression of anthocyanin pathway genes, an important mechanism for altering flower color (Tanaka et al. 2008), has been demonstrated in Arabidopsis (Solfanelli et al. 2006). Sucrose treatment followed by radiation treatment increased the frequency of flower-color mutation in chrysanthemum and petunia, although no measurements of anthocyanin pathway gene expression were made (Hase et al. 2010; Kim et al. 2016). Recently, Kim et al. (2019) demonstrated that

sucrose and methyl jasmonate treatment increases flower-color mutation induced by γ-irradiation in chrysanthemum, confirming up-regulated expression for several anthocyanin pathway genes.

For floricultural crops, flower and leaf color are considered to be among the most important characteristics that determine commercial value in the flower market. In particular, variegation of leaves in foliage plants is more important than that of flowers. In rice, variegation of leaves has been extensively studied to understand chlorophyll (Chl) biosynthesis and degradation, chloroplast development, and photosynthesis (Deng et al. 2014). So far, more than 50 leaf-color related genes have been cloned in rice (Deng et al. 2014; Ma et al. 2017). It was reported that mutations of 13 genes (*gra75*, *OsCAO*, *OsCHLD*, *OsCHLH*, *OsChlI*, *OsDET1*, *OsDVR*, *OsGluRS*, *OsPORB*, *lyl1-1*, *sdl*, *ygl1*, and *ygl7*) in the Chl biosynthesis pathway and five genes (*sgr*, *nol*, *nyc1*, *nyc3*, and *nyc4*) in the Chl degradation pathway caused phenotypic variations in rice (Yamatani et al. 2013; Deng et al. 2014; Ma et al. 2017; Qin et al. 2017). Chls are synthesized instantly upon light exposure (Zhu et al. 2017) and, in association with photosystem II, absorb light energy to drive essential photochemistry in photosynthesis (Baker 2008). In plants, there are two forms of Chls, Chl *a* and *b* (Zhu et al. 2017). Zhu et al. (2017) reported that phytohormones, such as ethylene, abscisic acid, and jasmonic acid, and light affect Chl degradation. In addition, it

was reported that salicylic acid (Morris et al. 2000) and brassinolide (Jeong et al. 2010) are promoters, and cytokinin (Lara et al. 2004) and gibberellic acid (Kim et al. 2006) are repressors of Chl degradation.

In this study, I determined the optimal conditions for light modulation to induce up-regulated expression of Chl biosynthesis and degradation genes and assessed the effects of light modulation on the frequency of γ-irradiation-induced Chl-related leaf-color mutation in *Cymbidium*.

MATERIALS AND METHODS

Plant materials

In this study, two *Cymbidium* hybrid (*C. sinense* × *C. goeringii*) cultivars, "RB003" and "RB012" were used. Rhizomes of those two cultivars were cultured at 24 ± 1 °C with a 16-h photoperiod provided by white fluorescent lights (PPFD = 50 μmol m^{-2} s^{-1}) on medium (pH 5.35) comprising 0.1% Hyponex (N:P:K = 20:20:20; Hyponex Japan Co., Ltd., Osaka, Japan), 0.2% Hyponex (N:P:K = 6.5:6:19), 0.3% peptone (Duchefa B.V.), 3% sucrose (Duchefa B.V., Haarlem, The Netherlands), 0.38% plant agar (Duchefa B.V.), and 0.075% activated charcoal (Sigma-Aldrich, St Louis, MO, USA).

Light modulation

One-month-old rhizomes were used for light modulation of both cultivars. Light modulation was conducted following dark treatment as follows: to degrade the Chl in the rhizomes, dark treatment was carried out for 0, 20, 40, 60, 75, or 90 days; next, to synthesize Chl in the rhizomes, light treatment with a 16-h photoperiod (same as the culture condition) was carried out for 0, 1, 5, 7,

10, 14, 15, 20, or 21 days.

Chl analysis

Rhizomes treated with light modulation following dark treatment were sampled for Chl content analysis. The amounts of Chl *a* and *b* were estimated by the method of Lichtenthaler (1987). Rhizomes were ground in liquid nitrogen, and the pigments were extracted in 95% ethanol (Sigma, St. Louis, MO, USA). The extract was vortexed for 24 h at room temperature in the dark. After centrifugation, the absorbance of the supernatants were quantitatively measured with a UV-1800 spectrometer (Shimadzu, Kyoto, Japan) at 664.2 nm, 648.6 nm, and 470 nm. Experiments were performed as three replicates.

RNA extraction and RT-qPCR analysis

Total RNA was isolated from the light-modulated rhizomes using an RNeasy Plant Mini Kit (Qiagen, Hilden, Germany). The concentration and quality of the extracted RNA were assessed using a Nonodrop 2000 spectrophotometer (Thermo Fisher Scientific, Waltham, MA, USA). First-strand cDNA synthesis was conducted using a ReverTra Ace-α kit (Toyobo Co. Ltd,

Osaka, Japan). Reverse transcription quantitative PCR (RT-qPCR) was carried out with iQ SYBR Green Supermix (Bio-Rad, Hercules, CA, USA) using the CFX96 Touch Real-Time PCR Detection System (Bio-Rad, Hercules, USA). PCR was performed following the method of Kim et al. (2013). Transcript levels of each gene were normalized to those of *Actin*. Three experimental replicates were performed. Primer sequences were as follows: *HEMD*, 5′-CTTCGCCTCTGCTTCTCCT-3′ and 5′-TGCCAGCACCAACAACTCC-3′; *HEME2*, 5′-TTATCGAGAACGCCCGTTT-3′ and 5′-TGTACCTCCCTGCTTGCCT-3′; *PORA*, 5′-GCCTCCTCTTTCCTCGCAC-3′ and 5′-GGCTGTTGCTGTCGTCTGG-3′; *CHLG*, 5′-GTCTCAGTCGCCGTCTCGA-3′ and 5′-TCTTCCATTTGTCCGTGCC-3′; *CLH2*, 5′-CATGGCTCCACCAGCAAAA-3′ and 5′-CCTCCTTGTGCTCCCAAGG-3′; *RCCR*, 5′-TTCACACCGCCTCTCATCA-3′ and 5′- AACCGAGGCGATCGTCAAC-3′; *Actin*, 5′-AATCCCAAGGCAAACAGA-3′ and 5′-CCATACCAGAATCCAG-3′.

γ-ray treatments and evaluation of induced leaf mutants

Light-modulated rhizomes of two cultivars were γ-irradiated (50 Gy for RB003, and 30 Gy for RB012) using a ^{60}Co source (150 TBq capacity; AECL,

Canada) for 24 h at the Korea Atomic Energy Research Institute, Jeongeup, Korea. γ-irradiation was conducted on the rhizomes treated with light modulation as follows: RB003, dark treatment (60 days) followed by light treatment (10 days); RB012, dark treatment (75 days) followed by light treatment (10 days). Experiments were performed with three biological replicates and 250 rhizomes per replicate.

Phenotype analysis of γ-irradiated RB003 and RB012 populations was conducted twice, at 6 and 10 months after γ-ray treatment, to measure regeneration rate, total mutation rate, and Chl-related mutation rate.

Statistical analyses

Student's *t*-tests were used to compare the significance of differences in means among treatments. The *p*-value was considered statistically significant at the 0.05 significance level.

RESULTS

Effect of light modulation on Chl degradation and biosynthesis

To induce Chl biosynthesis, light modulation was conducted on the rhizomes of two *Cymbidium* cultivars. Dark treatment was first conducted to degrade Chls and was then followed by light treatment to induce Chl biosynthesis. Chl degradation was visually apparent on the terminal parts of rhizomes after 40 days of dark treatment (Figure IV-1). There were differences in Chl degradation from dark treatment between the two cultivars because the rate of Chl degradation in RB003 rhizomes was higher than that in RB012 rhizomes. As a result, the minimum durations of dark treatment required to degrade Chls were 60 and 75 days for RB003 and RB012, respectively (Figure IV-1). For dark treatments that were longer than minimum durations, elongation of the rhizome terminal parts was more apparent than additional effects on Chl degradation (Figure IV-1).

Following dark treatment, Chl accumulation in rhizomes was observed after 10 and 5 days of light treatment in RB003 and RB012, respectively (Figure IV-2). The Chl accumulation in response to light treatment was more significant in RB012 rhizomes than in RB003 rhizomes. Chl levels increased rapidly after 7

days of light treatment in both cultivars (Figure IV-3). Chl levels in RB003 rhizomes reached at maximum at 20 days of light treatment, and decreased at 21 days, reaching a content level that was similar to controls. For RB012 rhizomes, Chl amounts continuously increased until 21 days of light treatment, but in amounts that were less than those in the control (Figure IV-3). The amount of Chl *a* was a little higher than the amount of Chl *b* in both cultivars (Figure IV-3). Additionally, the Chl content of an RB012 control that was not subjected to dark treatment, was more than 2-fold higher than that of the RB003 control. The rate of Chl degradation and biosynthesis was higher in RB003 rhizomes than in RB012 rhizomes, and the Chl content in RB012 was higher than that in RB003 (Figure IV-1–3).

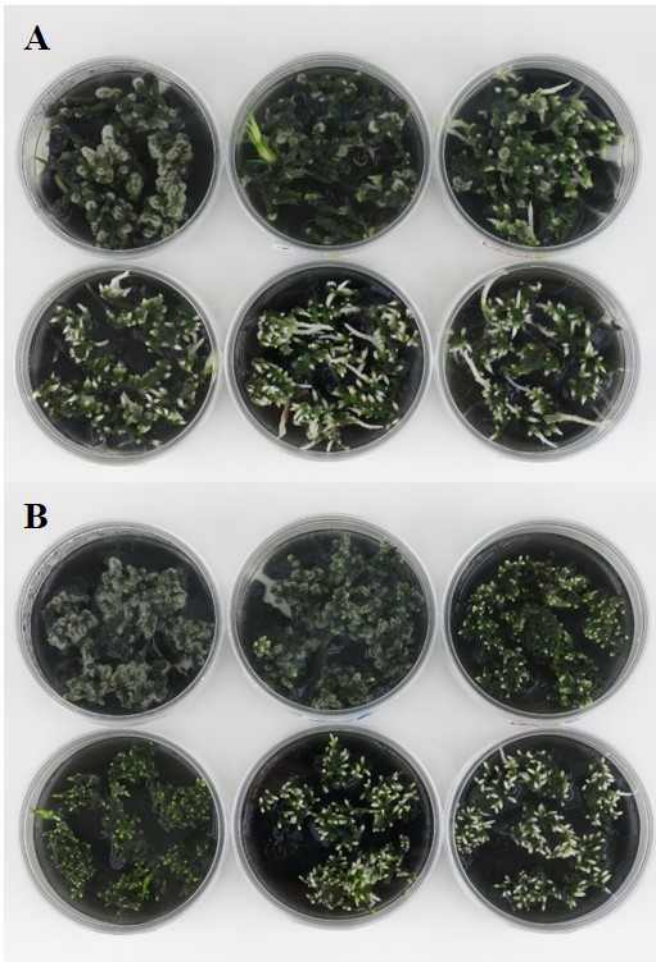

Figure IV-1. Chlorophyll degradation after dark treatment in rhizomes of *Cymbidium* hybrids RB003 and RB012. (a) RB003; (b) RB012. From the upper left, 0, 20, 40, 60, 75, and 90 days after dark treatment.

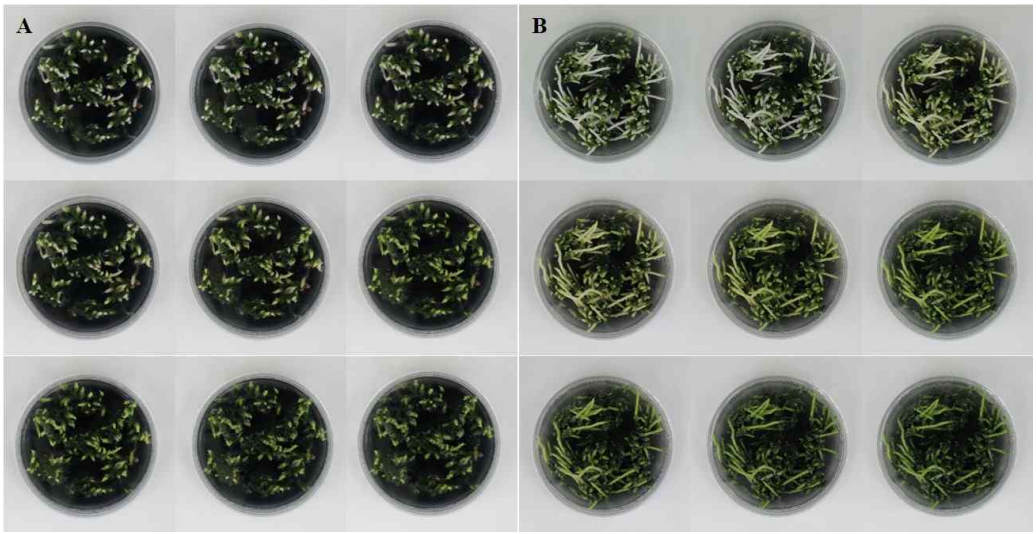

Figure IV-2. Chlorophyll accumulation after light treatment in rhizomes of *Cymbidium* hybrids RB003 and RB012. (a) RB003; (b) RB012. From the upper left, dark-treated rhizomes treated with light for 0, 1, 5, 7, 10, 14, 15, 20, and 21 days. Dark treatment of the rhizomes was 60 and 75 days for *Cymbidium* hybrids RB003 and RB012, respectively.

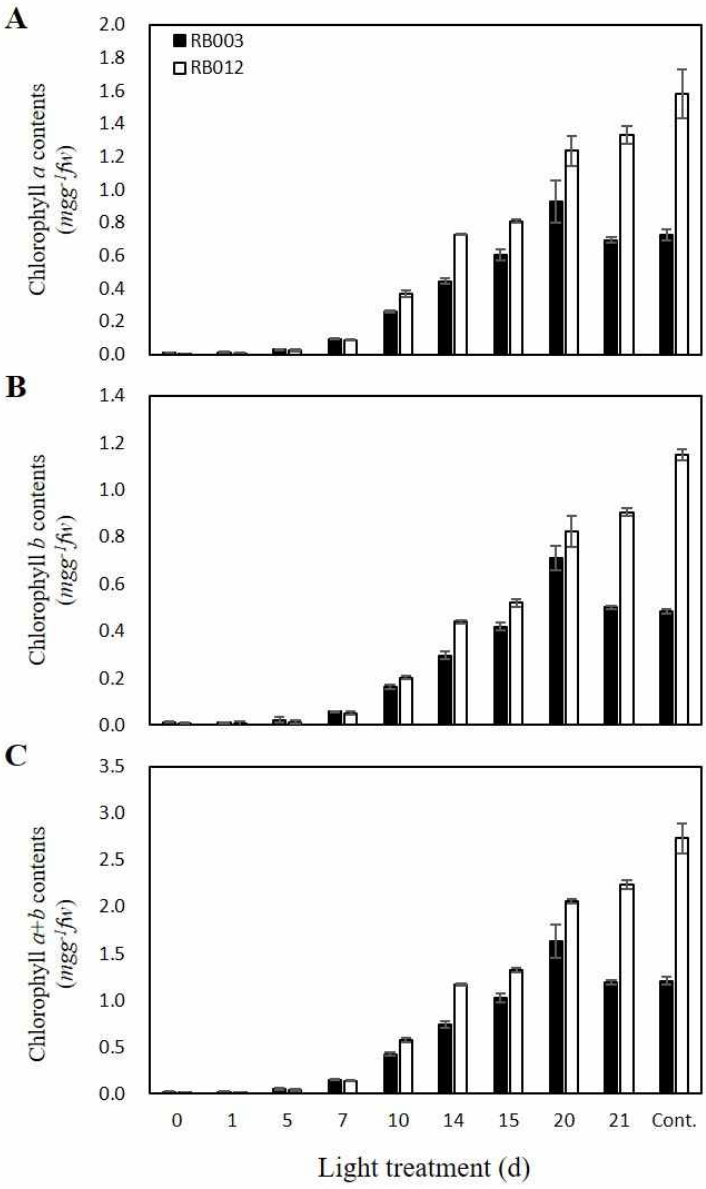

Figure IV-3. Chlorophyll contents of light-treated rhizomes in *Cymbidium* hybrids RB003 and RB012. Dark treatment of the rhizomes was 60 and 75 days for *Cymbidium* hybrids RB003 and RB012, respectively. Dark treatment was followed by light treatment.

Effect of light modulation on Chl pathway gene expression

To identify the effect of light modulation on Chl pathway genes expression, the expression patterns of four genes (*HEMD*, *HEME2*, *PORA*, and *CHLG*) involved in Chl biosynthesis and two genes (*CLH2* and *RCCR*) involved in Chl degradation were analyzed after various durations of light treatment that followed dark treatment (Figure IV-4). In the RB003 cultivar, the expression of *HEME2* and *CHLG* were highest at 14 and 10 days after light treatment, respectively, gradually increasing to those time points and then decreasing (Figure IV-4). The expression of *HEMD*, *PORA*, and *RCCR*, excepting *CLH2*, gradually increased until 10 days after light treatment and then decreased, although expression was not higher than that of untreated controls. In the RB012 cultivar, the expression of *HEMD*, *PORA*, and *CHLG* were highest at after 10 days of light treatment, with expression that gradually increased until that time point and then decreased, as seen with RB003 (Figure IV-4). The expression of *HEME2*, *CLH2*, and *RCCR* were highest at relatively early time points, after 5–7 days of light treatment. However, the expression of *PORA*, *CHLG*, *CLH2*, and *RCCR* remained high, even after relatively long light treatments, which differed from their expression pattern in RB003 Figure IV-4). Overall, though the expression patterns of the six genes were different depending on the target gene and the cultivar, 10 days of light treatment appeared to be optimal for inducing up-regulated expression of Chl pathway genes.

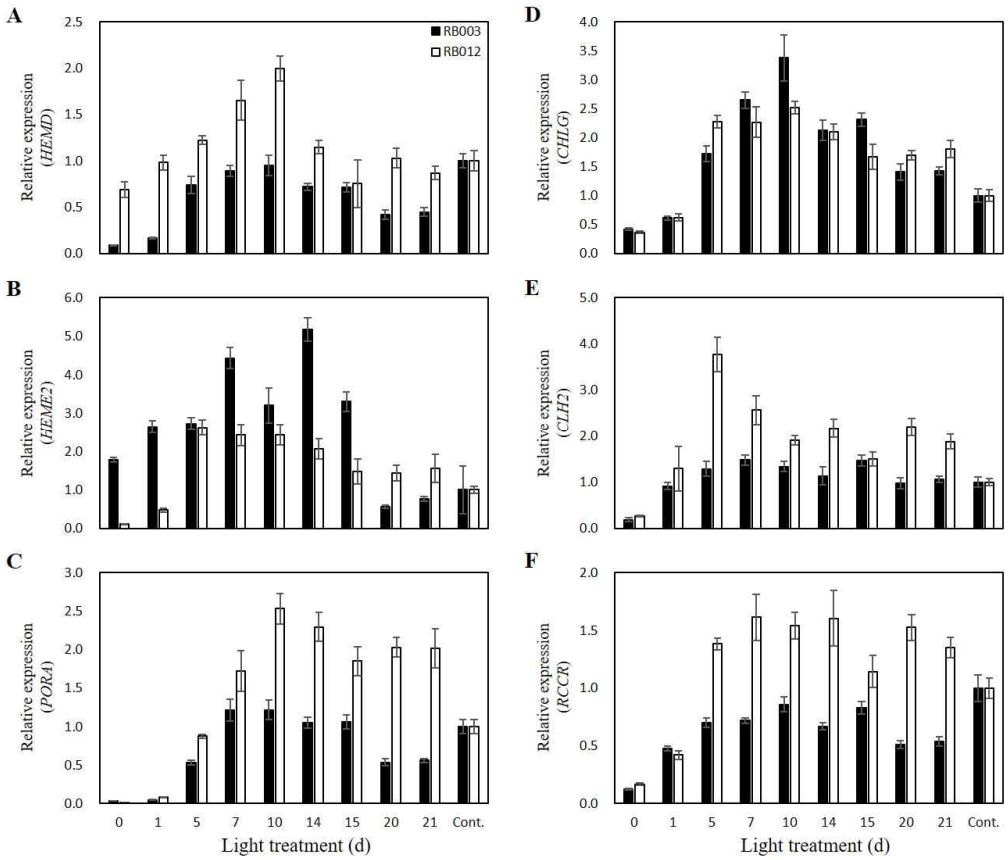

Figure IV-4. Relative expression of six genes involved in chlorophyll biosynthesis and degradation during light treatment of *Cymbidium* hybrids RB003 and RB012. Dark treatment of the rhizomes was 60 and 75 days for *Cymbidium* hybrids RB003 and RB012, respectively. Dark treatment was followed by light treatment.

Induction frequency of Chl-related leaf-color mutants

Light modulation [dark treatment for 60 days (RB003) and 75 days (RB012) followed by light treatment for 10 days] followed by γ-irradiation [50 Gy (RB003) and 30 Gy (RB012)] was performed, and phenotypes of RB003 and RB012 populations were analyzed to determine regeneration rate, total mutation rate, and Chl-related mutation rate. Regeneration rates of γ-irradiated populations were reduced compared with those of the two control populations [RB003: Cont., 7.9, Cont. (DL), 7.4, gamma-ray, 4.1, DL + gamma-ray, 4.6; RB012: Cont., 8.0, Cont. (DL), 7.2, gamma-ray, 5.7, DL + gamma-ray, 6.0] (Figure IV-6(a), (d)). Total mutation rates in light modulation followed by γ-irradiated populations were greater than those in only γ-irradiated populations (RB003: gamma-ray, 0.56, DL + gamma-ray, 0.75; RB012: gamma-ray, 0.26, DL + gamma-ray, 0.45) (Figure IV-6(b), (e)). In addition, somaclonal variations without γ-irradiation were also identified [RB003: Cont. (DL), 0.05; RB012: Cont., 0.07, Cont. (DL), 0.07] (Figure IV-6(b), (e)). Chl-related mutation rates in light modulation followed by γ-irradiated populations were greater than those in only γ-irradiated populations (RB003: gamma-ray, 0.37, DL + gamma-ray, 0.51; RB012: gamma-ray, 0.15, DL + gamma-ray, 0.30), although the difference was not statistically significant (Figure IV-6(c), (f)). Interestingly, in both cultivars, diverse mutants

were more abundant in the second regenerated populations than in the first regenerated populations (Figure IV-5–6), which should be considered for future selections of induced mutants in γ-irradiated populations.

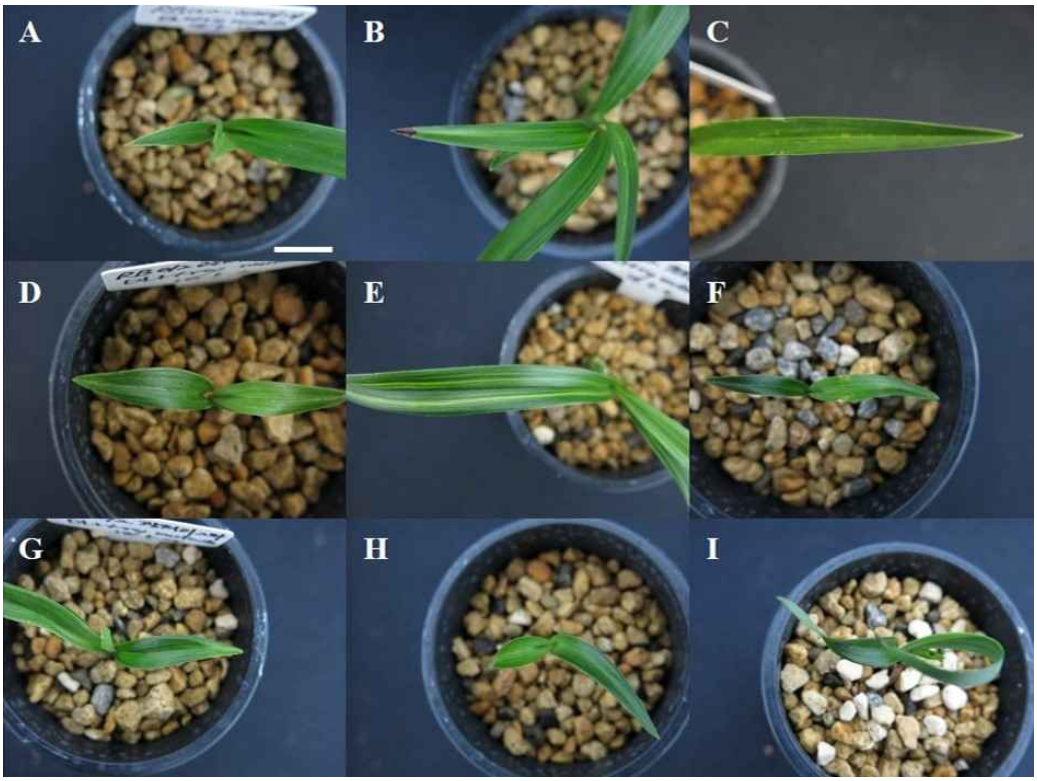

Figure IV-5. Representative leaf-color and -shape mutants induced by light modulation followed by γ-irradiation in *Cymbidium* hybrids RB003 and RB012. (a)–(c) mutants induced in *Cymbidium* hybrid RB003; (d)–(i) mutants induced in *Cymbidium* hybrid RB012. (a) and (c) yellow marginal leaf-color mutants; (b), (d), (e), and (g) yellow stripe leaf-color mutants; (f) dwarf leaf-shape mutant; (i) twisted leaf-shape mutant. Scale bar: 1 cm.

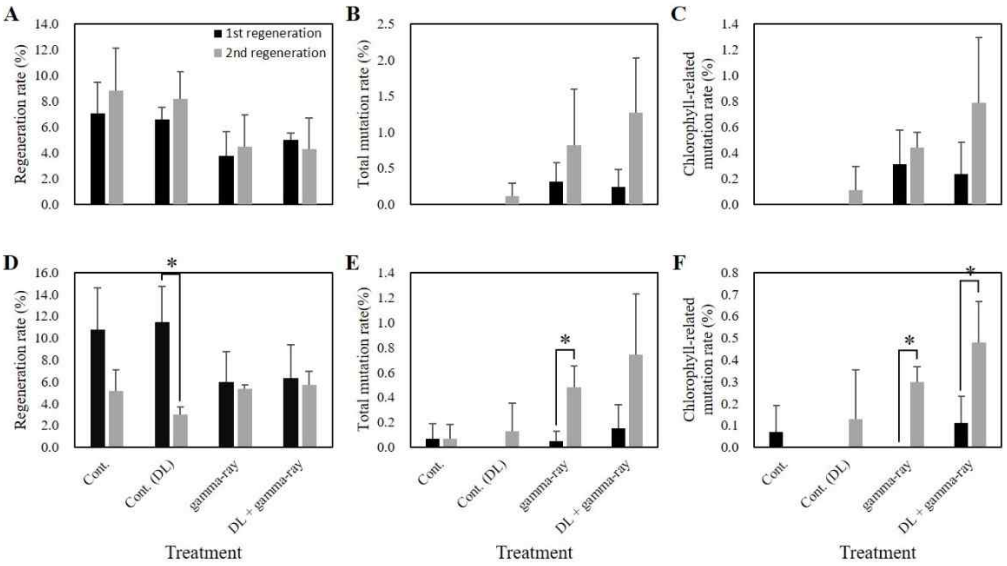

Figure IV-6. Regeneration, total mutation, and chlorophyll-related mutation rates of mutant populations induced by light modulation followed by γ-irradiation in *Cymbidium* hybrids RB003 and RB012. (a)–(c) regeneration rate, total mutation rate, and chlorophyll-related mutation rate in RB003 population; (d)–(f) regeneration rate, total mutation rate, and chlorophyll-related mutation rate in RB012 population. DL, light modulation (dark/light). Student's *t*-test was used to calculate statistical significance (*$p < 0.05$).

DISCUSSION

Light modulation up-regulates gene expression in Chl pathway

Chl plays important light-harvesting and energy transduction roles in photosynthesis, and almost every gene involved in Chl biosynthesis and degradation has been identified (Eckhardt et al. 2004). Chl biosynthesis and degradation can be summarized as follows (Eckhardt et al. 2004): biosynthesis, glutamyl tRNA followed by 5-aminolevulinic acid (ALA), protoporphyrin IX (Proto), protochlorophyllide *a* (Pchlide *a*), chlorophyllide *a* (Chlide *a*), and Chl *a*; degradation, Chl *a* followed by Chlide *a*, Pchlide *a*, red Chl catabolite (RCC), primary fluorescent Chl catabolite (pFCC), and nonfluorescent Chl catabolites.

In this study, I analyzed time-course expression of four biosynthesis pathway genes (*HEMD*, *HEME2*, *PORA*, and *CHLG*) and two degradation pathway genes (*CLH2* and *RCCR*) during light treatment that followed dark treatment (Figure IV-4). *HEMD* and *HEME2* function in the biosynthesis of ALA to Proto as follows (Eckhardt et al. 2004): *HEMD*, uroporphyrinogen III synthase, cyclizes and isomerizes hydroxymethylbilane to produce uroporphyrinogen III in the plastid (Lim et al. 1994); *HEME2*, uroporphyrinogen III decarboxylase, eliminates the carboxyl groups from the four acetate side chains of

uroporphyrinogen III to produce coproporphyrinogen III (Mock and Grimm 1997). *PORA* and *CHLG* function in the biosynthesis of Pchlide *a* to Chl *a* as follows (Eckhardt et al. 2004): *PORA*, NADPH-protochlorophyllide oxidoreductase (POR) A, catalyzes a light-dependent trans-reduction of the D-ring of Pchlide *a* to produce Chlide *a* in the plastid membranes (Su et al. 2001); *CHLG*, Chl synthase, catalyzes the esterification of Chlide *a* to produce Chl *a* in the plastid membranes (Gaubier et al. 1995). *CLH2* and *RCCR* function in the degradation of Chl *a* to Chlide *a* and RCC to pFCC, respectively (Eckhardt et al. 2004), as follows: *CLH2*, chlorophyllase, catalyzes the hydrolysis of Chl *a* to produce Chlide *a* in the plastid or vacuole (Tsuchiya et al. 1999); *RCCR*, red Chl catabolite reductase, catalyzes the cleavage of RCC to produce pFCC in the plastid or stroma (Wüthrich et al. 2000). Eckhardt et al. (2004) reported that the expression of most genes involved in Chl biosynthesis are light-inducible and developmental-dependent, while Chl degradation genes, except Pchlide *a* oxygenase, are constitutively expressed. In RB012, all four genes involved in Chl biosynthesis were highly expressed after light treatment (Figure IV-4(a)–(d)), which is consistent with a previous report; however, both genes involved in Chl degradation were also highly expressed after light treatment (Figure IV-4(e), (f)). In RB003, only two Chl biosynthesis genes, *HEME2* and *CHLG*, were highly expressed by light treatment (Figure IV-4(b), (d)). Overall, there were differences

between expression responses of Chl pathway genes in this study and those of a previous report (Eckhardt et al. 2004), which may result from different plant species being studied. It has been reported that when Chl accumulation in dark-grown seedlings under light treatment has reached a maximum level, POR activity decreased to an undetectable level (Forreiter et al. 1990). In this study, the relative expression of the six genes studied reached at maximum before maximal Chl accumulation was reached (Figure IV-3–4).

Light modulation followed by γ-ray treatment increases leaf-color mutation

In previous reports, effects of sucrose and plant hormones on the expression of anthocyanin pathway genes were definitively demonstrated in Arabidopsis (Solfanelli et al. 2006; Loreti et al. 2008). Using sucrose pre-treatment to up-regulate anthocyanin biosynthesis gene expression, Hase et al. (2010) and Kim et al. (2016) reported that the sucrose pre-treatment followed by carbon-ion and γ-ray treatments resulted in 2.5-fold and 2- to 10.5-fold increases in flower-color mutation rates in petunia (Hase et al. 2010) and chrysanthemum (Kim et al. 2016), respectively. Additionally, Kim et al. (2019) elucidated the optimal pre-treatment condition (50 mM sucrose with 100 μM methyl jasmonate for 18 h) and measured effects of pre-treatment on expression patterns for six

anthocyanin pathway genes. They reported that sucrose with methyl jasmonate pre-treatment followed by γ-irradiation resulted in a 1.5-fold increase in the rate of flower-color mutation in chrysanthemum (Kim et al. 2019).

Following the successful demonstration that the frequency of flower-color mutation could be increased by up-regulation of anthocyanin pathway gene expression, I have applied similar methodology to increase the frequency of leaf-color mutation in *Cymbidium*. In the present study, light modulation followed by γ-irradiation resulted in 1.4-fold (RB003) and 2.0-fold (RB012) increases in rates of Chl-related leaf-color mutation compared with those of γ-ray treatment alone, although a statistically significant difference was not confirmed because of a large variation among replicates (Figure IV-6). Presumably, this larger variation results from differences in mechanism, complexity, and the number of genes that determine the color in flower and leaf in anthocyanin and Chl pathways (Tanaka et al. 2008; Solfanelli et al. 2006; Chatterjee and Kundu 2015). In addition, it is known there are 19 types of anthocyanins (Tanaka et al. 2008) but only two types of Chls (Chl *a*, *b*) in higher plants (Zhu et al. 2017). Therefore, additional experiments will be necessary to establish optimal conditions for up-regulating Chl pathway gene expression to optimize mutation rates. Regardless, the present study supports the use of methodology that increases the mutation frequency of a target trait by controlling the expression of genes related to the target trait.

REFERENCES

Baker NR. 2008. Chlorophyll fluorescence: a probe of photosynthesis in vivo. Annu Rev Plant Biol. 59: 89–113.

Blasco M, Badenes ML.2015. Naval, M.M. Colchicine-induced polyploidy in loquat (*Eriobotrya japonica* (Thunb.) Lindle.). Plant Cell Tissue Organ Cult. 120: 453–461.

Bottino PJ, Sparrow AH, Schwemmer SS. Thompson, K.H. Interrelation of exposure and exposure rate in germinating seeds of barley and its concurrence with dose-rate theory. Radiat Bot. 15: 17–27.

Cai X, Cao Z, Xu S, Deng Z. 2015. Induction, regeneration and characterization of tetraploids and variants in 'Tapestry' caladium. Plant Cell Tissue Organ Cult. 120: 689–700.

Chatterjee A, Kundu S. Revisiting the chlorophyll biosynthesis pathway using genome scale metabolic model of *Oryza sativa japonica*. Sci Rep. 5: 14975.

Chen C, Hou X, Zhang H, Wang G, Tian L. 2011. Induction of *Anthurium andraeanum* "Arizona" tetraploid by colchicine in vitro. Euphytica. 181: 137–145.

Coe RA, Chatterjee J, Acebron K, Dionora J, Mogul R, Lin HC, Yin X. 2018. Bandyopadhyay, A.; Sirault, X.R.R.; Furbank, R.T.; et al. High-throughput chlorophyll fluorescence screening of *Setaria viridis* for mutants with altered CO_2 compensation points. Funct Plant Biol. 45: 1017–1025.

Deng X, Zhang H, Wang Y, He F, Liu J, Xiao X, Shu Z, Li W, Wang G, Wang G. 2014. Mapped clone and functional analysis of leaf-color gene *Ygl7* in a rice hybrid (*Oryza sativa* L. spp. *Indica*). PLoS ONE. 9: e99564.

Dewey DL. 1969. An oxygen-dependent X-ray dose-rate effect in *Serratia marcescens*. Radiat Res. 38: 467–474.

Eckhardt U, Grimm B, Hörtensteiner S. 2004. Recent advances in chlorophyll biosynthesis and breakdown in higher plants. Plant Mol Biol. 56: 1–14.

Forreiter C, van Cleve B, Schmidt A, Apel K. 1990. Evidence for a general light-dependent negative control of NADPH-protochlorophyllide oxidoreductase in angiosperms. Planta. 183: 126–132.

Gady ALF, Hermans FWK, de Wal MHBJV, van Loo EN, Visser RGF, Bachem CWB. 2009. Implementation of two high through-put techniques in a novel application: detecting point mutations in large EMS mutated plant populations. Plant Methods. 5: 13.

Garcia V, Bres C, Just D, Fernandez L, Tai FWJ, Mauxion JP, Paslier MCL, Bérard A, Brunel D, Aoki K, et al. Rapid identification of causal mutations in tomato EMS populations via mapping-by-sequencing. Nat Protoc. 11: 2401–2418.

Gaubier P, Wu HJ, Laudié M, Delseny M, Grellet F. 1995. A chlorophyll synthetase gene from *Arabidopsis thaliana*. Mol Genet Genomics. 249: 58.

Hase Y, Okamura M, Takeshita D, Narumi I, Tanaka A. 2010. Efficient induction of flower-color mutants by ion beam irradiation in petunia seedlings treated with high sucrose concentration. Plant Biotechnol. 27: 99–103.

Hase Y, Satoh K, Kitamura S, Oono Y. 2018. Physiological status of plant tissue affects the frequency and types of mutations induced by carbon-ion irradiation in Arabidopsis. Sci Rep. 8: 1394.

Hase Y, Yoshihara R, Nozawa S, Narumi I. 2012. Mutagenic effects of carbon ions near the range end in plants. Mutat Res. 731: 41–47.

Howden R, Andersen CR, Goldsbrough PB, Cobbett CS. 1995. A cadmium-sensitive, glutathione-deficient mutant of *Arabidopsis thaliana*. Plant Physiol. 107: 1067–1073.

Huang P, Jiang H, Zhu C, Barry K, Jenkins J, Sandor L, Schmutz J, Box MS, Kellogg EA, Brutnell TP. 2017. *Sparse panicle1* is required for inflorescence development in *Setaria viridis* and maize. Nat Plants. 3: 17054.

Jeong YJ, Shang Y, Kim BH, Kim SY, Song JH, Lee JS, Lee MM, Li J, Nam KH. 2010. BAK7 displays unequal genetic redundancy with BAK1 in brassinosteroid signaling and early senescence in Arabidopsis. Mol Cells. 29: 259–266.

Killion DD, Constantin MJ. 1971. Acute gamma irradiation of the wheat plant:

effects of exposure, exposure rate, and developmental stage on survival, height, and grain yield. Radiat Bot. 11: 367–373.

Kim HJ, Ryu H, Hong SH, Woo HR, Lim PO, Lee IC, Sheen J, Nam HG, Hwang I. 2006. Cytokinin-mediated control of leaf longevity by AHK3 through phosphorylation of ARR2 in *Arabidopsis*. Proc. Natl. Acad. Sci. U S A. 103: 814–819.

Kim SH, Jo YD, Ryu J, Hong MJ, Kang BC, Kim JB. 2019. Effects of the total dose and duration of γ-irradiation on the growth responses and induced SNPs of a *Cymbidium* hybrid. Int J Radiat Biol. (in press).

Kim SH, Kim YS, Jo YD, Kang SY, Ahn JW, Kang BC, Kim JB. 2019. Sucrose and methyl jasmonate modulate the expression of anthocyanin biosynthesis genes and increase the frequency of flower-color mutants in chrysanthemum. Sci Hortic. 256: 108602.

Kim SH, Kim YS, Lee HJ, Jo YD, Kim JB, Kang SY. 2019. Biological effects of three types of ionizing radiation on creeping bentgrass. Int J Radiat Biol. 95: 1295–1300.

Kim YS, Sakuraba Y, Han SH, Yoo SC, Paek NC. 2013. Mutation of the Arabidopsis NAC016 transcription factor delays leaf senescence. Plant Cell Physiol. 54: 1660–1672.

Kim YS, Sung SY, Jo YD, Lee HJ, Kim SH. 2016. Effects of gamma ray dose rate and sucrose treatment on mutation induction in chrysanthemum. Eur J Hortic Sci. 81: 212–218.

Kodym A, Afza R, Forster BP, Ukai Y, Nakagawa H, Mba C. 2012. Methodology for physical and chemical mutagenic treatments. *In*: Shu QY, Forster BP, Nakagawa H (eds.) Plant Mutation Breeding and Biotechnology, CAB International, Wallingford; FAO, Rome, pp. 123–134.

Kowyama Y, Saba T, Tsuji T, Kawase T. 1994. Specific developmental stages of gametogenesis for radiosensitivity and mutagenesis in rice. Euphytica 80: 27–38.

Lara MEB, Garcia MCG, Fatima T, Ehneß R, Lee TK, Proels R, Tanner W, Roitsch T. 2004. Extracellular invertase is an essential component of cytokinin-mediated delay of senescence. Plant Cell. 16: 1276–1287.

Lee YM, Jo YD, Lee HJ, Kim YS, Kim DS, Kim JB, Kang SY, Kim SH. 2015. DNA damage and oxidative stress induced by proton beam in

Cymbidium hybrid. Hort Environ Biotechnol. 56: 240–246.

Lee YM, Lee HJ, Kim YS, Kang SY, Kim DS, Kim JB, Ahn JW, Ha BK, Kim SH. 2016. Evaluation of the sensitivity to ionizing γ-radiation of a *Cymbidium* hybrid. J Hortic Sci Biotechnol. 91: 109–116.

Lichtenthaler HK. 1987. Chlorophylls and carotenoids: pigments of photosynthetic biomembranes. Meth Enzymol. 148: 350–382.

Lim SH, Witty M, Wallace-Cook ADM, Ilag LI, Smith AG. 1994. Porphobilinogen deaminase is encoded by a single gene in *Arabidopsis thaliana* and is targeted to the chloroplast. Plant Mol Biol. 26: 863–872.

Liu L, Guo H, Zhao L, Gu J, Zhao S. 2007. Achievements in the past twenty years and perspective outlook of crop space breeding in China. J Nucl Agric Sci. 21: 589–592.

Loreti E, Povero G, Novi G, Solfanelli C, Alpi A, Perata P. 2008. Gibberellins, jasmonate and abscisic acid modulate the sucrose-induced expression of anthocyanin biosynthetic genes in *Arabidopsis*. New Phytologist. 179: 1004–1016.

Ma X, Sun X, Li C, Huan R, Sun C, Wang Y, Xiao F, Wang Q, Chen P, Ma F, et al. 2017. Map-based cloning and characterization of the novel yellow-green leaf *ys83* in rice (*Oryza sativa*). Plant Physiol Biochem. 111: 1–9.

Mabuchi T, Matsumura S. 1064. Dose rate dependence of mutation rates from γ-irradiated pollen grains of maize. Jpn J Genet. 39: 131–135.

Mandal AKA, Chakrabarty D, Datta SK. 2000. Application of *in vitro* techniques in mutation breeding of chrysanthemum. Plant Cell Tissue Organ Cult. 60: 33–38.

Mock HP, Grimm B. 1997. Reduction of uroporphyrinogen decarboxylase by antisense RNA expression affects activities of other enzymes involved in tetrapyrrole biosynthesis and leads to light-dependent necrosis. Plant Physiol. 113: 1101–1112.

Morris K, Mackerness SAH, Page T, John CF, Murphy AM, Carr JP, Buchanan-Wollaston V. 2000. Salicylic acid has a role in regulating gene expression during leaf senescence. Plant J. 23: 677–685.

Natarajan AT, Maric MM. 1961. The time-intensity factor in dry seed irradiation. Radiat Bot. 1: 1–9.

Nishiyama I, Ikushima T, Ichikawa S. 1966. Radiological studies in plants–XI: further studies on somatic mutations induced by X-rays at the *al* locus of diploid oats. Radiat Bot. 6: 211–218.

Okamura M, Hase Y, Furusawa Y, Tanaka A. 2015. Tissue-dependent somaclonal mutation frequencies and spectra enhanced by ion beam irradiation in chrysanthemum. Euphytica. 202: 333–343.

Pestanana RKN, Amorim EP, Ferreira CF, Amorim VBO, Oliveira LS, Ledo CAS, Silva SO. 2011. Agronomic and molecular characterization of gamma ray induced banana (*Musa* sp.) mutants using a multivariate statistical algorithm. Euphytica. 178: 151–158.

Qin R, Zeng D, Liang R, Yang C, Akhter D, Alamin M, Jin X, Shi C. 2017. Rice gene *SDL*/*RNRS1*, encoding the small subunit of ribonucleotide reductase, is required for chlorophyll synthesis and plant growth development. Gene. 627: 351–362.

Roman G, Lubarsky B, Kieber JJ, Rothenberg M. 1995. Genetic analysis of ethylene signal transduction in *Arabidopsis thaliana*: five novel mutant loci integrated into a stress response pathway. Genetics. 139: 1393–1409.

Shikazono N, Suzuki C, Kitamura S, Watanabe H, Tano S, Tanaka A. 2005. Analysis of mutations induced by carbon ions in *Arabidopsis thaliana*. J Exp Bot. 56: 587–596.

Shikazono N, Yokota Y, Kitamura S, Suzuki C, Watanabe H, Tano S, Tanaka A. 2003. Mutation rate and novel *tt* mutants of *Arabidopsis thaliana* induced by carbon ions. Genetics 163: 1449–1455.

Shirasawa K, Hirakawa H, Nunome T, Tabata S, Isobe S. 2016. Genome-wide survey of artificial mutations induced by ethyl methanesulfonate and gamma rays in tomato. Plant Biotechnol J. 14: 51–60.

Shirley BW, Kubasek WL, Storz G, Bruggemann E, Koornneef M, Ausubel FM, Goodman HM. 1995. Analysis of *Arabidopsis* mutants deficient in flavonoid biosynthesis. Plant J. 8: 659–671.

Solfanelli C, Poggi A, Loreti E, Alpi A, Perata P. 2006. Sucrose-specific induction of the anthocyanin biosynthetic pathway in Arabidopsis. Plant Physiol. 140: 637–646.

Su Q, Frick G, Armstrong G, Apel K. 2001. POR C of *Arabidopsis thaliana*: a third light- and NADPH-dependent protochlorophyllide oxidoreductase

that is differentially regulated by light. Plant Mol Biol. 47: 805–813.

Takata H, Hanafusa T, Mori T, Shimura M, Iida Y, Ishikawa K, Yoshikawa K, Yoshikawa Y, Maeshima K. 2013. Chromatin compaction protects genomic DNA from radiation damage. PLoS ONE. 8: e75622.

Tanaka A, Shikazono N, Hase Y. 2010. Studies on biological effects of ion beams on lethality, molecular nature of mutation, mutation rate, and spectrum of mutation phenotype for mutation breeding in higher plants. J Radiat Res. 51: 223–233.

Tanaka Y, Sasaki N, Ohmiya A. 2008. Biosynthesis of plant pigments: anthocyanins, betalains and carotenoids. Plant J. 54: 733–749.

Tsuchiya T, Ohta H, Okawa K, Iwamatsu A, Shimada H, Masuda T, Takamiya K. 1999. Cloning of chlorophyllase, the key enzyme in chlorophyll degradation: Finding of a lipase motif and the induction by methyl jasmonate. Proc Natl Acad Sci. U S A. 96: 15362–15367.

Venkatesh P, Panyutin IV, Remeeva E, Neumann RD, Panyutin IG. 2016. Effect of chromatin structure on the extent and distribution of DNA double strand breaks produced by ionizing radiation; comparative study of hESC and differentiated cells lines. Int J Mol Sci. 17: 58.

Wüthrich KL, Bovet L, Hunziker PE, Donnison IS, Hörtensteiner S. 2000. Molecular cloning, functional expression and characterisation of RCC reductase involved in chlorophyll catabolism. Plant J. 21: 189–198.

Yamaguchi H, Hase Y, Tanaka A, Shikazono N, Degi K, Shimizu A, Morishita T. 2009. Mutagenic effects of ion beam irradiation on rice. Breed Sci. 59: 169–177.

Yamaguchi H, Shimizu A, Degi K, Morishita T. 2008. Effects of dose and dose rate of gamma ray irradiation on mutation induction and nuclear DNA content in chrysanthemum. Breed Sci. 58: 331–335.

Yamatani H, Sato Y, Masuda Y, Kato Y, Morita R, Fukunaga K, Nagamura Y, Nishimura M, Sakamoto W, Tanaka A, et al. NYC4, the rice ortholog of Arabidopsis THF1, is involved in the degradation of chlorophyll – protein complexes during leaf senescence. Plant J. 74: 652–662.

Yang R, Bai J, Fang J, Wang Y, Lee G, Piao Z. 2016. A single amino acid mutation of *OsSBEIIb* contributes to resistant starch accumulation in rice. Breed Sci. 66: 481–489.

Yu S, Luo H, Li J, Yu X. 2013. Molecular variation and application from aerospace mutagenesis in upland rice Huhan 3 and Huhan7. Rice Sci. 20: 249–258.

Zhu X, Chen J, Qiu K, Kuai B. 2017. Phytohormone and light regulation of chlorophyll degradation. Front Plant Sci. 8: 1911.

GENERAL CONCLUSION

In this study, I analyzed the optimal γ-irradiation condition, frequency and spectrum of mutation, stability of leaf chimeras, mechanism of leaf-color mutation, and induction frequency of mutation on the target trait in *Cymbidium*.

In chapter I, I analyzed the effects of the total dose and irradiation duration on the growth of *Cymbidium* hybrid RB001 protocorm-like bodies (PLBs). On the basis of the survival rate of γ-irradiated PLBs, the optimal doses (LD_{50}) for each irradiation duration were estimated: 1 h, 16.1 Gy; 4 h, 23.6 Gy; 8 h, 37.9 Gy; 16 h, 37.9 Gy; and 24 h, 40.0 Gy. The estimated optimal doses were duration-dependent at irradiation durations shorter than 8 h, but not at irradiation durations exceeding 8 h. A SNP comparison revealed a lack of significant differences among the mutations induced by γ-irradiations. These results indicate the irradiation duration affects PLB growth in response to γ-rays. Moreover, the mutations induced by a short-term treatment may be similar to those induced by a treatment over a longer period.

In chapter II, I analyzed the radiation-sensitivity, mutation frequency, and spectrum of mutants induced by diverse γ-ray treatments, and analyzed the stability of induced chimera mutants in the *Cymbidium* hybrid RB003 and RB012.

The optimal γ-irradiation conditions of each cultivar differed as follows: RB003, mutation frequency of 4.06% (under 35 Gy/4 h); RB012, 1.51% (20 Gy/1 h). Re-irradiation of γ-rays broadened the mutation spectrum observed in RB012. The stability of leaf-color chimera mutants was higher than that of leaf-shape chimeras, and stability was dependent on the chimera type and location of a mutation in the cell layers of the shoot apical meristem. These results indicated that short-term γ-irradiation was more effective to induce mutations in *Cymbidium*. Information on the stability of chimera mutants will be useful for mutation breeding of diverse ornamental plants.

In chapter III, I analyzed the candidate genes related to the fade leaf-color of S12 mutant, which is developed by γ-ray-based mutagenesis of a *Cymbidium* hybrid RB003, using RNA sequencing (RNA-Seq). A total of 144,918 unigenes obtained from over 25 million reads were assigned to 22 metabolic pathways in the Kyoto Encyclopedia of Genes and Genomes database. In addition, Gene Ontology was used to classify the predicted functions of transcripts into 73 functional groups. The RNA-Seq analysis identified 2,267 differentially expressed genes between wild-type and S12 mutant. Genes involved in chlorophyll biosynthesis and degradation as well as ion transport were identified and assayed for their expression levels in wild-type and S12

mutant using quantitative real-time profiling. No critical change was detected in genes involved in chlorophyll biosynthesis. In contrast, seven genes involved in ion transport, including two metal ion transporters were down-regulated, and chlorophyllase 2, associated with chlorophyll degradation was up-regulated. Together, these results suggest that alteration in chlorophyll metabolism and/or ion transport might contribute to leaf color in *Cymbidium* orchids.

In chapter IV, I determined the optimal light modulation for up-regulating the expression of six chlorophyll pathway genes and measured effects of light modulation on the γ-irradiation-induced frequency of leaf-color mutation in the *Cymbidium* hybrid RB003 and RB012. To degrade chlorophylls in rhizomes, 60–75 days of dark treatment was required. To up-regulate the expression of chlorophyll pathway genes, 10 days of light treatment was found to be optimal. Light modulation followed by γ-irradiation increased chlorophyll-related leaf mutants by 1.4- to 2.0-fold compared with γ-ray treatment alone. Light modulation combined with γ-irradiation increased the frequency of leaf-color mutants in *Cymbidium*, supporting wider implementation of plant breeding methodology that increases the mutation frequency of a target trait by controlling the expression of genes related to the target trait.

These results will be a guide on the mutation induction, selection of

mutants, and stabilization of chimeras in mutation breeding of orchids, including *Cymbidium*. Diverse leaf-color mutants developed by γ-ray mutagenesis may be used as important resources for understanding of the mechanism on photosynthesis and chlorophyll catabolism. Finally, light modulation combined with γ-irradiation could be a new methodology that increases the mutation frequency of a target trait.

ABSTRACT IN KOREAN

물리적 돌연변이원(감마선, X-선, 이온빔 등)을 이용한 방사선 돌연변이 육종법은 다양한 식물에 활용되어 현재까지 공식적으로 3,000종 이상이 개발되었다. 특히, 우수 품종의 1~2개 형질을 개량하는데 유용하게 활용되고 있으며, 종자번식 작물을 중심으로 돌연변이의 유기 기작, 적정 방사선 처리조건, 돌연변이 발생빈도 등에 대해 활발한 연구가 진행되었다. 반면, 영양번식 작물의 경우 국화를 제외하고는 관련 연구가 제한적으로 진행되었으며, 특히 한국, 중국, 일본의 화훼산업에서 중요한 화훼작물에 속하는 난의 경우 보고된 연구가 거의 없다. 본 연구에서는 심비디움을 대상으로 적정 방사선 처리조건, 돌연변이 발생빈도, 돌연변이체의 키메라 안정성, 변이 기작, 돌연변이 유기효율 증진에 대한 연구를 목적으로 한다.

심비디움의 적정 감마선 처리조건 분석은 다양한 조사시간(1, 4, 8, 16, 24시간) 및 조사선량(0, 20, 40, 60, 80, 120Gy)로 처리한 후 3, 6, 9개월에 생존율, 증식률, 재분화율을 비교한 결과 조사시간 1-8시간까지는 RD_{50} 및 LD_{50}이 조사시간에 비례적으로 증가하였으나, 8-24시간에서는 차이가 없는 것을 확인하였다. 1차 도출결과를

활용하여 다양한 감마선 처리집단을 구축하고 돌연변이 발생빈도를 분석한 결과 특정 조사조건(RB003: 35Gy/4h, 변이빈도 4.06%; RB012: 20Gy/1h, 변이빈도 1.51%)에서 높은 변이빈도 및 스펙트럼을 보이는 것으로 확인되었다. 반면, 감마선 재조사에서는 돌연변이 발생빈도에 차이가 없었다. 이러한 결과는 상대적으로 짧은 4시간 이하의 감마선 조사를 통해서 다수의 변이체를 유기할 수 있음을 의미한다. 또한 변이체의 키메라 안정성을 분석한 결과 추정되는 키메라의 발생 형태에 따라 안정성에 차이가 있음을 확인하였다.

감마선에 의한 심비디움 엽색변이체(RB003-S12, 엽록소 감소 돌연변이체)의 변이 메커니즘을 분석하기 위해 대조구와 돌연변이체의 RNA를 추출하여 염기서열을 분석하였다. 그 결과 대조구와 돌연변이체 간의 유전자 발현 차이를 보이는 2,267개(724개 증가, 529개 감소)의 유전자를 도출하였으며, 엽록소 합성 및 분해, 금속이온 전달자에 연관된 유전자가 다수 포함된 것으로 확인되었다. 해당 유전자의 유전자 발현을 정량적 PCR로 분석한 결과 엽록소 생합성과 연관된 유전자는 확인되지 않았으며, 7개의 이온 전달자 유전자는 발현이 감소되었고 엽록소 분해 유전자(chlorophyllase 2)는 발현이 증가되는 것으로 확인되었다. 이러한 결과는 엽록소 및 금속이온 전달 대사과정에서 발생된 돌연변이가 엽색의 변화를

미친다는 것을 의미한다.

특정 전 처리를 통해 목표 형질의 유전자 발현이 증가된 상태에서 감마선을 처리할 경우 목표 형질의 돌연변이 유기효율이 증진될 수 있는지를 분석하기 위해 심비디움의 엽색을 대상으로 분석을 하였다. 심비디움 기내배양 라이좀을 광 조절(암처리 및 광처리)를 통해 엽록소 생합성을 유도한 후 감마선을 조사하고 엽색 돌연변이의 발생 빈도를 분석하였다. 그 결과 1차 재분화체에 비해 2차 재분화체에서 엽색 돌연변이의 발생 빈도가 높았으며, 광 조절 후 감마선을 조사한 경우(RB003: 변이빈도 0.51%, RB012: 변이빈도 0.30%) 감마선만 조사한(RB003: 변이빈도 0.37%, RB012: 변이빈도 0.15%) 시험구에 비해 엽색 돌연변이의 발생 빈도가 1.4-2.0배 증진된 것으로 분석되었다.

본 연구결과는 심비디움의 돌연변이 육종연구에서 돌연변이 유기 및 키메라의 안정화, 변이 유기증진 등에 중요한 기초자료로 활용될 것으로 기대한다.

주요어: 감마선, 돌연변이, 빈도, 안정성, 기작, 유기 효율

학 번: 2013-30323